CT-imaging in Acute Ischemic Stroke: Thrombus Characterization and Technique Optimization

Joris Martijn Niesten

J.M. Niesten, Amsterdam, 2014
jmniesten@gmail.com

ISBN: 978-94-90944-09-4
Cover design: Joris Niesten and Christiaan van Kesteren
Lay-out: Vincent van Zandvoord
Printed by: Printsupport4u

CT-imaging in Acute Ischemic Stroke: Thrombus Characterization and Technique Optimization

CT-beeldvorming bij Acuut Herseninfarct: Thrombuskarakterisering en Techniekoptimalisatie

(met een samenvatting in het Nederlands)

Proefschrift

ter verkrijging van de graad van doctor aan de Universiteit Utrecht op gezag van de rector magnificus, prof.dr. G.J. van der Zwaan, ingevolge het besluit van het college voor promoties in het openbaar te verdedigen op vrijdag 28 maart 2014 des middags te 2.30 uur

door

Joris Martijn Niesten

geboren op 30 december 1984 te Nijmegen

Promotor:	Prof. dr. W.P.Th.M. Mali
Co-promotoren:	Dr. I.C. van der Schaaf
	Dr. B.K. Velthuis

The research described in this thesis was supported by a grant of the Dutch Heart Foundation (NHS-2008T034) and NutsOhra Foundation (NHS 0903-012).

Financial support by the Dutch Heart Foundation for the publication of this thesis is gratefully acknowledged.

This thesis was also generously sponsored by Chipsoft BV, Covidien BV, Lundbeck BV, Philips Healthcare, Rontgenstichting Utrecht and Terumo Europe NV.

CONTENTS

General introduction

CHAPTER 1

Stroke is the third leading cause of death worldwide and the most common cause of long term disability with an approximate incidence of 795.000 per year in America and 41.000 in the Netherlands [1, 2]. Around 20% of all stroke patients die within one year after the stroke event [2]. Two important types of stroke can be distinguished: hemorrhagic stroke, occurring in 13% of patients (3% subarachnoid and 10% intracerebral), and ischemic stroke, accounting for 87% of strokes [2, 3].

Recanalization of the occluded artery is the main aim of treatment in ischemic stroke [4]. Intravenous thrombolysis with recombinant tissue-type plasminogen activator (IV-rtPA) is the most important first-line treatment. However, recanalization is achieved in only 50% of occluded arteries [5].
Being able to predict in which patients IV-rtPA will be successful may facilitate the choice for other treatment options such as mechanical thrombectomy or intra-arterial thrombolysis. The composition of thrombi may influence the efficacy of rtPA [6-9]. Improved knowledge about thrombus composition and its relation with radiologic imaging characteristics could help to predict the success of rtPA and individualize treatment.
On arrival at the emergency department CT-imaging plays a critical first-line role in evaluating patients with symptoms of an acute stroke. After a non-contrast CT (NCCT) has excluded hemorrhage, CT-Perfusion (CTP) and CT-angiography (CTA) are well-established scan series to identify and determine the extent and potential reversibility of ischemia, the site and extent of vessel occlusion, and for early identification of the stroke subtype [10-12]. With the growing use of CTP and CTA as diagnostic studies in many institutions, it is important to optimise these techniques in order to achieve a balance between the best possible image quality with the least possible radiation dose.
The first part of this thesis explores the histopathological and CT-imaging characteristics of cerebral thrombi in acute stroke patients. The second part focuses on techniques to optimize CTP- and CTA-imaging.

PART 1: CT-IMAGING IN ACUTE ISCHEMIC STROKE: THROMBUS CHARACTERIZATION

Different causes of ischemic stroke can be distinguished. Cardioembolism is the origin of stroke in about 18-30%, large artery atherosclerosis in 13-36%, and small artery occlusion in 14-27% [13-15]. Although only a relative small source of overall stroke (2%), dissection of an artery is responsible for approximately 15% of stroke in younger patients [16, 17].
According to the current guidelines all patients without contra-indications, admitted within 4.5 hours after stroke onset, are treated with IV-rTPA. The main complication of IV-rtPA is intracerebral hemorrhage and as this risk increases with time, IV-rtPA should be applied as soon as possible [18, 19]. Other treatment options such as mechanical thrombectomy or intra-arterial thrombolysis can

be considered in patients who do not achieve timely recanalization with IV-rtPA, or who are not eligible for IV-rtPA because of the time-restriction or other contraindications. Intra-arterial thrombolysis allows for direct delivery to the thrombus but is restricted to a six-hour window [20]. Mechanical thrombectomy establishes recanalization through thrombus extraction, providing a possibility to extend the treatment time window to 8 hours [21], although recent randomized controlled trials have not yet proven the benefit [22, 23] . Although the overall recanalization rates for intra-arterial thrombolysis (around 65%) and for mechanical thrombectomy (around 87%) are high [5, 20, 22, 24] , there is an increased risk of hemorrhage [22].

In patients who are eligible for IV-rtPA, there are no straightforward tools to predict whether this treatment will be successful. To understand and predict the pathways of thrombus lysability better, both pathologic studies and radiologic imaging are important. The traditional thought is that "red thrombi", containing a mixture of mainly red blood cells (RBC) and fibrin, originate from low flow regions such as in cardioembolism thrombi; while "white thrombi", containing mainly platelets and fibrin, arise in regions of fast moving blood, as to be expected in large artery atherosclerosis thrombi [25, 26]. This thrombus consistency may influence the efficacy of IV-rtPA as RBC-rich thrombi may be more sensitive to IV-rtPA as compared to platelet-rich thrombi [6-9]. Furthermore, RBCs in thrombi increase the attenuation on NCCT, whereas platelets, atheromatous and cellular debris are known to decrease the HU-values [27-29]. Measuring thrombus attenuation on NCCT could therefore be a rapid non-invasive tool for predicting thrombus composition, stroke subtype and recanalization rate. More knowledge about histopathological and CT-imaging characteristics of thrombi may help to gain insight in the etiopathogenesis of stroke and to individualize treatment.

Chapter 2 describes the relation between the presence of hyperdense vessel signs and the attenuation of intracranial thrombi on NCCT and different stroke subtypes.

Chapter 3 presents the relationship between the histopathologic composition of thrombi and stroke subtypes as well as thrombus attenuation on NCCT.

Chapter 4 discusses whether thrombus density is related to the likelihood of recanalization after IV-rtPA and whether persistent occlusions can be predicted by HU-measurements of thrombi on NCCT.

PART 2: CT-IMAGING IN ACUTE ISCHEMIC STROKE: TECHNIQUE OPTIMIZATION

CTP and CTA are valuable additions to NCCT in the evaluation of acute ischemic stroke patients, with the possibility of twenty-four/seven availability, low costs, and rapid assessment in most clinical facilities [10, 30]. CTP is a functional CT-imaging technique that provides information about hemodynamics

of the brain parenchyma. In ischemic stroke it can be used to determine the extent of irreversibly damaged brain parenchyma (infarct core) and ischemic but potentially salvageable tissue (penumbra) [31]. Several quantitative perfusion parameters are used for perfusion measurements, including Cerebral Blood Flow (CBF), Cerebral Blood Volume (CBV), Mean Transit Time (MTT), and Time to Peak (TTP) [31]. Typically, on CTP the whole ischemic area of brain parenchyma is defined as the area with prolonged MTT or decreased CBF, and CBV is used to differentiate the infarct core (decreased CBV) from the penumbra (normal or increased CBV) [32].

The accuracy of CTP for detecting ischemic stroke lesions has been the subject of several studies but a systematic review comparing all these studies has not yet been performed.
Furthermore, CTP has some limitations with regard to radiation dose, brain coverage, and the validity of quantitative perfusion parameters. Increased diagnostic information gained by adding CTP is at the expense of increased ionising radiation dose. A combination of NCCT, CTP and CTA will triplicate the radiation dose in comparison to NCCT alone [33]. With the on-going replacement of current CTP brain coverage, up to 6 cm in z-direction, by full-brain CTP in many institutions the radiation exposure of the CTP will increase even further [33, 34]. One of the most promising new techniques to reduce radiation exposure is the recently introduced iterative reconstruction (IR) algorithm [35-37]. IR optimises CT data with a noise- and artefact-reducing model and has the possibility to significantly reduce radiation dose while maintaining the image quality compared to the standard reconstruction method filtered back projection (FBP) [36, 37].
Another problem concerning the validity of CTP is the number of operator-dependent steps that are necessary to calculate the CBV, CBF, MTT and TTP. One important step is the selection of the Arterial Input Function (AIF) and Venous Output Function (VOF) [38, 39] with an inter-observer variability between 10% and 27% [40]. The selection of different vessels as the AIF and VOF can result in different estimations of quantitative perfusion parameters and subsequently diverging predictions of the final infarct volume and the infarct-penumbra index [41-43].
CTA of the head (circle of Willis) and neck (carotid and vertebral arteries) in acute ischemic stroke patients can help to assess the extent and cause of arterial occlusion, the collateral circulation, and the grade of extracranial vessel stenosis [44, 45]. The extent of the arterial occlusion and the collateral circulation are important factors in predicting infarct size and stroke outcome [46, 47]. Accurate measurement of the carotid artery stenosis grade is essential as it can influence treatment in both acute and later phase. A disadvantage of the standard reconstruction method FBP to create CTA images is the increased amount of noise when radiation dose is reduced. Recently introduced IR algorithms could potentially replace standard FBP to improve CTA image quality while maintaining the same radiation dose.

Chapter 5 presents a systematic review to determine the accuracy of CTP for the detection of ischemic stroke.
Chapter 6 describes the possibility to reduce radiation dose in CTP imaging with the use of IR algorithms.
Chapter 7 reports the accuracy and reproducibility of CTP by assessment of the optimal artery for the AIF and re-evaluating the necessity of the VOF.
Chapter 8 investigates image quality of head and neck CTA reconstructed with standard FBP reconstruction and two different IR algorithms.

REFERENCES

1. Hartstichting. Factsheet, feiten en cijfers beroerte. *Available via http://webshop.hartstichting.nl/Producten/download.aspx?pID=2574*. 2011
2. Go AS, Mozaffarian D, Roger VL, Benjamin EJ, Berry JD, Borden WB, Bravata DM, Dai S, Ford ES, Fox CS, Franco S, Fullerton HJ, Gillespie C, Hailpern SM, Heit JA, Howard VJ, Huffman MD, Kissela BM, Kittner SJ, Lackland DT, Lichtman JH, Lisabeth LD, Magid D, Marcus GM, Marelli A, Matchar DB, McGuire DK, Mohler ER, Moy CS, Mussolino ME, Nichol G, Paynter NP, Schreiner PJ, Sorlie PD, Stein J, Turan TN, Virani SS, Wong ND, Woo D, Turner MB. Heart disease and stroke statistics--2013 update: A report from the american heart association. *Circulation*. 2013;127:e6-e245
3. Ahmed N, Wahlgren N, Grond M, Hennerici M, Lees KR, Mikulik R, Parsons M, Roine RO, Toni D, Ringleb P. Implementation and outcome of thrombolysis with alteplase 3-4.5 h after an acute stroke: An updated analysis from sits-istr. *Lancet neurology*. 2010;9:866-874
4. Rha JH, Saver JL. The impact of recanalization on ischemic stroke outcome: A meta-analysis. *Stroke*. 2007;38:967-973
5. Mazighi M, Serfaty JM, Labreuche J, Laissy JP, Meseguer E, Lavallee PC, Cabrejo L, Slaoui T, Guidoux C, Lapergue B, Klein IF, Olivot JM, Abboud H, Simon O, Niclot P, Nifle C, Touboul PJ, Raphaeli G, Gohin C, Claeys ES, Amarenco P. Comparison of intravenous alteplase with a combined intravenous-endovascular approach in patients with stroke and confirmed arterial occlusion (recanalise study): A prospective cohort study. *Lancet neurology*. 2009;8:802-809
6. Caplan LR. Antiplatelet therapy in stroke prevention: Present and future. *Cerebrovasc Dis*. 2006;21 Suppl 1:1-6
7. Jang IK, Gold HK, Ziskind AA, Fallon JT, Holt RE, Leinbach RC, May JW, Collen D. Differential sensitivity of erythrocyte-rich and platelet-rich arterial thrombi to lysis with recombinant tissue-type plasminogen activator. A possible explanation for resistance to coronary thrombolysis. *Circulation*. 1989;79:920-928
8. Niessen F, Hilger T, Hoehn M, Hossmann KA. Differences in clot preparation determine outcome of recombinant tissue plasminogen activator treatment in experimental thromboembolic stroke. *Stroke*. 2003;34:2019-2024
9. Molina CA, Montaner J, Arenillas JF, Ribo M, Rubiera M, Alvarez-Sabin J. Differential pattern of tissue plasminogen activator-induced proximal middle cerebral artery recanalization among stroke subtypes. *Stroke*. 2004;35:486-490
10. Wintermark M, Meuli R, Browaeys P, Reichhart M, Bogousslavsky J, Schnyder P, Michel P. Comparison of ct perfusion and angiography and mri in selecting stroke patients for acute treatment. *Neurology*. 2007;68:694-697
11. Muir KW, Halbert HM, Baird TA, McCormick M, Teasdale E. Visual evaluation of perfusion computed tomography in acute stroke accurately estimates infarct volume and tissue viability. *Journal of neurology, neurosurgery, and psychiatry*. 2006;77:334-339
12. Tan JC, Dillon WP, Liu S, Adler F, Smith WS, Wintermark M. Systematic comparison of perfusion-ct and ct-angiography in acute stroke patients. *Ann Neurol*. 2007;61:533-543
13. Bejot Y, Caillier M, Ben Salem D, Couvreur G, Rouaud O, Osseby GV, Durier J, Marie C, Moreau T, Giroud M. Ischaemic stroke subtypes and associated risk factors: A french population based study. *Journal of neurology, neurosurgery, and psychiatry*. 2008;79:1344-1348
14. Schulz UG, Rothwell PM. Differences in vascular risk factors between etiological subtypes of ischemic stroke: Importance of population-based studies. *Stroke*. 2003;34:2050-2059
15. Kolominsky-Rabas PL, Weber M, Gefeller O, Neundoerfer B, Heuschmann PU. Epidemiology of ischemic stroke subtypes according to toast criteria: Incidence, recurrence, and long-term survival in ischemic stroke subtypes: A population-based study. *Stroke*. 2001;32:2735-2740
16. Bejot Y, Daubail B, Debette S, Durier J, Giroud M. Incidence and outcome of cerebrovascular events related to cervical artery dissection: The dijon stroke registry. *International journal of stroke : official journal of the International Stroke Society*. 2013
17. Putaala J, Metso AJ, Metso TM, Konkola N, Kraemer Y, Haapaniemi E, Kaste M, Tatlisumak T. Analysis of 1008 consecutive patients aged 15 to 49 with first-ever ischemic stroke: The helsinki young stroke registry. *Stroke*. 2009;40:1195-1203
18. Saver JL. Time is brain - quantified. *Neurology*. 2005;64:A295-A295
19. Tissue plasminogen activator for acute ischemic stroke. The national institute of neurological disorders and stroke rt-pa stroke study group. *The New England journal of medicine*. 1995;333:1581-1587
20. Furlan A, Higashida R, Wechsler L, Gent M, Rowley H, Kase C, Pessin M, Ahuja A, Callahan F, Clark WM, Silver F, Rivera F. Intra-arterial prourokinase for acute ischemic stroke. The proact ii study: A randomized controlled trial. Prolyse in acute cerebral thromboembolism. *JAMA : the journal of the American Medical Association*. 1999;282:2003-2011
21. Tenser MS, Amar AP, Mack WJ. Mechanical thrombectomy for acute ischemic stroke using the merci retriever and penumbra aspiration systems. *World neurosurgery*. 2011;76:S16-23
22. Broderick JP, Palesch YY, Demchuk AM, Yeatts SD, Khatri P, Hill MD, Jauch EC, Jovin TG, Yan B, Silver FL, von Kummer R, Molina CA, Demaerschalk BM, Budzik R, Clark WM, Zaidat OO, Malisch TW, Goyal M, Schonewille WJ, Mazighi M, Engelter ST, Anderson C, Spilker J, Carrozzella J, Ryckborst KJ, Janis LS, Martin RH, Foster LD, Tomsick TA. Endovascular therapy after intravenous t-pa versus t-pa alone for stroke. *The New England journal of medicine*. 2013;368:893-903

23. Kidwell CS, Jahan R, Gornbein J, Alger JR, Nenov V, Ajani Z, Feng L, Meyer BC, Olson S, Schwamm LH, Yoo AJ, Marshall RS, Meyers PM, Yavagal DR, Wintermark M, Guzy J, Starkman S, Saver JL. A trial of imaging selection and endovascular treatment for ischemic stroke. *The New England journal of medicine*. 2013;368:914-923
24. Ciccone A, Valvassori L. Endovascular treatment for acute ischemic stroke. *The New England journal of medicine*. 2013;368:2433-2434
25. Chaves CJ, Caplan LR. Heparin and oral anticoagulants in the treatment of brain ischemia. *Journal of the neurological sciences*. 2000;173:3-9
26. Jerjes-Sanchez C. Venous and arterial thrombosis: A continuous spectrum of the same disease? *European heart journal*. 2005;26:3-4
27. Liebeskind DS, Sanossian N, Yong WH, Starkman S, Tsang MP, Moya AL, Zheng DD, Abolian AM, Kim D, Ali LK, Shah SH, Towfighi A, Ovbiagele B, Kidwell CS, Tateshima S, Jahan R, Duckwiler GR, Vinuela F, Salamon N, Villablanca JP, Vinters HV, Marder VJ, Saver JL. Ct and mri early vessel signs reflect clot composition in acute stroke. *Stroke*. 2011;42:1237-1243
28. Kim EY, Heo JH, Lee SK, Kim DJ, Suh SH, Kim J, Kim DI. Prediction of thrombolytic efficacy in acute ischemic stroke using thin-section noncontrast ct. *Neurology*. 2006;67:1846-1848
29. Besachio DA, Quigley EP, 3rd, Shah LM, Salzman KL. Noncontrast computed tomographic hounsfield unit evaluation of cerebral venous thrombosis: A quantitative evaluation. *Neuroradiology*. 2013;55:941-945
30. Rother J, Jonetz-Mentzel L, Fiala A, Reichenbach JR, Herzau M, Kaiser WA, Weiller C. Hemodynamic assessment of acute stroke using dynamic single-slice computed tomographic perfusion imaging. *Arch Neurol*. 2000;57:1161-1166
31. Konstas AA, Goldmakher GV, Lee TY, Lev MH. Theoretic basis and technical implementations of ct perfusion in acute ischemic stroke, part 1: Theoretic basis. *AJNR Am J Neuroradiol*. 2009;30:662-668
32. Shetty SK, Lev MH. Ct perfusion in acute stroke. *Neuroimaging clinics of North America*. 2005;15:481-501, ix
33. Abels B, Klotz E, Tomandl BF, Villablanca JP, Kloska SP, Lell MM. Ct perfusion in acute ischemic stroke: A comparison of 2-second and 1-second temporal resolution. *AJNR Am J Neuroradiol*. 2011;32:1632-1639
34. Kloska SP, Fischer T, Sauerland C, Buerke B, Dziewas R, Fischbach R, Heindel W. Increasing sampling interval in cerebral perfusion ct: Limitation for the maximum slope model. *Acad Radiol*. 2010;17:61-66
35. Mnyusiwalla A, Aviv RI, Symons SP. Radiation dose from multidetector row ct imaging for acute stroke. *Neuroradiology*. 2009;51:635-640
36. Willemink MJ, de Jong PA, Leiner T, de Heer LM, Nievelstein RA, Budde RP, Schilham AM. Iterative reconstruction techniques for computed tomography part 1: Technical principles. *Eur Radiol*. 2013;23:1623-1631
37. Willemink MJ, Leiner T, de Jong PA, de Heer LM, Nievelstein RA, Schilham AM, Budde RP. Iterative reconstruction techniques for computed tomography part 2: Initial results in dose reduction and image quality. *Eur Radiol*. 2013
38. Turk AS, Grayev A, Rowley HA, Field AS, Turski P, Pulfer K, Mukherjee R, Haughton V. Variability of clinical ct perfusion measurements in patients with carotid stenosis. *Neuroradiology*. 2007;49:955-961
39. Zussman B, Jabbour P, Talekar K, Gorniak R, Flanders AE. Sources of variability in computed tomography perfusion: Implications for acute stroke management. *Neurosurg Focus*.30:E8
40. Soares BP, Dankbaar JW, Bredno J, Cheng S, Bhogal S, Dillon WP, Wintermark M. Automated versus manual post-processing of perfusion-ct data in patients with acute cerebral ischemia: Influence on interobserver variability. *Neuroradiology*. 2009;51:445-451
41. Kealey SM, Loving VA, Delong DM, Eastwood JD. User-defined vascular input function curves: Influence on mean perfusion parameter values and signal-to-noise ratio. *Radiology*. 2004;231:587-593
42. Ferreira RM, Lev MH, Goldmakher GV, Kamalian S, Schaefer PW, Furie KL, Gonzalez RG, Sanelli PC. Arterial input function placement for accurate ct perfusion map construction in acute stroke. *AJR Am J Roentgenol*.194:1330-1336
43. Sanelli PC, Lev MH, Eastwood JD, Gonzalez RG, Lee TY. The effect of varying user-selected input parameters on quantitative values in ct perfusion maps. *Acad Radiol*. 2004;11:1085-1092
44. Saake M, Goelitz P, Struffert T, Breuer L, Volbers B, Doerfler A, Kloska S. Comparison of conventional cta and volume perfusion cta in evaluation of cerebral arterial vasculature in acute stroke. *AJNR Am J Neuroradiol*. 2012;33:2068-2073
45. Josephson SA, Bryant SO, Mak HK, Johnston SC, Dillon WP, Smith WS. Evaluation of carotid stenosis using ct angiography in the initial evaluation of stroke and tia. *Neurology*. 2004;63:457-460
46. Puetz V, Dzialowski I, Hill MD, Subramaniam S, Sylaja PN, Krol A, O'Reilly C, Hudon ME, Hu WY, Coutts SB, Barber PA, Watson T, Roy J, Demchuk AM. Intracranial thrombus extent predicts clinical outcome, final infarct size and hemorrhagic transformation in ischemic stroke: The clot burden score. *International journal of stroke : official journal of the International Stroke Society*. 2008;3:230-236
47. McVerry F, Liebeskind DS, Muir KW. Systematic review of methods for assessing leptomeningeal collateral flow. *AJNR Am J Neuroradiol*. 2012;33:576-582

PART 1

CT-imaging in Acute Ischemic Stroke: Thrombus Characterization

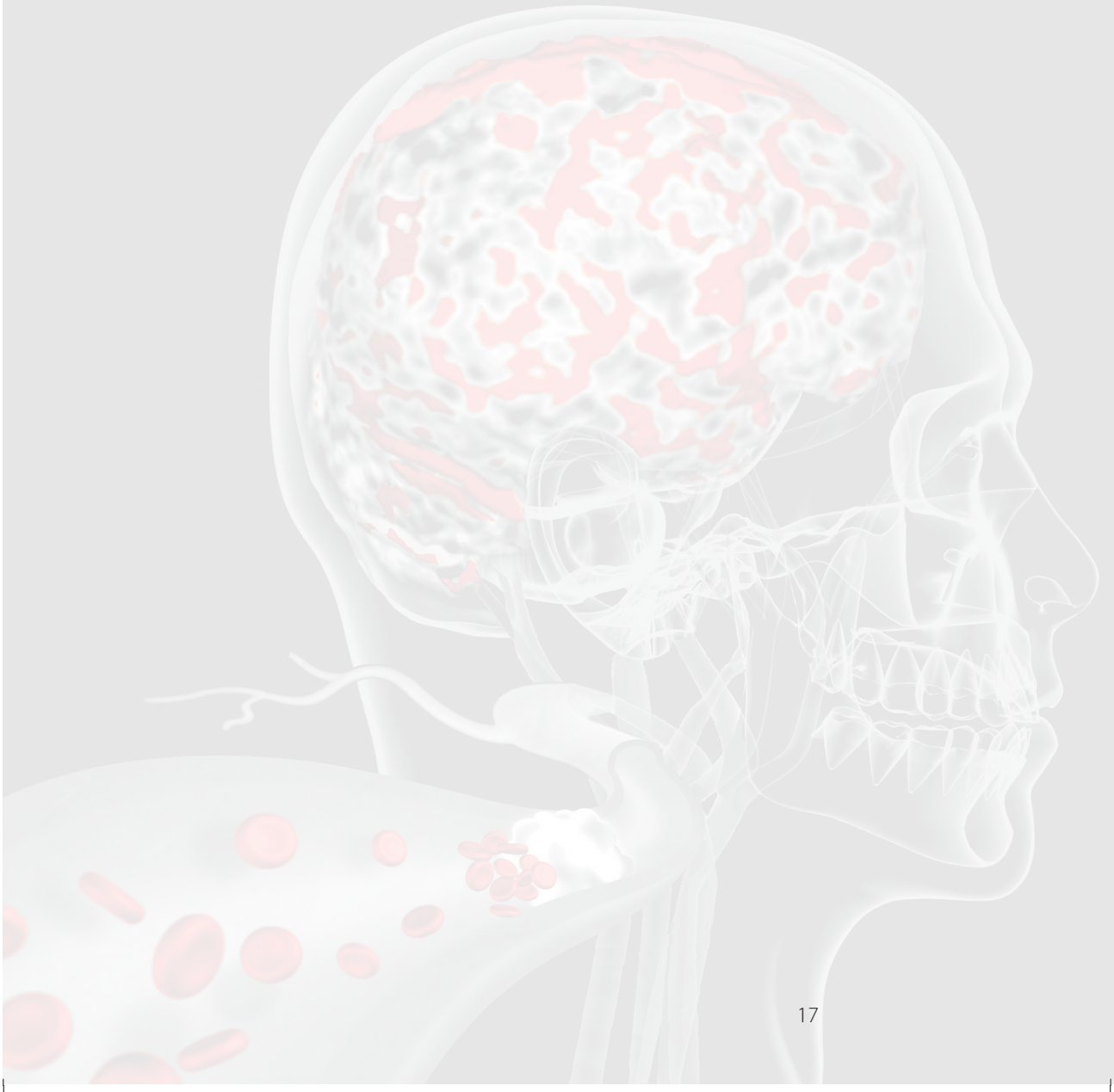

Relationship between thrombus attenuation and different stroke subtypes

JM Niesten, IC van der Schaaf, GJ Biessels, AE van Otterloo, T van Seeters, AD Horsch, MJA Luitse, Y van der Graaf, LJ Kappelle, WPTM Mali, BK Velthuis, on behalf of the DUtch acute Stroke Trial (DUST)

Neuroradiology, 2013

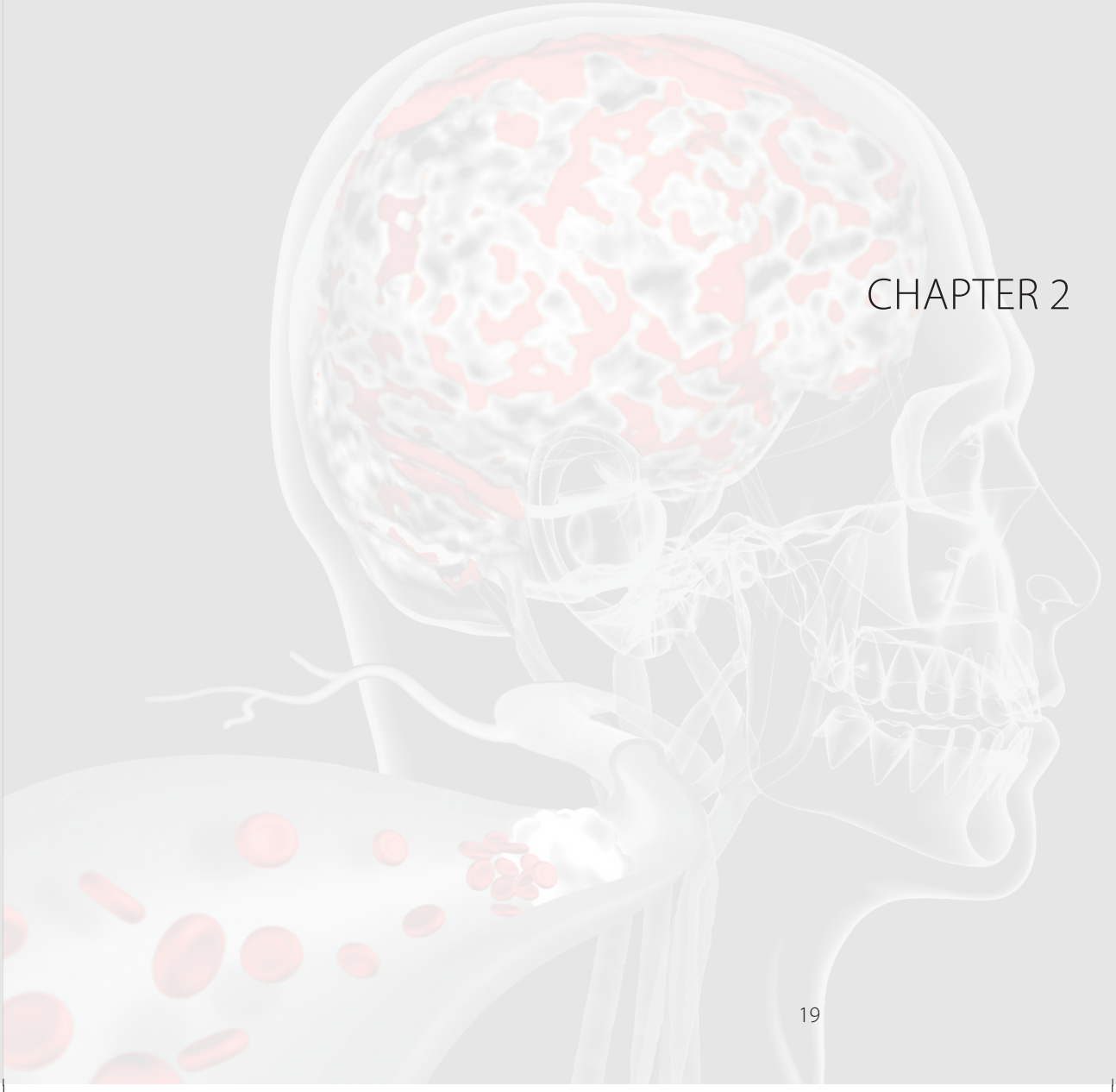

CHAPTER 2

ABSTRACT

Introduction

More insights in the etiopathogenesis of thrombi could be helpful in the treatment of patients with acute ischemic stroke. The aim of our study was to determine the relationship between presence of a hyperdense vessel sign and thrombus density with different stroke subtypes.

Methods

We included 123 patients with acute ischemic anterior circulation stroke and a visible occlusion on CT-angiography caused by cardioembolism (n=53), large artery atherosclerosis (n=55) or dissection (n=15). Presence or absence of a hyperdense vessel sign was assessed and thrombus density was measured in Hounsfield Units (HU) on non-contrast 1 mm thin slices CT. Subsequently, occurrence of hyperdense vessel sign and thrombus density (absolute HU and rHU (=HU thrombus / HU contralateral) were related with stroke subtypes.

Results

The presence of hyperdense vessel signs differed significantly among subtypes and was found in 45%, 64% and 93% of patients with cardioembolism, large artery atherosclerosis and dissection, respectively (p=0.003). The mean HU and rHU (+ 95%CI) of the thrombi in all vessels were respectively 56.1 (53.2-59.0) and 1.39 (1.33-1.45) in cardioembolism, 64.6 (62.2-66.9) and 1.59 (1.54-1.64) in large artery atherosclerosis and 76.4 (73.0-79.8) and 1.88 (1.79-1.97) in dissection (p<0.0001). We found the same significant ranking order in the density of thrombi with hyperdense vessel signs (mean HU and rHU (+ 95%CI) respectively): cardioembolism 61.3 (57.4-65.3) and 1.49 (57.4-65.3); large artery atherosclerosis 67.3 (64.9-69.7) and 1.65 (1.58-1.71); dissection 76.4 (72.6-80.1) and 1.89 (1.79-1.99, p<0.0001).

Conclusion

Presence of a hyperdense vessel sign and thrombus density are related to stroke subtype.

INTRODUCTION

Acute ischemic stroke is the third leading cause of death and the leading cause of long term disability worldwide [1,2]. About three-quarters of ischemic strokes are caused by arterial thrombo-embolism [3]. Ischemic stroke of arterial origin is caused by cardioembolism in 18-30%, by large artery atherosclerosis in 13-36% and by small artery occlusion in 14-27% [4-6]. Dissection of a vertebral or carotid artery is a relatively infrequent cause of ischemic stroke and responsible for approximately 15% of stroke in younger patients [7].

Intravenous thrombolysis with recombinant tissue-type plasminogen activator (rtPA) should be considered in the acute stage of ischemic stroke, but results in timely recanalization in only 50% of occluded arteries [8]. The reasons for this treatment failure are still not fully understood. Being able to predict which type of thrombus is likely to be resolved by rtPA may be helpful for choosing other recanalization strategies such as mechanical thrombectomy or intra-arterial thrombolysis. Currently there are no straightforward tools to predict in which patients rtPA will be helpful in lysing the thrombus. Improved knowledge about the rtPA-vulnerability of a thrombus may facilitate the choice of treatment.

Thrombus subtype (cardioembolic, atherosclerotic or dissection) and consistency may influence the efficacy of thrombolysis with rtPA [9-15]. Thrombi have complex and variable architecture with fibrin, erythrocytes, leukocytes and platelets as most important components [16]. Platelet rich thrombi have lower attenuation on non-contrast CT than erythrocyte rich thrombi [17-19]. The erythrocyte component of the thrombus has been shown to correspond to the presence of a hyperdense vessel sign in a pathological study [20].

The aim of the current study is to investigate the relation between the presence of hyperdense vessel signs and the attenuation of intra-cranial thrombi on non-contrast CT with the different stroke subtypes to gain insights in the etiopathogenesis of the thrombus.

METHODS

We reviewed the records of a prospectively included series of patients who participated in a large prospective multicenter observational cohort study between May 2009 and November 2012. Inclusion criteria for this study are: age ≥ 18 years, onset of stroke symptoms < 9 hours, NIHSS ≥ 2 and informed consent for follow-up from patient or family. Exclusion criteria are: known renal failure; contrast allergy and patients who had already received therapy before neuroimaging. All patients undergo non-contrast CT, CT-perfusion (CTP) and CT-angiography (CTA) on admission with similar protocols.

For this substudy we only included patients with a visible middle cerebral artery (MCA) or intracranial internal carotid artery (ICA) occlusion on CTA and a diagnosis of acute ischemic anterior stroke due to cardioembolism, large artery atherosclerosis or dissection. Large artery atherosclerosis was defined

as imaging findings of either significant (>50%) stenosis or occlusion of a major cerebropetal artery on CTA ipsilateral to the symptomatic hemisphere, presumed to be due to atherosclerosis according to the Trial of Org 10172 in Acute Stroke Treatment (TOAST) criteria [21] if other diagnostic studies had excluded potential sources of cardiac embolism. Stroke was defined as cardioembolic if at least one cardiac source for an embolus had been identified in the absence of significant ipsilateral stenosis (>50%) and atherosclerosis [21]. Criteria for diagnosing dissection at CTA were a narrowed eccentric lumen surrounded by crescent-shaped mural thickening or a tapered occlusion with an associated increase in external vessel diameter [22,23]. Further inclusion criteria were: imaging performed with CT-scanners from the same vendor with non-contrast CT 1 mm thin-slices available for evaluation. We excluded patients in which it was not possible to determine the cause of stroke with enough certainty, e.g. if atherosclerosis was present in combination with a possible cardiac cause such as atrial fibrillation (*figure 1)*.

Figure 1 *Flowchart of total enrolment of patients.*

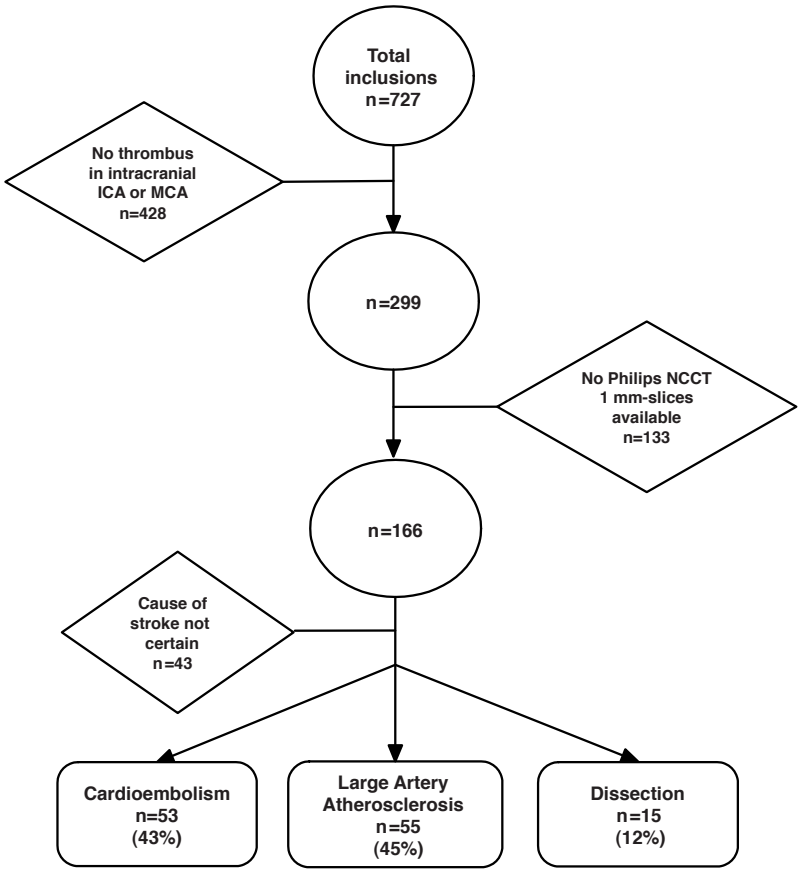

The following baseline data were collected for all patients: demographic features, cardiovascular risk factors (hypertension, diabetes, hyperlipidemia, smoking, stroke or transient ischemic attack (TIA) in history), location of the thrombus, onset time to imaging and baseline NIHSS on admission (*table 1*).

Scan parameters of the non-contrast CT were: 120 kVp, 300 mAs, and 1 mm reconstructed slice thickness. For CTA 60-80 ml of contrast agent (300mg I/ml) were injected into the antecubital vein (18-gauge needle) at a rate of 6 mL/s followed by a 40-mL saline flush at a rate of 6 mL/s. The scan parameters for the CTA were: 120 kVp, 150 mAs, 1 mm reconstructed slice thickness.
For evaluation of the presence or absence of a hyperdense vessel sign each non-contrast CT-scan was evaluated separately by two observers of which at least one had experience for 5 or more years in neurovascular imaging. The observers were blinded for all radiologic, neurologic and clinical data, except for side of symptoms. In case of disagreement consensus was reached with a third reader. The definition for hyperdense vessel sign was derived from earlier publications [24-28] as the appearance of an unilateral hyperattenuating cerebral artery on non-contrast CT. If a hyperdense vessel sign was present, the attenuation of the thrombus was measured on non-contrast CT in Hounsfield Units (HU) by a third observer. All hyperdense vessel signs were confirmed to be caused by thrombi on CTA. If no hyperdense vessel sign was detected on non-contrast CT, we used CTA information to identify the location of a thrombus and subsequently performed the attenuation measurements in the corresponding location on non-contrast CT.
In all patients the attenuation of the corresponding contralateral vessel (without thrombus) was also measured to investigate the variance in attenuation in non-occluded vessels. Per patient a standardised small round region of interest was drawn three separate times within the thrombus and mean HU-values were used for analysis to improve reproducibility. The same measurements were performed in the corresponding contralateral vessel.
Subsequently, the thrombus HU was corrected for hematocrit, by calculating the rHU (=HU thrombus / HU contralateral vessel). Length of the hyperdense arteries were also measured on the 1 mm non-contrast images. With use of a rotation center images were orientated along the exact course of the hyperdense artery so that the length could be measured accurately.
Statistical analyses were performed to investigate differences in clinical data between patients with a different stroke subtype using Chi-square for nominal variables and One-Way ANOVA for continuous data. For the three subtypes of stroke the proportion of patients with a hyperdense vessel sign, the mean thrombus length and the mean HU and rHU-values (with 95%confidence intervals (CI)) of the thrombus and of the contralateral vessel were calculated and values were respectively compared by X^2-test (comparing all subtypes) and analysis of covariance (ANCOVA, general linear model) to adjust mean HU and rHU-values for age, sex and potential confounders (the presence of hypertension, diabetes and hyperlipidemia and time from symptom onset to imaging). A p-value of <0.05 was considered statistical significant. To investi-

gate the interobserver agreement of the presence of hyperdense artery signs and the intraobserver reliability of the HU-measurements respectively Cohen's kappa and intraclass correlation coefficients (ICCs) were used.

RESULTS

We included 123 patients with a stroke that was caused by cardioembolism (n=53), large artery atherosclerosis (n=55) or dissection (n=15). The included patients consisted of 50 women (41%) and had an average age of 68 years (±13) (*table 1*).

Table 1 *Patient characteristics in different stroke subtypes*

Characteristics	***Stroke subtype***			***P-value***
	Cardioembolism	*Large Artery Atherosclerosis*	*Dissection*	
Patient numbers, n	53	55	15	
Demographics				
Age, mean years (± SD)	68 (13)	72 (11)	52 (11)	0.001
Female, n (%)	27 (51)	20 (36)	3 (20)	0.07
Risk factors[a], n (%)				
Hypertension	27 (51)	31 (56)	4 (27)	0.12
Diabetes	4 (8)	7 (13)	0	0.28
Hyperlipidemia	14 (28)	19 (35)	1 (7)	0.10
Smoking	16 (33)	11 (22)	3 (21)	0.37
Stroke or TIA in history	11 (21)	6 (11)	1 (7)	0.23
Baseline NIHSS[b], mean (± SD)	11 (7)	12 (6)	13 (5)	0.50
Time to Imaging[c], minutes (± SD)	102 (72)	112 (76)	111 (93)	0.81
Location thrombus[d], n (%)				
MCA - M1	22 (42)	27 (49)	7 (47)	0.73
MCA - M2	30 (57)	21 (38)	3 (20)	0.02
Intracranial ICA	1 (2)	7 (13)	5 (33)	0.002

[a] Hypertension: according to WHO criteria; blood pressure: systolic ≥ 140 mmHg and/ or diastolic ≥ 90 mmHg
Diabetes: according to WHO criteria; fasting plasma glucose ≥ 7.0mmol/l or 2hr plasma glucose ≥ 11.1mmol/l
Hyperlipidemia: abnormally elevated levels of any or all lipids and/or lipoproteins in the blood
Smoking: includes both daily and non-daily tobacco smoking

[b] Baseline NIHSS: NIH Stroke Scale on admission

[c] Time to imaging: time between onset of stroke symptoms and first CT-scan

[d] MCA: middle cerebral artery; M1: M1 segment; M2: M2 segment; ICA: internal carotid artery

A hyperdense vessel sign was found in 24 patients (45%) with cardioembolism, in 35 patients (64%) with large artery atherosclerosis and in all but one patient (n=14, 93%) with a dissection (X^2, p=0.003) (*table 2*).

Table 2 *Thrombus characteristics in different stroke subtypes*

	Stroke subtype			***P-value***
Characteristics	*Cardioembolism*	*Large Artery Atherosclerosis*	*Dissection*	
Hyperdense Vessel, n (%, 95%CI)	24 (45, 31-59)	35 (64, 51-77)	14 (93, 79-100)	0.003
Attenuation thrombus, mean (95%CI)				
All thrombi				
Absolute HU	56.1 (53.2-59.0)	64.6 (62.2-66.9)	76.4 (73.0-79.8)	<0.001
rHU	1.39 (1.33-1.45)	1.59 (1.54-1.64)	1.88 (1.79-1.97)	<0.001
Thrombi with hyperdense vessel				
Absolute HU	61.3 (57.4-65.3)	67.3 (64.9-69.7)	76.4 (72.6-80.1)	<0.001
rHU	1.49 (1.40-1.59)	1.65 (1.58-1.71)	1.89 (1.79-1.99)	<0.001
Thrombi without hyperdense vessel				
Absolute HU	51.9 (48.2-55.5)	59.8 (55.6-64.0)	77.0 (n.a)	0.002
rHU	1.31 (1.24-1.37)	1.50 (1.41-1.59)	1.75 (n.a)	<0.001
Contralateral vessel	40.4 (39.0-41.8)	40.8 (39.4-42.2)	40.9 (38.7-43.1)	0.91
Hyperdense artery length, mean (± 95% CI)	8.7 (6.1-11.3)	12.2 (8.7-15.7)	13.9 (8.2-19.6)	0.15

The interobserver agreement for the presence of a hyperdense vessel sign was excellent (*k*=0.93).

Mean HU and rHU-values of all thrombi (with and without hyperdense vessel) on non-contrast CT were significantly different between all subtypes (ANCOVA-test, p<0.0001) and were lowest in the cardioembolism subtype (56.1 95%CI 53.2-59.0 and 1.39 (95%CI 1.33-1.45), respectively), higher in the large artery atherosclerosis subtype (64.6, 95%CI 62.2-66.9 and 1.59 (95%CI 1.54-1.64), respectively), and highest in the dissection subtype (76.4, 95%CI 73.0-79.8 and 1.88 (95%CI 1.79-1.97, respectively) *(table 2, figure 2 and 3)*. The intraobserver reliability for the HU-measurements was excellent (ICC=0.82). Considering only the HU and rHU-value of thrombi in hyperdense vessels, we also found a significant difference between all subtypes (mean HU-value and mean rHU-value): cardioembolism 61.3 (95%CI 57.4-65.3) and 1.49 (95%CI 57.4-65.3); large artery atherosclerosis 67.3 (95%CI 64.9-69.7) and 1.65 (95%CI 1.58-1.71); dissection 76.4 (95%CI 73.0-79.8) and 1.89 (95%CI 1.79-1.99), *table 2*, ANCOVA-test, both p<0.0001). The mean HU and rHU-values were significantly higher in hyperdense vessels (mean HU 67.0, 95%CI 64.9-69.2 and mean rHU 1.64, 95%CI 1.59-1.70) than in non-hyperdense vessels (mean HU 55.5, 95%CI 52.6-58.5 and mean rHU 1.39, 95%CI 1.33-1.45, student's t-test, both p<0.0001).

Figure 2 *Boxplot of attenuation thrombus (in HU) in different stroke subtypes*

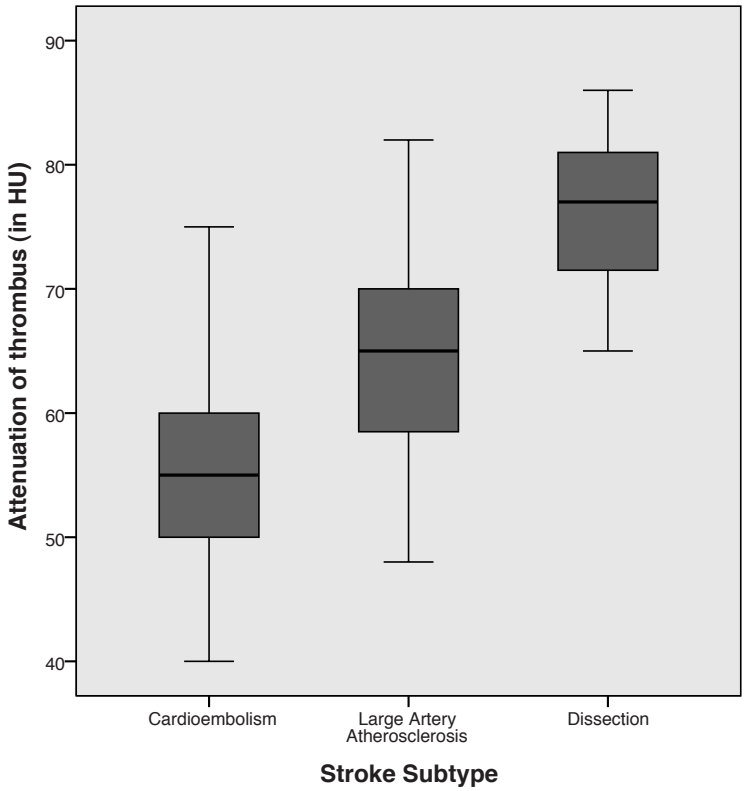

HU-value of contralateral (non-occluded) vessels was comparable for cardioembolism (mean 40.4, 95%CI 39.0-41.8), large artery atherosclerosis (mean 40.8, 95%CI 39.4-42.2) and dissection (mean 40.9, 95%CI 38.7-43.1) (*table 2,* ANCOVA-test, p=0.912).

There were no significant differences in length of the hyperdense arteries between different stroke subtypes (*table 2,* ANCOVA-test, p=0.15).

Figure 3 *Percentage of different stroke subtypes divided by HU-quartiles*

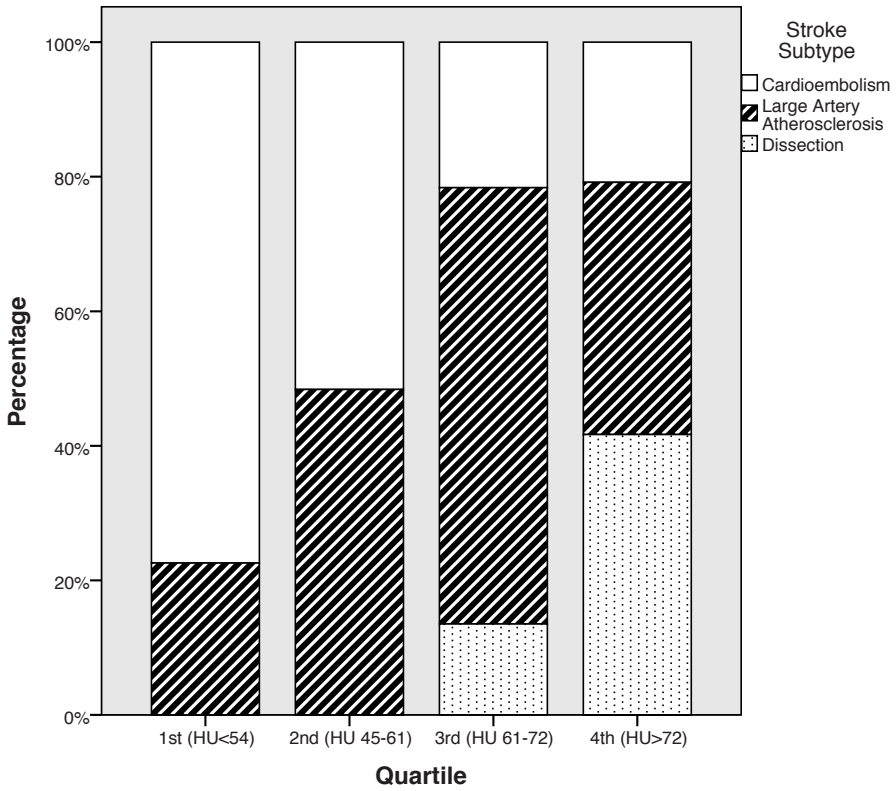

DISCUSSION

This study shows the significant relation between the presence of a hyperdense vessel sign and the thrombus attenuation on 1 mm thin slice non-contrast CT with different stroke subtypes. Cardioembolic thrombi showed the least hyperdense vessel signs and the lowest attenuation, followed by thrombi due to large artery atherosclerosis while thrombi due to dissections nearly always showed a hyperdense vessel sign and had the highest thrombus attenuation. The thrombus attenuation and presence of hyperdense vessel sign is thought to be related to the constituents and composition of the thrombus. The attenuation of the thrombus has a linear correlation with the concentration of hemoglobin while platelets and atheromatous or cellular debris are known to decrease the attenuation of the thrombus on CT [9,17,18,19,28]. Most studies on this topic, however, are experimental or animal studies. The increased use of mechanical thrombectomy devices allows correlation between thrombus density and thrombus composition. One recent study, based on mechanical retrieved thrombi of 50 patients with MCA occlusion, related CT and MRI early vessels sign (hyperdense vessel sign and blooming artefact respectively) to histological clot composition. In 20 patients the presence or absence of

hyperdense vessel signs on CT were related to the thrombus composition. They showed that the presence of a hyperdense vessel sign was related to red blood cell dominance in the thrombus, describing that 100% of red blood cell dominant, versus 67% of mixed and only 20% of fibrin-dominant thrombi showed a hyperdense vessel sign [20].

The relationship between thrombus density and stroke subtype is still unclear. A recently published study relating thrombus attenuation measured on 3 mm non-contrast CT slices to stroke subtype and recanalization found, in accordance to our findings, significantly more hyperdense vessel signs in large artery atherosclerosis thrombi compared to cardioembolism thrombi [15]. In contrast to our finding they described a higher relative thrombus attenuation) in cardioembolism thrombi compared to large artery atherosclerosis. We measured the thrombus attenuation three times on 1 mm thin slices, therefore we do not think that our results are biased by measurement errors or partial volume effects.

The traditional assumption is that the so called "red clots" contain mainly a mixture of platelets and erythrocytes and originate from low flow regions, as would be expected in cardioembolism thrombi [29,13]. In contrast, white clots, containing mainly platelets and high amount of fibrin, were thought to arise in regions of fast moving blood, as in large artery atherosclerosis thrombi [29]. However, histopathology information about thrombi leading to cerebral stroke is limited and therefore interpretations have mainly been derived from coronary studies. Thrombi causing myocardial infarction are all thought to originate from a localised occlusion due to the atherosclerotic process. Although traditionally erythrocytes were thought to be of no importance in this process, more recently the role of erythrocytes in atherosclerosis has been described as major [30,31]. Several investigators have revealed that erythrocytes originating from intraplaque hemorrhage are not only a driving force in the progression of atherosclerosis [32,33] but also causes instability with rupture and re-hemorrhage in the ulcerated atherosclerotic plaques, promoting the transition from a stable to an unstable lesion causing coronary occlusions [32,34,35]. The role of erythrocytes in the pathogenesis of coronary artery disease was confirmed in carotid artery disease by a large pathological study performed on carotids plaques which confirmed that fresh plaque haemorrhage had occurred in all patients who suffered a recent cerebral stroke [36].

Concerning the composition of cardioembolic thrombi the only study [37] investigating the histopathology of cardioembolisms found the opposite to the assumption that cardioembolic thrombi are erythrocyte-rich. They concluded that all cardiac thrombi consisted mainly out of fibrin, platelets and debris. Furthermore, an important difference between cardiac in situ thrombus and embolized thrombi was found; embolized thrombi showed twice as much platelet-rich domains (40% of total) compared to non-embolized atrial thrombi (20%).

Dissections typically begin with a tear on the innermost intimal layer or the middle layer of the blood vessel wall. This allows blood to enter the vascular wall under arterial pressure, resulting in an acute intramural hematoma with

consequent luminal stenosis or thromboembolic event [38,39]. As this hematoma consists mostly out of erythrocytes, dissection thrombi are likely to have high amounts of erythrocytes.

To our knowledge only three histopathological studies (number of patients 5, 25 and 50 respectively) were performed on thrombi retrieved from cerebral arteries of patients having acute stroke [20,40,41]. The investigators showed no relation between stroke etiology and thrombus composition.

The three relative small histopathological studies on cerebral thrombi disprove the traditional assumption and the literature discussed above strengthens our speculated mechanism that cerebral thrombi originating from atherosclerosis are erythrocyte-rich and of high density while cerebral clots from cardioembolism are fibrin and platelets rich and will have low density on NCCT. However, large histopathological studies of cerebral thrombi are needed to validate this assumption.

Recanalization is associated with good clinical outcome [42,43] and thrombus composition influences the rate of recanalization [44-46]. In this context, stroke subtypes may represent a surrogate marker of clot composition and therefore might reflect differences in the response to rtPA in terms of recanalization [47]. Some investigators describe that cardioembolic thrombi are more likely to recanalize after treatment than large artery atherosclerosis thrombi [13,14] However, more recent or larger studies found either no relation between etiology and recanalization [47,48] or outcome [49] or even described a worse outcome in cardioembolic stroke compared to the other stroke subtypes [50] Therefore the relationship between the etiology of stroke and the rate of recanalization remains uncertain.

The success of IV- and IA-thrombolysis seems to be related more strongly to the HU-value of thrombi. Recent studies found that high HU-values can predict full recanalization after rtPA because erythrocyte rich thrombi are described to be more vulnerable to rtPA [15,18,46]. Moftakhar et al. found that the HU-values are not only related to rtPA vulnerability but also related to the success rate of mechanical thrombectomy. Our results show that presence of a hyperdense vessel sign and thrombus attenuation are both related to stroke subtype with cardioembolic thrombi having least hyperdense vessel signs and lowest attenuation, followed by large artery atherosclerosis and dissections. Therefore it seems plausible to assume that in our population the cardioembolic subtype will have a lower recanalization rate compared to large artery atherosclerosis. However, as the purpose of our study was to gain more insights in the etiopathogenesis of stroke, we did not investigate the recanalization rate and therefore we cannot conclude about the relationships between the recanalization rate and subtype of stroke or HU-values of thrombi in our population.

Although our study does not have histological confirmation of thrombus composition we did find significant differences in hyperdense vessel signs and thrombus attenuation in different stroke subtypes. Since the presence of hyperdense vessel sign and attenuation are related to the hemoglobin component our findings suggest that dissection subtype contains the highest

proportion of erythrocytes, followed by large artery atherosclerosis, and that cardioembolism contains the least proportion of erythrocytes. Based on previous recent articles and the findings in our current study the traditional etiopathogenetic assumption of red clots arising from cardiac origin and white clots forming from atherosclerotic arterial origin seems to be invalid. Future studies, combining thrombus attenuation and presence of hyperdense vessel sign on imaging with stroke subtype and histological investigation of thrombus composition may further elucidate the etiopathogenesis of thrombus composition.

This study has some aspects that merit consideration. First, it is not always possible to determine the cause of stroke with certainty, e.g. if atherosclerosis is present in combination with a possible cardiac cause such as atrial fibrillation. These patients were excluded from this study. The possibility of still having misclassified some of our included patients in different stroke subtypes would have biased our results towards less strong results, therefore overestimation of our findings could not have been introduced by misclassification. Second, we only investigated patients with the dissection subtype if the thrombus extended to intracranial level. Therefore, different results might be found in dissection patients with extracranial thrombus only.

In conclusion, our study shows that the presence of a hyperdense vessel sign and thrombus attenuation are both related to stroke subtype. Cardioembolic thrombi showed the least hyperdense vessel signs and the lowest attenuation, followed by thrombi due to large artery atherosclerosis while thrombi due to dissections nearly always showed a hyperdense vessel sign and had the highest thrombus attenuation.

REFERENCES

1. Carod-Artal FJ, Egido JA (2009) Quality of life after stroke: the importance of a good recovery. Cerebrovasc Dis 27 Suppl 1: 204-214.
2. Roger VL, Go AS, Lloyd-Jones DM, Benjamin EJ, Berry JD, Borden WB, Bravata DM, Dai S, Ford ES, Fox CS, Fullerton HJ, Gillespie C, Hailpern SM, Heit JA, Howard VJ, Kissela BM, Kittner SJ, Lackland DT, Lichtman JH, Lisabeth LD, Makuc DM, Marcus GM, Marelli A, Matchar DB, Moy CS, Mozaffarian D, Mussolino ME, Nichol G, Paynter NP, Soliman EZ, Sorlie PD, Sotoodehnia N, Turan TN, Virani SS, Wong ND, Woo D, Turner MB (2012) Heart disease and stroke statistics--2012 update: a report from the American Heart Association. Circulation 125: e2-e220.
3. Williams GR, Jiang JG, Matchar DB, Samsa GP (1999) Incidence and occurrence of total (first-ever and recurrent) stroke. Stroke 30: 2523-2528
4. Bejot Y, Caillier M, Ben Salem D, Couvreur G, Rouaud O, Osseby GV, Durier J, Marie C, Moreau T, Giroud M (2008) Ischaemic stroke subtypes and associated risk factors: a French population based study. Journal of neurology, neurosurgery, and psychiatry 79: 1344-1348.
5. Schulz UG, Rothwell PM (2003) Differences in vascular risk factors between etiological subtypes of ischemic stroke: importance of population-based studies. Stroke 34: 2050-2059.
6. Kolominsky-Rabas PL, Weber M, Gefeller O, Neundoerfer B, Heuschmann PU (2001) Epidemiology of ischemic stroke subtypes according to TOAST criteria: incidence, recurrence, and long-term survival in ischemic stroke subtypes: a population-based study. Stroke 32: 2735-2740
7. Putaala J, Metso AJ, Metso TM, Konkola N, Kraemer Y, Haapaniemi E, Kaste M, Tatlisumak T (2009) Analysis of 1008 consecutive patients aged 15 to 49 with first-ever ischemic stroke: the Helsinki young stroke registry. Stroke 40: 1195-1203.
8. Mazighi M, Serfaty JM, Labreuche J, Laissy JP, Meseguer E, Lavallee PC, Cabrejo L, Slaoui T, Guidoux C, Lapergue B, Klein IF, Olivot JM, Abboud H, Simon O, Niclot P, Nifle C, Touboul PJ, Raphaeli G, Gohin C, Claeys ES, Amarenco P (2009) Comparison of intravenous alteplase with a combined intravenous-endovascular approach in patients with stroke and confirmed arterial occlusion (RECANALISE study): a prospective cohort study. Lancet neurology 8: 802-809.
9. Caplan LR (2006) Antiplatelet therapy in stroke prevention: present and future. Cerebrovasc Dis 21 Suppl 1: 1-6.
10. Jang IK, Gold HK, Ziskind AA, Fallon JT, Holt RE, Leinbach RC, May JW, Collen D (1989) Differential sensitivity of erythrocyte-rich and platelet-rich arterial thrombi to lysis with recombinant tissue-type plasminogen activator. A possible explanation for resistance to coronary thrombolysis. Circulation 79: 920-928
11. Zivin JA, Fisher M, DeGirolami U, Hemenway CC, Stashak JA (1985) Tissue plasminogen activator reduces neurological damage after cerebral embolism. Science 230: 1289-1292
12. Niessen F, Hilger T, Hoehn M, Hossmann KA (2003) Differences in clot preparation determine outcome of recombinant tissue plasminogen activator treatment in experimental thromboembolic stroke. Stroke 34: 2019-2024.
13. Molina CA, Montaner J, Arenillas JF, Ribo M, Rubiera M, Alvarez-Sabin J (2004) Differential pattern of tissue plasminogen activator-induced proximal middle cerebral artery recanalization among stroke subtypes. Stroke 35: 486-490.
14. Cho KH, Lee DH, Kwon SU, Choi CG, Kim SJ, Suh DC, Kim JS, Kang DW (2012) Factors and outcomes associated with recanalization timing after thrombolysis. Cerebrovasc Dis 33: 255-261.
15. Puig J, Pedraza S, Demchuk A, Daunis IEJ, Termes H, Blasco G, Soria G, Boada I, Remollo S, Banos J, Serena J, Castellanos M (2012) Quantification of thrombus hounsfield units on noncontrast CT predicts stroke subtype and early recanalization after intravenous recombinant tissue plasminogen activator. AJNR Am J Neuroradiol 33: 90-96.
16. Wohner N (2008) Role of cellular elements in thrombus formation and dissolution. Cardiovascular & hematological agents in medicinal chemistry 6: 224-228
17. Kirchhof K, Welzel T, Mecke C, Zoubaa S, Sartor K (2003) Differentiation of white, mixed, and red thrombi: value of CT in estimation of the prognosis of thrombolysis phantom study. Radiology 228: 126-130
18. Kim EY, Heo JH, Lee SK, Kim DJ, Suh SH, Kim J, Kim DI (2006) Prediction of thrombolytic efficacy in acute ischemic stroke using thin-section noncontrast CT. Neurology 67: 1846-1848.
19. New PF, Aronow S (1976) Attenuation measurements of whole blood and blood fractions in computed tomography. Radiology 121: 635-640
20. Liebeskind DS, Sanossian N, Yong WH, Starkman S, Tsang MP, Moya AL, Zheng DD, Abolian AM, Kim D, Ali LK, Shah SH, Towfighi A, Ovbiagele B, Kidwell CS, Tateshima S, Jahan R, Duckwiler GR, Vinuela F, Salamon N, Villablanca JP, Vinters HV, Marder VJ, Saver JL (2011) CT and MRI early vessel signs reflect clot composition in acute stroke. Stroke 42: 1237-1243.
21. Adams HP, Jr., Bendixen BH, Kappelle LJ, Biller J, Love BB, Gordon DL, Marsh EE, 3rd (1993) Classification of subtype of acute ischemic stroke. Definitions for use in a multicenter clinical trial. TOAST. Trial of Org 10172 in Acute Stroke Treatment. Stroke 24: 35-41

22. Kim YK, Schulman S (2009) Cervical artery dissection: pathology, epidemiology and management. Thrombosis research 123: 810-821.

23. Chen CJ, Tseng YC, Lee TH, Hsu HL, See LC (2004) Multisection CT angiography compared with catheter angiography in diagnosing vertebral artery dissection. AJNR Am J Neuroradiol 25: 769-774

24. Leys D, Pruvo JP, Godefroy O, Rondepierre P, Leclerc X (1992) Prevalence and significance of hyperdense middle cerebral artery in acute stroke. Stroke 23: 317-324

25. Rauch RA, Bazan C, 3rd, Larsson EM, Jinkins JR (1993) Hyperdense middle cerebral arteries identified on CT as a false sign of vascular occlusion. AJNR Am J Neuroradiol 14: 669-673

26. Barber PA, Demchuk AM, Hudon ME, Pexman JH, Hill MD, Buchan AM (2001) Hyperdense sylvian fissure MCA "dot" sign: A CT marker of acute ischemia. Stroke 32: 84-88

27. Bastianello S, Pierallini A, Colonnese C, Brughitta G, Angeloni U, Antonelli M, Fantozzi LM, Fieschi C, Bozzao L (1991) Hyperdense middle cerebral artery CT sign. Comparison with angiography in the acute phase of ischemic supratentorial infarction. Neuroradiology 33: 207-211

28. Moulin T, Tatu L, Vuillier F, Cattin F (1999) [Brain CT scan for acute cerebral infarction: early signs of ischemia]. Revue neurologique 155: 649-655

29. Chaves CJ, Caplan LR (2000) Heparin and oral anticoagulants in the treatment of brain ischemia. Journal of the neurological sciences 173: 3-9

30. Vila A, Korytowski W, Girotti AW (2002) Spontaneous transfer of phospholipid and cholesterol hydroperoxides between cell membranes and low-density lipoprotein: assessment of reaction kinetics and prooxidant effects. Biochemistry 41: 13705-13716

31. Kockx MM, Cromheeke KM, Knaapen MW, Bosmans JM, De Meyer GR, Herman AG, Bult H (2003) Phagocytosis and macrophage activation associated with hemorrhagic microvessels in human atherosclerosis. Arteriosclerosis, thrombosis, and vascular biology 23: 440-446.

32. Kolodgie FD, Gold HK, Burke AP, Fowler DR, Kruth HS, Weber DK, Farb A, Guerrero LJ, Hayase M, Kutys R, Narula J, Finn AV, Virmani R (2003) Intraplaque hemorrhage and progression of coronary atheroma. The New England journal of medicine 349: 2316-2325.

33. Takaya N, Yuan C, Chu B, Saam T, Polissar NL, Jarvik GP, Isaac C, McDonough J, Natiello C, Small R, Ferguson MS, Hatsukami TS (2005) Presence of intraplaque hemorrhage stimulates progression of carotid atherosclerotic plaques: a high-resolution magnetic resonance imaging study. Circulation 111: 2768-2775.

34. Rao DS, Goldin JG, Fishbein MC (2005) Determinants of plaque instability in atherosclerotic vascular disease. Cardiovascular pathology : the official journal of the Society for Cardiovascular Pathology 14: 285-293.

35. Virmani R, Kolodgie FD, Burke AP, Finn AV, Gold HK, Tulenko TN, Wrenn SP, Narula J (2005) Atherosclerotic plaque progression and vulnerability to rupture: angiogenesis as a source of intraplaque hemorrhage. Arteriosclerosis, thrombosis, and vascular biology 25: 2054-2061.

36. Redgrave JN, Lovett JK, Gallagher PJ, Rothwell PM (2006) Histological assessment of 526 symptomatic carotid plaques in relation to the nature and timing of ischemic symptoms: the Oxford plaque study. Circulation 113: 2320-2328.

37. Wysokinski WE, Owen WG, Fass DN, Patrzalek DD, Murphy L, McBane RD, 2nd (2004) Atrial fibrillation and thrombosis: immunohistochemical differences between in situ and embolized thrombi. Journal of thrombosis and haemostasis. JTH 2: 1637-1644.

38. Mohan IV (2013) Current Optimal Assessment and Management of Carotid and Vertebral Spontaneous and Traumatic Dissection. Angiology. doi:10.1177/0003319712475154

39. Stevic I, Chan HH, Chan AK (2011) Carotid artery dissections: thrombosis of the false lumen. Thrombosis research 128: 317-324.

40. Marder VJ, Chute DJ, Starkman S, Abolian AM, Kidwell C, Liebeskind D, Ovbiagele B, Vinuela F, Duckwiler G, Jahan R, Vespa PM, Selco S, Rajajee V, Kim D, Sanossian N, Saver JL (2006) Analysis of thrombi retrieved from cerebral arteries of patients with acute ischemic stroke. Stroke 37: 2086-2093.

41. Almekhlafi MA, Hu WY, Hill MD, Auer RN (2008) Calcification and endothelialization of thrombi in acute stroke. Ann Neurol 64: 344-348.

42. Bhatia R, Hill MD, Shobha N, Menon B, Bal S, Kochar P, Watson T, Goyal M, Demchuk AM (2010) Low rates of acute recanalization with intravenous recombinant tissue plasminogen activator in ischemic stroke: real-world experience and a call for action. Stroke 41: 2254-2258.

43. Khatri P, Abruzzo T, Yeatts SD, Nichols C, Broderick JP, Tomsick TA (2009) Good clinical outcome after ischemic stroke with successful revascularization is time-dependent. Neurology 73:1066-1072.

44. Wu JH, Siddiqui K, Diamond SL (1994) Transport phenomena and clot dissolving therapy: an experimental investigation of diffusion-controlled and permeation-enhanced fibrinolysis. Thrombosis and haemostasis 72: 105-112

45. Blinc A, Keber D, Lahajnar G, Stegnar M, Zidansek A, Demsar F (1992) Lysing patterns of retracted blood clots with diffusion or bulk flow transport of plasma with urokinase into clots--a magnetic resonance imaging study in vitro. Thrombosis and haemostasis 68: 667-671

46. Moftakhar P, English JD, Cooke DL, Kim WT, Stout C, Smith WS, Dowd CF, Higashida RT, Halbach VV, Hetts SW (2013) Density of Thrombus on Admission CT Predicts Revascularization Efficacy in Large Vessel Occlusion Acute Ischemic Stroke. Stroke 44: 243-245.

47. Rocha S, Pires A, Gomes J, Rocha J, Sousa F, Pinho J, Rodrigues M, Ferreira C, Machado A, Mare R, Fontes JR (2011) Intravenous thrombolysis is more effective in ischemic cardioembolic strokes than in non-cardioembolic? Arquivos de neuro-psiquiatria 69: 905-909

48. Hsia AW, Sachdev HS, Tomlinson J, Hamilton SA, Tong DC (2003) Efficacy of IV tissue plasminogen activator in acute stroke: does stroke subtype really matter? Neurology 61: 71-75

49. Mustanoja S, Meretoja A, Putaala J, Viitanen V, Curtze S, Atula S, Artto V, Happola O, Kaste M (2011) Outcome by stroke etiology in patients receiving thrombolytic treatment: descriptive subtype analysis. Stroke 42: 102-106.

50. Grau AJ, Weimar C, Buggle F, Heinrich A, Goertler M, Neumaier S, Glahn J, Brandt T, Hacke W, Diener HC (2001) Risk factors, outcome, and treatment in subtypes of ischemic stroke: the German stroke data bank. Stroke 32: 2559-2566

Histopathologic composition of cerebral thrombi of acute stroke patients is correlated with stroke subtype and thrombus attenuation

JM Niesten, IC van der Schaaf, L van Dam, A Vink, JA Vos, WJ Schonewille, PC de Bruin, WPTM Mali, BK Velthuis

Plos One, 2014

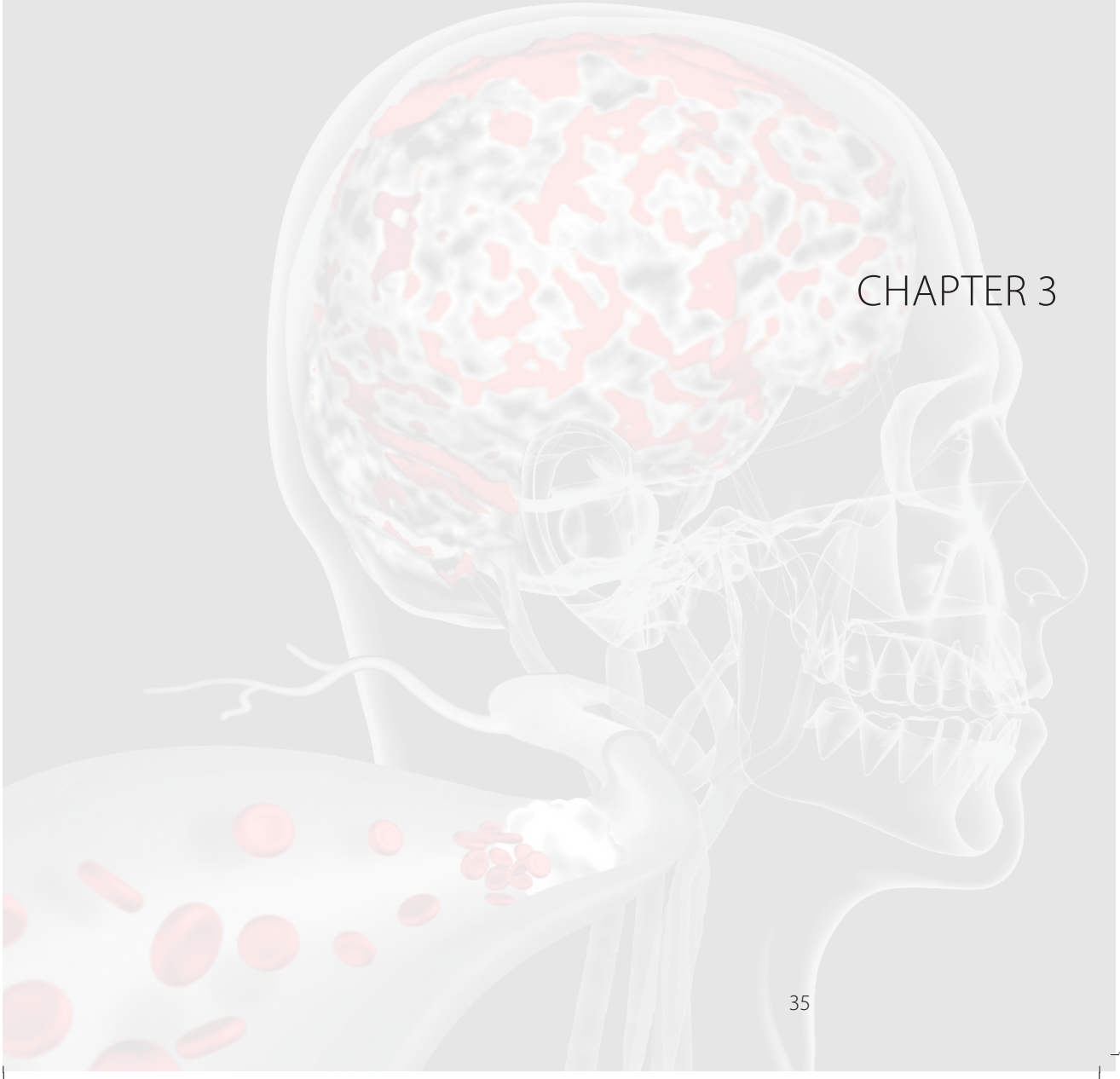

CHAPTER 3

ABSTRACT

Introduction

We related composition of cerebral thrombi to stroke subtype and attenuation on non-contrast CT (NCCT) to gain more insight in etiopathogenesis and to validate thrombus attenuation as a new imaging biomarker for acute stroke.

Methods

We histopathologically investigated 22 thrombi retrieved after mechanical thrombectomy in acute stroke patients. First, thrombi were classified as fresh, lytic or organized. Second, percentages of red blood cells (RBCs), platelets and fibrin and number of red, white (respectively RBCs or platelets outnumbering other components with ≥15%) or mixed thrombi were compared between large artery atherosclerosis (LAA), cardioembolism, dissection and unknown subtype. Third, correlation between attenuation and RBCs, platelets and fibrin was calculated using Pearson's correlation coefficients (*r*).

Results

Thrombi were fresh in 73% (n=16), lytic in 18% (n=4) and organized in 9% (n=2)**.** The stroke cause was LAA in eight (36%), cardioembolism in six (27%), dissection in three (14%), and unknown in five (23%) patients.

LAA thrombi showed the highest percentage RBCs (median 50 (range 35-90)), followed by dissection (35 (20-40), p=0.05), cardioembolism (35 (5-45), p=0.013) and unknown subtype (25 (2-40), p=0.006). No differences in platelets (p=0.16) and fibrin (p=0.52) between subtypes were found.

LAA thrombi were classified as red or mixed (both n=4), cardioembolisms as mixed (n=5) or white (n=1) and dissection as mixed (n=3).

There was a moderate positive correlation between attenuation and RBCs (r=0.401, p=0.049), and weak negative correlations with platelets (r=-0.368, p=0.09) and fibrin (r=-0.073, p=0.75).

Conclusions

The majority of cerebral thrombi is fresh. There are no differences in age of thrombi between subtypes. LAA thrombi have highest percentages RBCs, cardioembolism and unknown subtype lowest. No relationship exists between subtype and platelets or fibrin percentages. We found a correlation between the RBC-component and thrombus attenuation, which improves validation of thrombus attenuation on NCCT as an imaging biomarker for stroke management.

INTRODUCTION

Thromboembolism is the cause of ischemic stroke in the majority of acute stroke patients [1]. These thrombi originate mainly from large artery atherosclerosis (LAA) and cardioembolisms, and more infrequently from dissection [2-4] .
The use of mechanical thrombectomy devices allows retrieval of cerebral thrombi from the intracranial vessels and subsequent histopathologic analysis. The first histopathologic studies showed that the architecture of cerebral thrombi is variable with different main components such as fibrin, red blood cells (RBC) and platelets [5-7]. The composition of thrombi may influence the efficacy of thrombolysis with recombinant tissue plasminogen activator (rtPA) since RBC-rich or red thrombi are described to be more vulnerable for current thrombolysis compared to platelet-rich or white thrombi [8-10].
Furthermore, the age of thrombi could also play a role in success rate of thrombolysis, which is only about 50% with current IV-rtPA therapy. Recanalization depends on the time from stroke onset to intravenous (IV) rtPA-treatment, hence it may be more effective in fresh than old thrombi [11].
On non-contrast CT (NCCT) platelet-rich thrombi have lower attenuation than RBC-rich thrombi since the attenuation has a linear correlation with the concentration of hemoglobin [9, 12-14]. Recent studies found that the attenuation is also related to stroke subtype [15, 16] and could be helpful in predicting the rate of recanalization after rtPA [17, 18].
Improved knowledge about thrombus age and composition and its relation with stroke subtypes and attenuation could help to gain more insight in the etiopathogenesis of stroke. The aims of this study were to relate the age and histopathologic composition of thrombi to the stroke subtype and to thrombus attenuation on NCCT.

METHODS

Patient population

We histopathologically investigated thrombi retrieved after mechanical thrombectomy of acute stroke patients admitted to the University Medical Center Utrecht or the St. Antonius Hospital Nieuwegein, between December 2010 and April 2013. Inclusion criteria were: age ≥ 18 years, National Institutes of Health Stroke Scale (NIHSS) ≥ 2, acute stroke patients with an intracranial thrombus on CT-Angiography (CTA) eligible for thrombectomy, retrieval of thrombus material available for histopathologic analysis. Exclusion criteria were the collection of thrombus material that was unsuitable for histopathologic analyses and a poor quality NCCT that was unsuitable for thrombus density measurements.
The following baseline data were collected: demographic features, cardiovascular risk factors (hypertension, diabetes mellitus, smoking), NIHSS on admission, location of the thrombus, and onset time to CT-imaging, to IV-rtPA treatment and thrombus retrieval.

LAA was defined as imaging findings of either significant (>50%) stenosis or occlusion of a major cervical (carotid or vertebral) artery or intracranial artery on CTA ipsilateral to the symptomatic hemisphere, presumed to be due to atherosclerosis according to the Trial of Org 10172 in Acute Stroke Treatment (TOAST) criteria [19] if other diagnostic studies had excluded potential sources of cardiac embolism. Cardioembolism was defined as at least one cardiac source for an embolus identified in the absence of significant ipsilateral stenosis (>50%) of ipsilateral large extracrianal arteries or atherosclerosis. Criteria for diagnosing dissection as the cause of stroke were a narrowed eccentric lumen surrounded by crescent-shaped mural thickening or tapered occlusion with associated increase in external vessel diameter on CTA [20, 21].

Ethics statement

The medical ethics committee of the University Medical Center Utrecht approved the study. If patients had the capacity to consent, written informed consent was obtained from themselves. If this was not the case, written informed consent was obtained from their nearest relative(s).

Treatment prior to thrombectomy

Based on clinical and imaging information IV-rtPA was administered to patients when considered eligible by a team of experienced neuroradiologists and neurologists. If IV-rtPA failed or could not be administrated due to contra-indications, the administration of intra-arterial (IA) rtPA followed by thrombectomy or thrombectomy alone was done, in all cases under systemic heparin. The heparin was given IV at a dose of 2500 IU.

Thrombectomy Procedure

Informed consent was obtained prior to the procedure. Mechanical thrombectomy was performed in accordance with local guidelines. All patients had heparin administered during the percutaneous intervention. The occlusion was reached using a guiding catheter through the femoral artery. The thrombus was removed by a Merci retriever, a Trevo retriever or a Solitair stent and thrombus material was collected in a formalin equipped bottle.

Histopathologic Procedure

Specimens were embedded in paraffin and 4 consecutive 5-µm thick slices were cut. All thrombi were stained with hamatoxylin and eosin, Mallory's phosphotungstic acid-hematoxilin (identifying fibrin), glycophorin A (identifying RBCs) and CD31 (identifying platelets) immunostains.

Subsequently, thrombi were histopathologic analysed by an experienced vascular pathologist (A.V.) together with two other investigators (J.N. and L.v.D.) on all 4 slices. Histological analysis was conducted in a blinded fashion without any knowledge of patient and stroke characteristics. First, all thrombi were classified as fresh (<1 day), lytic (1-5 days) or organized (>5 days), based on previously published definitions of thrombus age [22]. Thrombi were classified

according to the age of the largest part of the thrombus. Second, percentages of RBCs, platelets and fibrin were quantitatively determined in consensus. Subsequently, thrombi were classified as red if RBCs outnumbered platelets and fibrin by at least 15% and as white if platelets outnumbered RBCs and fibrin with at least 15% difference. If this was not the case, thrombi were classified as mixed. Furthermore, we also investigated the presence of other components (white blood cells, atheromatous material, calcification) in the thrombi.

Scan protocol and attenuation measurements

All imaging studies were performed using 64- or 256-slice MDCT–scanner (Philips, Philips Healthcare, Best, the Netherlands). CT parameters of the NCCT were: 120 kVp, 300 mAs, and 3-mm reconstructed slice thickness. For the CTA 65-70 ml of contrast agent (300mg Iopromide/mL) was injected into the antecubital vein (18-gauge needle) at a rate of 6 mL/s followed by a 40-mL saline flush at the same rate.

The attenuation of the thrombus was measured on 3-mm NCCT in Hounsfield Units (HU) by two independent observers, both blinded for any data except localization of the thrombus on CTA. Within the thrombus a standardised small round region of interest was drawn three separate times and mean HU-values were used for analysis. The same measurements were performed in the corresponding contralateral vessel and by calculating the relative HU (HU thrombus / HU contralateral) we corrected for hematocrit. If the thrombus was situated in the basilar artery, a more proximal non-thrombosed portion of the basilar artery was used for the control measurements. If the proximal end was not open, the supraclinoid ICA was used (n=3).

Statistical Analyses

Baseline characteristics were summarised as means (with standard deviation (SD)), medians (with range) or frequency counts and proportions.

First, the percentages of RBCs, platelets and fibrin were compared between the subtypes of stroke by the Kruskal-Wallis test. Significant group differences were further analysed by the Mann-Whitney U test to determine individual differences.

Intraclass correlation coefficients (ICCs) were used to evaluate the interobserver variation in HU-measurements of the thrombus. We considered ICC values <0.20 as poor, 0.21-0.40 as fair, 0.41-0.60 as moderate, 0.61-0.80 as good, and 0.81-1.00 as excellent. The correlation between attenuation and percentages of RBCs, platelets and fibrin was calculated using Pearson's correlation with a coefficient (*r*) of 0.90–1 as very strong; 0.70–0.89 as strong; 0.40–0.69 as moderate; 0.20–0.39 as weak and 0.01–0.19 as a negligible relationship. Statistical analysis was performed using SPSS (version 20.0, SPSS Inc., Chicago). Results were considered statistically significant if P-values were <0.05.

RESULTS

A total of 22 thrombi were retrieved from 22 patients with an average age of 60 years (± 13) and 50% female *(Table 1)*. No patients had to be excluded. The median time from onset to thrombus retrieval of was 287 minutes (125-455). The mean NIHSS was 14, with a minimum of 5 and a maximum of 35. In 17 patients (77%) IV-rtPA was administrated with a median time of 88 minutes from onset. Only 2 patients (9%) were on chronic anticoagulation medication and 3 patients (14%) received IA-rtPA prior to mechanical thrombectomy. The cause of stroke was classified as LAA in eight (36%), cardioembolism in six (27%), dissection in three (14%), and as unknown in five (23%) patients.

Table 1 *Patient characteristics*

Age in years, mean (±SD)	60 (± 13)
Sex (female), n (%)	11 (50)
Subtype, n (%)	
Large artery atherosclerosis	8 (36)
Cardioembolism	6 (27)
Dissection	3 (14)
Unknown	5 (23)
Cardiovascular risk factors, n (%)	
Current smoking	10 (45)
Hypertension	9 (41)
Diabetes Mellitus	1 (5)
Chronic anti-coagulation use, n (%)	2, (9)
Baseline NIHSS, median (range)	14 (5-35)
Intravenous thrombolysis (rtPA), n (%)	17 (77)
Intra-arterial thrombolysis (rtPA), n (%)	3 (14)
Location thrombus, n (%)	
Middle Cerebral Artery	14 (64)
Basilar Artery	7 (32)
Internal Carotid Artery	1 (5)
Onset time to CT in minutes, median (range)	107 (20-386)
Onset time to retrieval in minutes, median (range)	287 (125-455)
Onset time to IV-rtPA in minutes, median (range)*	88 (35-290)

* based on 17 patients received IV-rtPA. SD: standard deviation, NIHSS: National Institutes of Health Stroke Scale, rtPA: recombinant tissue plasminogen activator, CT: Computed Tomography

Thrombi were fresh in 73% (n=16), as lytic in 18% (n=4) and as organized in 9% (n=2). No significant differences were found in the age of thrombi between the different subtypes (p=0.54). All lytic and organized thrombi also revealed a component of the thrombus that was fresh. All thrombi that were fresh did not have any organized parts and only a very few fresh thrombi showed minimal lytic parts.

The median (range) percentages of components across all thrombi were 40% (2-90%) RBCs, 40% (5-80%) platelets, and 20% (5-65%) fibrin *(Figure 1)*.

Figure 1 *Histopathologic composition of all thrombi*

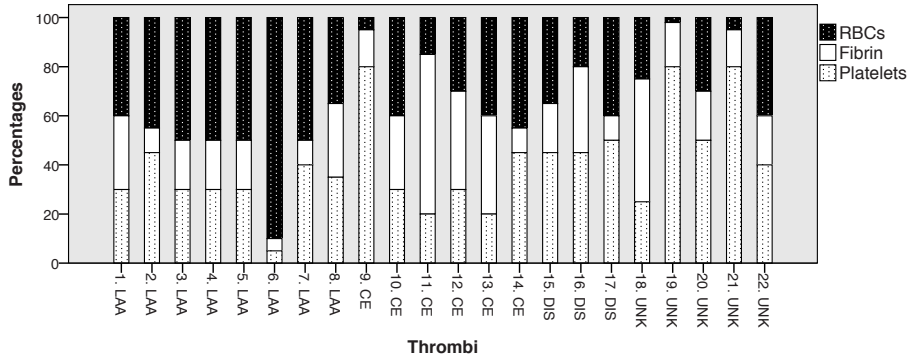

RBC: Red blood cell

The median percentages of RBCs differed significantly between the different stroke subtypes as a group (p=0.010) while there were no significant differences in the median percentages of platelets (p=0.16) and fibrin (p=0.52) between the different subtypes *(table 2 and figure 2)*.

Table 2 *Thrombus components: relation with stroke subtypes and correlation with attenuation on non-contrast CT*

Component		Stroke subtype					Correlation with attenuation	
		LAA	*CE*	*DIS*	*UNK*	*P-value*		
RBC	*mean (range)*	50% (35-90%)	35% (5-45%)	35% (20-40%)	25% (2-40%)	0.010	*r (p-value)*	0.401 (0.049)
Platelets	*mean (range)*	30% (5-45%)	30% (20-80%)	45% (45-50%)	50% (25-80%)	0.16	*r (p-value)*	-0.368 (0.09)
Fibrin	*mean (range)*	20% (5-30%)	35% (10-65%)	20% (10-35%)	20% (15-50)	0.52	*r (p-value)*	-0.073 (0.75)

LAA: large artery atherosclerosis, CE: cardioembolism, DIS: dissection, UNK: unknown, RBC: Red blood cell

Comparing the individual stroke subtypes; thrombi originating from LAA showed the highest percentage of RBCs (median 50% (35-90%)), which was not significantly different from the dissection subtype (median 35% (20-40%), p=0.05) but was significantly higher than thrombi from cardioembolisms (median 35% (5-45%), p=0.013) and unknown subtype (median 25% (2-40%), p=0.006). The median percentages of RBCs in thrombi from dissection and cardioembolisms (p=0.82), dissection and unknown subtype (p=0.33) and cardioembolism and unknown (p=0.39) were comparable *(Figure 2)*. White blood cells were present in most thrombi but in very small amounts only, in one thrombus a small volume of atheromatous material was seen and calcification was not visible in any thrombus.

Figure 2 *Boxplots of percentage red blood cells, platelets and fibrin of thrombi by subtype of stroke*

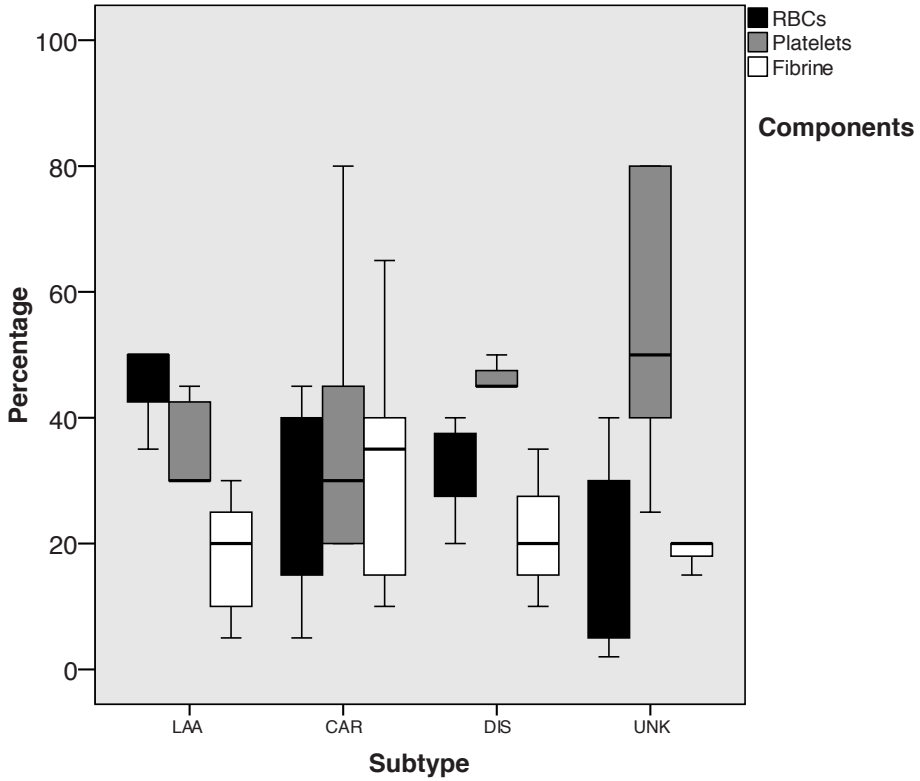

LAA: large artery atherosclerosis, CE: cardioembolism, DIS: dissection, UNK: unknown, RBC: Red blood cell

Thrombi were defined as red (RBC-rich) in 4 (18%), as white (platelet-rich) in 4 (18%) and as mixed in 14 (64%) cases *(figure 3)*. Thrombi from LAA were classified as red in half of the cases (n=4) and as mixed in the other half. Cardioembolic thrombi were defined 5 times (83%) as mixed and once as white (17%). All 3 dissection thrombi were classified as mixed, while the unknown subtype contained 3 white (60%) and 2 mixed thrombi (40%). No white thrombi were found in LAA and none of the cardioembolic, dissection, or unknown subtype thrombi were classified as red. Thrombi in patients with LAA had a significantly higher proportion of red thrombi than in cardioembolisms ($p=0.04$), and significantly less white thrombi than the unknown subtype ($p=0.012$) while differences between all other subtypes in number of red and white thrombi were insignificant ($p>0.06$).

Figure 3 *The number of red, white and mixed thrombi by subtypes*

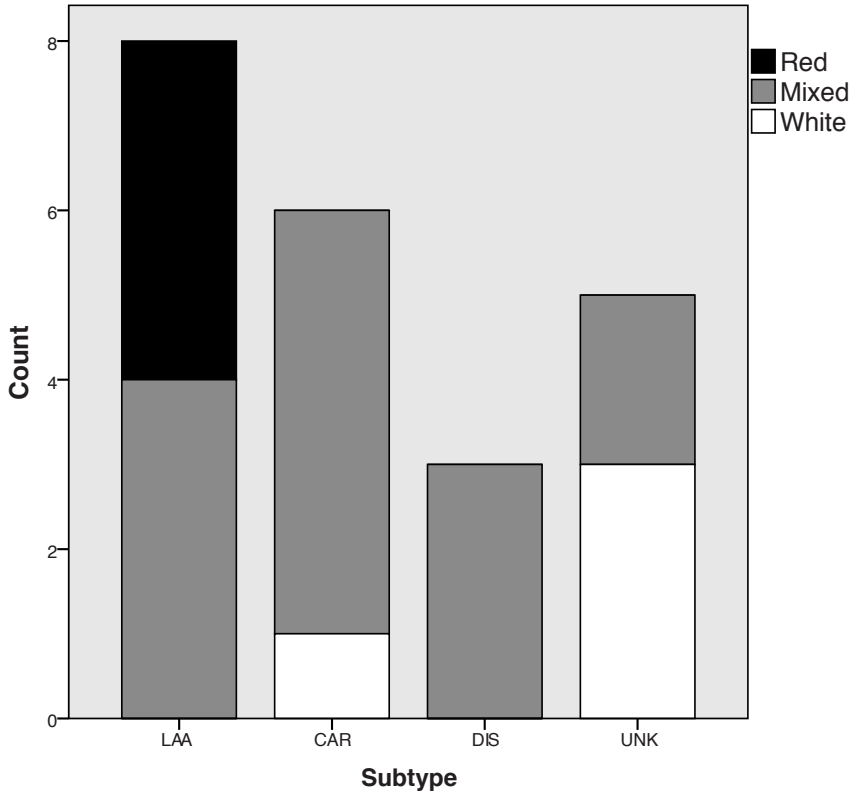

LAA: large artery atherosclerosis, CAR: cardioembolism, DIS: dissection, UNK: unknown.

The interobserver reliability for the HU-measurements was excellent (ICC=0.98). There was a moderate linear correlation between the attenuation and percentage of RBCs (r=0.401, p=0.049), a weak negative linear correlation between attenuation and platelets (r=-0.368, p=0.09) and a negligible negative linear correlation for fibrin (r=-0.073 p=0.75, *table 2*).

DISCUSSION

We found that most cerebral thrombi were fresh and that thrombi originating from LAA had the highest percentage of RBCs and were the only stroke subtype with red thrombi. There was a moderate correlation between the percentage of RBCs and the attenuation on NCCT.

Traditional teaching emphasizes that fresh red thrombi, containing mixtures of fibrin and RBCs, originate from low flow-regions while white thrombi, existing mainly out of platelets and fibrin, arise in regions of fast moving blood [23, 24]. In cerebral stroke, thrombi from LAA are thought to originate from regions of fast moving blood, while most cardioembolic thrombi are assumed

to develop from low flow-regions, such as the left atrial appendage. However, histopathology examination of cerebral stroke thrombi is limited and interpretations about the pathophysiology of cerebral thrombi have mainly been derived from coronary circulation studies.

Thrombi causing myocardial infarction originate from a local coronary artery occlusion due to the atherosclerotic process. In this process RBCs were formerly described to be of little importance [25]. However, more recently the influence of RBCs in coronary atherosclerosis has been described as major, especially in the transition from a stable to an unstable lesion causing occlusions [26-29]. It is therefore more likely that thrombi originating from (unstable) atherosclerotic plaques have a high RBC-component, especially in cerebral thrombi where the majority of atherosclerotic thrombi are due to acute thromboembolic events immediately after intraplaque hemorrhage [30-32].

In regard to the composition of cardioembolic thrombi, only one study investigated the histopathology of in vivo derived cardioembolic thrombi from patients with atrial fibrillation by either extraction from atrial thrombi during cardiac valve surgery (11 patients) or by removal of embolized cardioembolic thrombi from ilio-femoral and subclavian-brachial arteries during vascular surgery (11 patients) [33]. They found that all cardiac thrombi consisted mainly out of fibrin, platelets and debris. Furthermore, an important difference between cardiac in situ thrombus and embolized thrombi was found; embolized thrombi showed twice as much platelet-rich domains (40% of total) compared to non-embolized atrial thrombus material (20%).

Our findings are not in line with the traditional assumption. We observed that thrombus from LAA contain the highest amount of RBCs and that all red thrombi originate from LAA and none from cardioembolisms.

Our findings are, however, to a great extent in line with the previous histopathologic studies investigating cerebral thrombi, which also found that the traditional assumption is not valid for stroke patients. To our knowledge only three histopathologic studies were performed on thrombi retrieved from cerebral arteries of patients having acute stroke [5-7]. The first two studies, performing histological analyses of thrombi retrieved from intracranial vessels in respectively 5 and 25 patients with ischemic stroke, showed no relation between thrombus composition and stroke subtype [6, 7]. These investigators found similar cell components of thrombi derived from either arterial or cardiac sources and also demonstrated that atherosclerotic thrombi contain significant amounts of RBCs. The most recent histopathologic study measured the percentages RBCs, white blood cells and fibrin in 50 patients and related thrombus composition to stroke subtype [5]. They found a broad histopathologic distribution of thrombus composition, although white blood cells were consistently marginal and platelets were not investigated. They also mentioned that no relation between thrombus histopathology and stroke subtype was found. However, any other details about this relationship were not provided. In our study results we do not report percentages of white blood cells or other thrombus components because they were not or only in small amounts present.

Other than only one brief report on a thrombus from a single patient with a dissection, in which the histological examination was described as "serpentine" (fibrin:platelet bands interspersed with accumulations of nucleated cells and RBC-rich accumulations) [6], there are no studies available about the histology of strokes caused by dissection.

To our knowledge this is the first study investigating the age of thrombi in acute cerebral stroke patients. While the traditional assumption emphasizes that fresh thrombi originate mainly from cardioembolisms, we found no differences in age of thrombi between the stroke subtypes. Furthermore, we found a higher percentage of fresh thrombi compared to studies of myocardial infarction patients, in which at least half of the cardiac thrombi were days or weeks old [22]. This discrepancy increases the thought that the pathogenesis of cardiac and cerebral thrombi may be different. We also found that all lytic and organised thrombi also contained a component that was fresh (less than one day old). Fresh thrombus may occur around the local plaque rupture or an organised thrombus can embolize to the brain, incompletely occlude a brain artery, and then acquire fresh thrombus elements which may ultimately lead to complete vessel thrombosis.

As mentioned, thrombus attenuation could be related to the constituents and composition of the thrombus. The concentration of hemoglobin is one of the determining factors as it has a linear correlation with the attenuation while platelets and atheromatous or cellular debris are known to decrease the attenuation of the thrombus on CT [9, 12-14, 34-36]. Studies on this topic, however, are experimental, animal studies, or investigations of the venous sinus thrombus. Other than a recent histopathological study briefly mentioning that they did not find a significant relation between attenuation and composition [5], little is know about the relation between the attenuation of thrombi on NCCT and the histological composition of retrieved cerebral thrombi. We are the first study describing a correlation between the histopathological RBC-component of thrombi and the attenuation on NCCT. This correlation could be stronger in reality as attenuation was measured before IV-rtPA administration while most thrombi were histopathologically investigated after thrombolysis which could have influenced thrombus composition. As RBCs are more vulnerable for rtPA compared to platelets it is likely that the especially RBCs were influenced before histopathological examination.

There are some aspects that merit consideration. First, only a relative small number of thrombi were investigated, consequently making it hard to draw strong conclusions. Second, no clear definition of "red" and "white" thrombi exists which is probably due to the fact that just a few studies have pathologically assessed cerebral thrombi in vivo. Most histopathologic studies based the division in red or white thrombi on "macroscopic evaluation" without any thresholds [5,6,37-40]. To increase the objectivity and reproducibility, we introduced a cut-off value to distinguish between red and white thrombi. Third, the majority of the histopathologically investigated thrombi were resistant to IV-rtPA and we could not investigate thrombi with successful recanalization on IV-rtPA, This may bias the percentage of thrombus composition but not the cor-

relation between histopathology and thrombus attenuation. Fourth, besides the administration of IV-rtPA, the mechanism and timing of the procedures also varied and could have influenced the thrombus composition. Therefore we cannot assess the predictive value of thrombus composition, but this was not the purpose of the study. Fifth, attenuation measurement were performed on 3-mm slices, the thinnest slices available for evaluation. Partial volume effects may have influenced our attenuation results since some thrombi could be smaller than 3 mm or not completely included in one slice. However, this would have probably only led to less differences between subtypes and thus resulting in an underestimation of the results.Due to these considerations larger histopathologic studies of prospectively collected cerebral thrombi are needed to validate our findings. Ideally, the attenuation measurements will be performed on thin slices and the predictive value of clot composition for recanalization after treatment will be determined.

CONCLUSIONS

In our study with relatively small numbers important findings were seen: we found that the majority of cerebral thrombi is fresh and that there are no differences in age of thrombi between the stroke subtypes. Thrombi originating from large artery atherosclerosis have the highest percentages of red blood cells followed by thrombi due to dissection, while cardioembolic and unknown stroke subtype thrombi have the least red blood cells. A moderate correlation was found between the red blood cell-component and attenuation on non-contrast CT, improving the validation of thrombus attenuation on non-contrast CT as an imaging biomarker for acute ischemic stroke management. These findings will have to be validated in a larger study.

REFERENCES

1. Williams GR, Jiang JG, Matchar DB, Samsa GP. Incidence and occurrence of total (first-ever and recurrent) stroke. *Stroke*. 1999;30:2523-2528
2. Kolominsky-Rabas PL, Weber M, Gefeller O, Neundoerfer B, Heuschmann PU. Epidemiology of ischemic stroke subtypes according to toast criteria: Incidence, recurrence, and long-term survival in ischemic stroke subtypes: A population-based study. *Stroke*. 2001;32:2735-2740
3. Bejot Y, Caillier M, Ben Salem D, Couvreur G, Rouaud O, Osseby GV, Durier J, Marie C, Moreau T, Giroud M. Ischaemic stroke subtypes and associated risk factors: A french population based study. *Journal of neurology, neurosurgery, and psychiatry*. 2008;79:1344-1348
4. Schulz UG, Rothwell PM. Differences in vascular risk factors between etiological subtypes of ischemic stroke: Importance of population-based studies. *Stroke*. 2003;34:2050-2059
5. Liebeskind DS, Sanossian N, Yong WH, Starkman S, Tsang MP, Moya AL, Zheng DD, Abolian AM, Kim D, Ali LK, Shah SH, Towfighi A, Ovbiagele B, Kidwell CS, Tateshima S, Jahan R, Duckwiler GR, Vinuela F, Salamon N, Villablanca JP, Vinters HV, Marder VJ, Saver JL. Ct and mri early vessel signs reflect clot composition in acute stroke. *Stroke*. 2011;42:1237-1243
6. Marder VJ, Chute DJ, Starkman S, Abolian AM, Kidwell C, Liebeskind D, Ovbiagele B, Vinuela F, Duckwiler G, Jahan R, Vespa PM, Selco S, Rajajee V, Kim D, Sanossian N, Saver JL. Analysis of thrombi retrieved from cerebral arteries of patients with acute ischemic stroke. *Stroke*. 2006;37:2086-2093
7. Almekhlafi MA, Hu WY, Hill MD, Auer RN. Calcification and endothelialization of thrombi in acute stroke. *Ann Neurol*. 2008;64:344-348
8. Niessen F, Hilger T, Hoehn M, Hossmann KA. Differences in clot preparation determine outcome of recombinant tissue plasminogen activator treatment in experimental thromboembolic stroke. *Stroke*. 2003;34:2019-2024
9. Kirchhof K, Welzel T, Mecke C, Zoubaa S, Sartor K. Differentiation of white, mixed, and red thrombi: Value of ct in estimation of the prognosis of thrombolysis phantom study. *Radiology*. 2003;228:126-130
10. Zivin JA, Fisher M, DeGirolami U, Hemenway CC, Stashak JA. Tissue plasminogen activator reduces neurological damage after cerebral embolism. *Science*. 1985;230:1289-1292
11. Kimura K, Iguchi Y, Shibazaki K, Aoki J, Watanabe M, Matsumoto N, Yamashita S. Early stroke treatment with iv t-pa associated with early recanalization. *Journal of the neurological sciences*. 2010;295:53-57
12. New PF, Aronow S. Attenuation measurements of whole blood and blood fractions in computed tomography. *Radiology*. 1976;121:635-640
13. Lee SY, Cha SH, Lee SH, Shin DI. Evaluation of the effect of hemoglobin or hematocrit level on dural sinus density using unenhanced computed tomography. *Yonsei medical journal*. 2013;54:28-33
14. Black DF, Rad AE, Gray LA, Campeau NG, Kallmes DF. Cerebral venous sinus density on noncontrast ct correlates with hematocrit. *AJNR Am J Neuroradiol*. 2011;32:1354-1357
15. Niesten JM, van der Schaaf IC, Biessels GJ, van Otterloo AE, van Seeters T, Horsch AD, Luitse MJ, van der Graaf Y, Kappelle LJ, Mali WP, Velthuis BK. Relationship between thrombus attenuation and different stroke subtypes. *Neuroradiology*. 2013;55:1071-1079
16. Puig J, Pedraza S, Demchuk A, Daunis IEJ, Termes H, Blasco G, Soria G, Boada I, Remollo S, Banos J, Serena J, Castellanos M. Quantification of thrombus hounsfield units on noncontrast ct predicts stroke subtype and early recanalization after intravenous recombinant tissue plasminogen activator. *AJNR Am J Neuroradiol*. 2012;33:90-96
17. Moftakhar P, English JD, Cooke DL, Kim WT, Stout C, Smith WS, Dowd CF, Higashida RT, Halbach VV, Hetts SW. Density of thrombus on admission ct predicts revascularization efficacy in large vessel occlusion acute ischemic stroke. *Stroke*. 2013;44:243-245
18. Nam HS, Kim EY, Kim SH, Kim YD, Kim J, Lee HS, Nam CM, Heo JH. Prediction of thrombus resolution after intravenous thrombolysis assessed by ct-based thrombus imaging. *Thrombosis and haemostasis*. 2012;107:786-794
19. Adams HP, Jr., Bendixen BH, Kappelle LJ, Biller J, Love BB, Gordon DL, Marsh EE, 3rd. Classification of subtype of acute ischemic stroke. Definitions for use in a multicenter clinical trial. Toast. Trial of org 10172 in acute stroke treatment. *Stroke*. 1993;24:35-41
20. Chen CJ, Tseng YC, Lee TH, Hsu HL, See LC. Multisection ct angiography compared with catheter angiography in diagnosing vertebral artery dissection. *AJNR Am J Neuroradiol*. 2004;25:769-774
21. Kim YK, Schulman S. Cervical artery dissection: Pathology, epidemiology and management. *Thrombosis research*. 2009;123:810-821
22. Rittersma SZ, van der Wal AC, Koch KT, Piek JJ, Henriques JP, Mulder KJ, Ploegmakers JP, Meesterman M, de Winter RJ. Plaque instability frequently occurs days or weeks before occlusive coronary thrombosis: A pathological thrombectomy study in primary percutaneous coronary intervention. *Circulation*. 2005;111:1160-1165
23. Chaves CJ, Caplan LR. Heparin and oral anticoagulants in the treatment of brain ischemia. *Journal of the neurological sciences*. 2000;173:3-9

24. Jerjes-Sanchez C. Venous and arterial thrombosis: A continuous spectrum of the same disease? *European heart journal*. 2005;26:3-4

25. Lin HL, Xu XS, Lu HX, Zhang L, Li CJ, Tang MX, Sun HW, Liu Y, Zhang Y. Pathological mechanisms and dose dependency of erythrocyte-induced vulnerability of atherosclerotic plaques. *Journal of molecular and cellular cardiology*. 2007;43:272-280

26. Rao DS, Goldin JG, Fishbein MC. Determinants of plaque instability in atherosclerotic vascular disease. *Cardiovascular pathology : the official journal of the Society for Cardiovascular Pathology*. 2005;14:285-293

27. Kolodgie FD, Gold HK, Burke AP, Fowler DR, Kruth HS, Weber DK, Farb A, Guerrero LJ, Hayase M, Kutys R, Narula J, Finn AV, Virmani R. Intraplaque hemorrhage and progression of coronary atheroma. *The New England journal of medicine*. 2003;349:2316-2325

28. Kockx MM, Cromheeke KM, Knaapen MW, Bosmans JM, De Meyer GR, Herman AG, Bult H. Phagocytosis and macrophage activation associated with hemorrhagic microvessels in human atherosclerosis. *Arteriosclerosis, thrombosis, and vascular biology*. 2003;23:440-446

29. Takaya N, Yuan C, Chu B, Saam T, Polissar NL, Jarvik GP, Isaac C, McDonough J, Natiello C, Small R, Ferguson MS, Hatsukami TS. Presence of intraplaque hemorrhage stimulates progression of carotid atherosclerotic plaques: A high-resolution magnetic resonance imaging study. *Circulation*. 2005;111:2768-2775

30. Sitzer M, Muller W, Siebler M, Hort W, Kniemeyer HW, Jancke L, Steinmetz H. Plaque ulceration and lumen thrombus are the main sources of cerebral microemboli in high-grade internal carotid artery stenosis. *Stroke*. 1995;26:1231-1233

31. Mathiesen EB, Bonaa KH, Joakimsen O. Echolucent plaques are associated with high risk of ischemic cerebrovascular events in carotid stenosis: The tromso study. *Circulation*. 2001;103:2171-2175

32. Kim JS, Nah HW, Park SM, Kim SK, Cho KH, Lee J, Lee YS, Kim J, Ha SW, Kim EG, Kim DE, Kang DW, Kwon SU, Yu KH, Lee BC. Risk factors and stroke mechanisms in atherosclerotic stroke: Intracranial compared with extracranial and anterior compared with posterior circulation disease. *Stroke*. 2012;43:3313-3318

33. Wysokinski WE, Owen WG, Fass DN, Patrzalek DD, Murphy L, McBane RD, 2nd. Atrial fibrillation and thrombosis: Immunohistochemical differences between in situ and embolized thrombi. *Journal of thrombosis and haemostasis : JTH*. 2004;2:1637-1644

34. Kim EY, Heo JH, Lee SK, Kim DJ, Suh SH, Kim J, Kim DI. Prediction of thrombolytic efficacy in acute ischemic stroke using thin-section noncontrast ct. *Neurology*. 2006;67:1846-1848

35. Besachio DA, Quigley EP, 3rd, Shah LM, Salzman KL. Noncontrast computed tomographic hounsfield unit evaluation of cerebral venous thrombosis: A quantitative evaluation. *Neuroradiology*. 2013;55:941-945

36. Buyck PJ, De Keyzer F, Vanneste D, Wilms G, Thijs V, Demaerel P. Ct density measurement and h:H ratio are useful in diagnosing acute cerebral venous sinus thrombosis. *AJNR Am J Neuroradiol*. 2013;34:1568-1572

37. Uchida Y, Sakurai T, Kanai M, Shirai S, Morita T. Characterization of coronary fibrin thrombus in patients with acute coronary syndrome using dye-staining angioscopy. *Arteriosclerosis, thrombosis, and vascular biology*. 2011;31:1452-1460

38. Okamatsu K, Takano M, Sakai S, Ishibashi F, Uemura R, Takano T, Mizuno K. Elevated troponin t levels and lesion characteristics in non-st-elevation acute coronary syndromes. *Circulation*. 2004;109:465-470

39. Tabata H, Mizuno K, Arakawa K, Satomura K, Shibuya T, Kurita A, Nakamura H. Angioscopic identification of coronary thrombus in patients with postinfarction angina. *Journal of the American College of Cardiology*. 1995;25:1282-1285

40. Quadros AS, Cambruzzi E, Sebben J, David RB, Abelin A, Welter D, Sarmento-Leite R, Mehta RH, Gottschall CA, Lopes RD. Red versus white thrombi in patients with st-elevation myocardial infarction undergoing primary percutaneous coronary intervention: Clinical and angiographic outcomes. *American heart journal*. 2012;164:553-560

Predictive value of thrombus attenuation on thin-slice non-contrast CT for persistent occlusion after intravenous thrombolysis

JM Niesten, IC van der Schaaf, Y van der Graaf, LJ Kappelle, GJ Biessels, AD Horsch, JW Dankbaar, EJ Smit, WPTM Mali, BK Velthuis, on behalf of the DUtch acute Stroke Trial (DUST)

Cerebrovascular Diseases, 2014

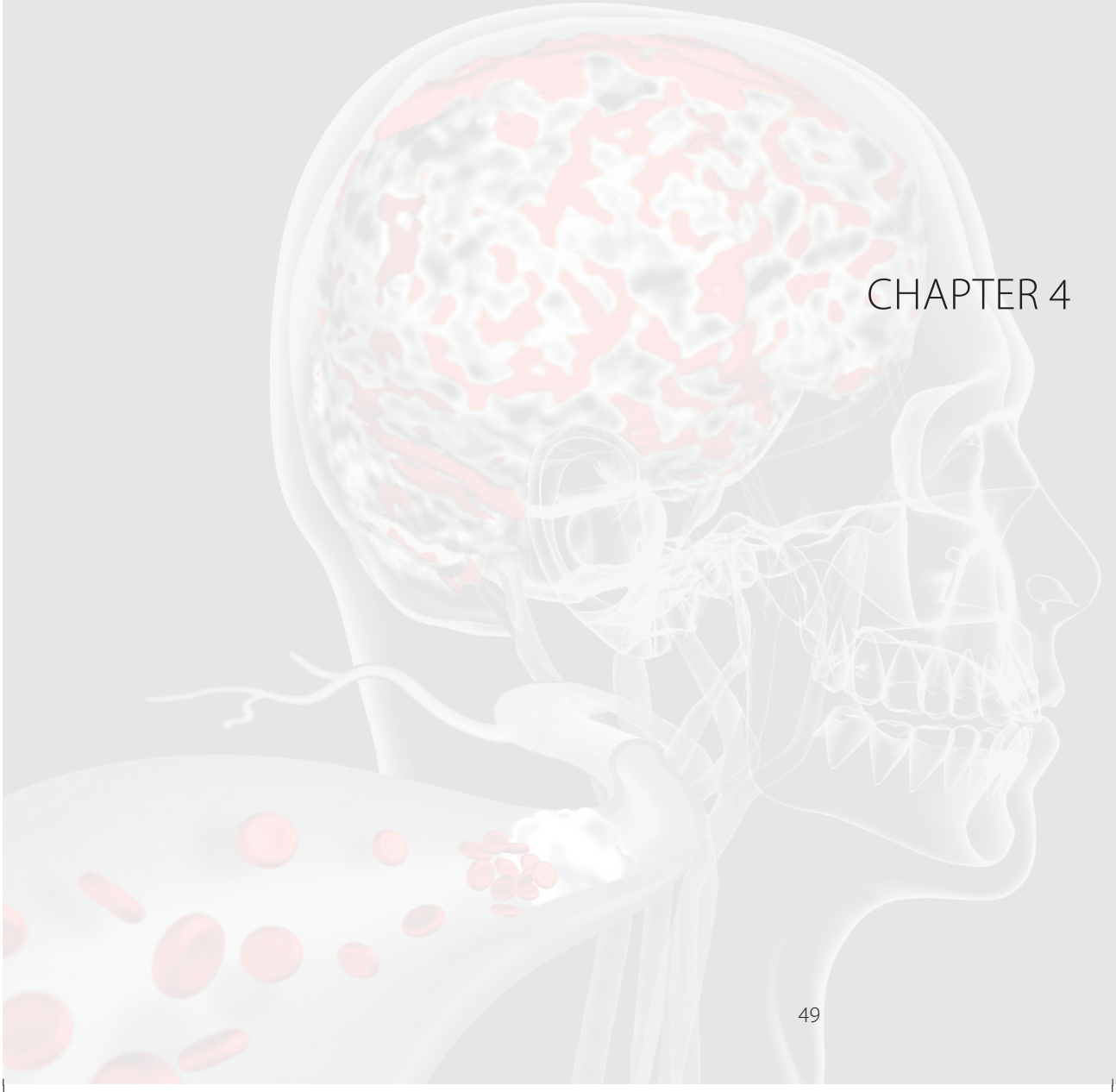

CHAPTER 4

ABSTRACT

Background

In stroke erythrocyte-rich thrombi are more sensitive to IV-rtPA and have higher density on non-contrast CT (NCCT). We investigated the relationship between thrombus density and recanalization and whether persistent occlusions can be predicted by HU-measurements.

Methods

In 88 IV-rtPA treated patients with intracranial ICA or MCA occluding thrombus and follow-up imaging, thrombus and contralateral vessel attenuation measurements were performed on thin-slice NCCT. Mean absolute and relative Hounsfield Units (HU) were compared between patients with persistent occlusion (modified TICI-system grade 0/1/2a) and recanalization (grade 2b/3). Univariate and multivariate (adjusted for stroke subtype, clot burden score, occlusion site and time to thrombolysis) odds ratios for persistent occlusion were calculated. Additional prognostic value for persistent occlusion was estimated by adding HU-measurements to the AUC of known determinants and calculating optimal cut-off values.

Results

Patients with persistent occlusion (n=19) had significant lower mean HU (absolute 52.2 ± 9.5, relative 1.29 ± 0.20) compared to recanalization (absolute 63.1 ± 10.7, relative 1.54 ± 0.23, both p<0.0001). Odds ratios for persistent occlusion were 3.1 (95%CI 1.6-6.0) univariate and 3.1 (95%CI 1.7-5.7) multivariate per 10 absolute HU-decrease and 3.2 (95%CI 1.6-6.5) univariate and 4.1 (95%CI 1.8-9.1) multivariate per 0.20 relative HU-decrease. Attenuation measurements significantly increased AUC (0.67) of the known determinants to 0.84 (absolute HU) and 0.86 (rHU). Cut-off values of <56.5 absolute HU and <1.38 relative HU showed optimal predictive values for persistent occlusion.

Thrombus density is related to recanalization rate. Lower absolute and relative HU are independently related to persistent occlusion and HU-measurements significantly increase discriminative performances of known recanalization determinants.

INTRODUCTION

In patients with acute ischemic stroke successful recanalization favours good clinical outcome and is the aim of acute stroke treatment [1]. Because earlier treatment is associated with better outcomes appropriate treatment should be applied as soon as possible [2]. However, intravenous thrombolysis with recombinant tissue plasminogen activator (IV-rtPA) results in timely recanalization in about 50% of occluded arteries only [3]. In patients with persistent occlusion after IV-rtPA other recanalization strategies such as intra-arterial thrombolysis or mechanical thrombectomy can be considered if initiated in time, although this is not evidence based. The success of IV-rtPA to achieve recanalization may be related to the composition of the thrombus. An erythrocyte-rich thrombus may be more sensitive to thrombolysis as compared to platelet rich thrombi [4, 5].

Thin-slice non-contrast CT (NCCT) allows accurate detection of thrombi and can be used to determine the thrombus density [6-9]. Erythrocytes increase the thrombus density, measured in Hounsfield Units (HU), whereas platelets, atheromatous and cellular debris are known to decrease the HU-value [5, 9-11]. The measurement of thrombus attenuation on NCCT could therefore be a rapid non-invasive tool for predicting persistent occlusions after IV-rtPA and may play a role in initiating additional intra-arterial treatment if recanalization is expected to be unsuccessful.
The aims of our study were to investigate whether thrombus density is related to the likelihood of recanalization after IV-rtPA and whether persistent occlusion can be predicted by HU-measurements of thrombi on thin-slice NCCT independent of the known determinants of recanalization subtype of stroke, clot burden score, time to thrombolysis and site of occlusion.

METHODS

Patients

We reviewed the records of prospectively included patients who participated in a large multicenter observational cohort study (DUtch acute Stroke Trial, DUST) between May 2009 and December 2012. Inclusion criteria for DUST are: age ≥ 18 years, onset of stroke symptoms < 9 hours, National Institutes of Health Stroke Scale (NIHSS) ≥ 2 and informed consent (including permission for follow-up imaging) on admission from patient or family. For this substudy additional inclusion criteria were: scanned on admission with thin-slice NCCT and CTA, an occlusion of the intracranial ICA or MCA (segment M1 or M2) on admission CTA and treated with IV-rtPA only and follow-up CTA or MRA available. All patients received IV-rtPA (Alteplase) within 4.5 hours after symptom onset using a bolus of 0.09 mg/kg, followed by 1-hour infusion of 0.81 mg/kg. Exclusion criteria are: known renal failure or contrast allergy and patients who had already received therapy before neuroimaging. All patients underwent

NCCT, CT-perfusion (CTP) and CT-angiography (CTA) on admission with similar protocols.
The following clinical data were collected for all patients; demographic features, cardiovascular risk factors (hypertension, diabetes, hyperlipidemia, severe carotid disease, atrial fibrillation), onset time to thrombolysis, NIHSS on admission, presence of a dense vessel, clot burden score and final stroke diagnosis with large artery atherosclerosis, cardioembolism and unknown subtype according to the Trial of Org 10172 in Acute Stroke Treatment (TOAST) criteria [12] and dissection defined as a narrowed eccentric lumen surrounded by crescent-shaped mural thickening or tapered occlusion with associated increase in external vessel diameter on CTA [13, 14].

Imaging

All included patients were scanned with NCCT and CTA on admission and CTA (n=82) or MRA (n=6) on follow-up. Follow-up imaging was performed between one and five days after admission. In this multicenter study CT imaging studies were performed on a Philips 256-slice, Philips 64-slice, Toshiba 64-slice or Toshiba 320-slice CT scanner. For this substudy only the admission NCCT and CTA and the follow-up CTA or MRA were used. Scan parameters of the NCCT were: 120 kVp, 300 mAs, and 1 mm and 5 mm reconstructed slice thickness and for the CTA: 120 kVp, 150 mAs, 1 mm reconstructed slice thickness.

One neuroradiologist and one experienced radiology resident blinded for all the clinical data except side of symptoms reviewed the NCCT and the CTA for presence and the location of an intracranial thrombus. Thrombus location and extent on CTA were also classified according to the clot burden score [15]. On the 1 mm NCCT attenuation measurements of the thrombus were performed, blinded to all data, except for location of thrombus on CTA. Additionally, the attenuation of the corresponding contralateral vessel (without thrombus) was measured. Per patient a small round region of interest was drawn three separate times within the thrombus and contralateral vessel, and mean HU-values were used for analysis to improve reproducibility. Because some variation in HU-measurements could be introduced by patient variation in haematocrit level and by the different vendors of CT scanners we additionally calculated the relative HU of the thrombus (attenuation thrombus/ attenuation contralateral vessel).
To assess the recanalization rate the modified Thrombolysis in Cerebral Infarction (mTICI)-system was used with mTICI grade 0 (no perfusion), 1 (perfusion past the initial obstruction, but limited distal branch filling with little or slow distal perfusion), 2a (partial perfusion of less than half of the vascular distribution of the occluded artery (e.g., filling and perfusion trough one M2 division)) representing a persistent occlusion and mTICI grade 2b (partial perfusion of half or greater of the vascular distribution of the occluded artery (e.g., filling and perfusion through 2 or more M2 divisions)) and Grade 3 (full perfusion with filling of all distal branches) representing successful recanalization [16, 17].

Analysis

We used descriptive statistics for demographics, cardiovascular risk factors, stroke subtype, thrombus location, NIHSS at admission, onset time to thrombolysis, proportion of hyperdense vessels and clot burden score to compare patients with a successful recanalization and patients with a persistent occlusion. These baseline characteristics were summarised as means (with standard deviation (SD)) or frequency counts and proportions. To estimate the relation between thrombus HU-values and recanalization, differences in means of the absolute HU-values of the thrombus and contralateral vessel as well as relative HU-values in patients with persistent occlusion and successful recanalization were calculated and compared with the student's t-test.
We performed univariate and multivariate binary logistic regression and calculated odds ratios for persistent occlusion with corresponding 95% confidence interval for absolute HU-values (per 10 HU-decrease) and relative HU-values (per 0.20 relative HU-decrease). In the multivariate analyses we included four additional determinants: subtype of stroke, clot burden score, time to thrombolysis and site of occlusion. These factors have been described as the most important determinants of recanalization [1, 15, 18-22].

Receiver Operating Characteristic (ROC) curves were used to determine the additional prognostic value for persistent occlusion by comparing multivariate models for both the absolute HU and relative HU-values. A first model contained the aforementioned determinants (subtype of stroke, time to thrombolysis, clot burden score and site of occlusion). Additional models contained the same determinants plus the absolute or relative HU-values. An area under the ROC curve (AUC) of more than 0.80 is considered a test with good discriminative performance [23]. The AUC of the first model was compared with the AUCs of the second models using the method as described by Delong *et al.* [24], which correct for correlation between two AUCs based on the same population. Absolute HU and relative HU cut-off values for persistent occlusions with the optimal test characteristics (sensitivity, specificity, positive predictive value and negative predictive value) were calculated. Statistical analysis were performed by using SPSS, version 19.0; SPSS Inc., Chicago, Ill. Results were considered statistically significant when P-values were <0.05 and when the 95% confidence interval of the odds ratios did not include 1.

RESULTS

A total of 88 patients were included. Table 1 summarizes the baseline characteristics of all patients, the mean age was 66.6 years and 43% were female. Of all patients 69 (78%) had a successful recanalization while 19 patients showed a persistent occlusion.

Table 1 *Baseline characteristics of patients with successful recanalizations and persistent occlusions*

Variable	*Total (n=88)*	*Successful recanalization (n=69)*	*Persistent occlusion (n=19)*
Demographics			
Mean age, years (SD)	66.6 (13.1)	66.6 (12.3)	66.7 (16.1)
Female, n (%)	38 (43)	32 (46)	6 (32)
Cardiovascular risk factors, n (%)			
Hypertension	37 (43)	27 (39)	10 (56)
Diabetes	4 (5)	3 (4)	1 (5)
Hyperlipidemia	25 (30)	22 (33)	3 (16)
Atrial fibrillation	8 (9)	6 (9)	2 (11)
Carotid disease[¤]	27 (31)	23 (33)	4 (21)
Stroke Subtype, n (%)			
Large artery atherosclerosis	29 (33)	21 (30)	8 (42)
Cardioembolism	28 (32)	22 (32)	6 (32)
Dissection	6 (7)	6 (9)	0
Unknown	25 (28)	20 (29)	5 (26)
Site of occlusion, n (%)			
ICA	5 (6)	4 (6)	1 (5)
M1 proximal	9 (10)	7 (10)	2 (11)
M1 distal	35 (40)	30 (44)	5 (26)
M2	39 (44)	28 (41)	11 (58)
NIHSS at admission, mean (SD)	12.2 (6.4)	12.8 (6.5)	10.2 (5.8)
Onset Time to rtPA (minutes), mean (SD)	103.8 (42.0)	104.2 (45.6)	102.5 (26.4)
Hyperdense vessel signs, n (%)	39 (44)	32 (46)	7 (37)
Clot Burden Score, mean (SD)	7.2 (1.9)	7.0 (2.0)	7.8 (1.5)

ICA: internal carotid artery; M1: MCA-M1 segment; M2: MCA-M2 segment

[¤]=Carotid disease was defined as atherosclerosis with a lumen diameter stenosis of ≥50%

Table 2 displays the differences in mean thrombus HU-values (absolute and relative) and HU-values of the contralateral vessel between patients with persistent occlusion and successful recanalization. Patients with persistent occlusion (mean ± SD: absolute HU 52.2 ± 9.5 and relative HU 1.29 ± 0.20) had significant lower thrombus attenuation compared to patients with successful recanalization (mean absolute HU 63.1 ± 10.7 and mean relative HU 1.54 ± 0.23, both p<0.0001, *table 2)*. HU-values of the contralateral vessel did not differ between the groups.

The odds ratios of thrombus density for persistent occlusion in the univariate analyses were 3.1 (95%CI 1.6-6.0) per 10 absolute HU-decrease and 3.2 (95%CI 1.6-6.5) per 0.20 relative HU-decrease. In the multivariate analyses adjusted for subtype of stroke, clot burden score, time to thrombolysis and site of occlusion both the absolute HU-value (OR 3.1, 95%CI 1.7-5.7) and relative HU (OR 4.1, 95%CI 1.8-9.1) were independently related to persistent occlusion *(table 2)*.

Table 2 *Relation of thrombus density with rate of recanalization*

Thrombus Density	*Total (n=88)*	*Successful recanalization (n=69)*	*Persistent occlusion (n=19)*	*P-value*	*Odds Ratios (95 %CI)*	
					Uni-variate	*Multi-variate±*
Absolute HU, mean (95 %CI)						
Thrombus attenuation	60.7 (58.3-63.1)	63.1 (60.5-65.7)	52.2 (47.6-56.8)	<0.001	3.1 (1.6-6.0)	3.1 (1.7-5.7)
Contralateral vessel	41.0 (40.0-42.0)	41.2 (39.9-42.4)	40.4 (39.0-41.9)	0.56		
Relative HU¤, mean (95 %CI)	1.49 (1.43-1.54)	1.54 (1.48-1.60)	1.29 (1.19-1.39)	<0.001	3.2 (1.6-6.5)	4.1 (1.8-9.1)

P-values of difference between thrombus attenuation with successful recanalizations and persistent occlusions and results of univariate and multivariate logistic regression in odds ratios for persistent occlusions per 10 absolute HU- and 0.20 relative HU-decrease are shown.

¤=Relative HU of the thrombus was calculated as thrombus attenuation divided by attenuation of contralateral vessel ±=Adjusted for subtype of stroke, clot burden score, time to thrombolysis and site of occlusion.

The AUC of the first model with determinants subtype of stroke, time to thrombolysis, clot burden score and site of occlusion was 0.67 (95CI% 0.55-0.80). The AUC of these four predictors combined with the HU-values was 0.84 (95CI% 0.74-0.94) with absolute HU-values and 0.86 (95CI% 0.77-0.95) with relative HU-values, a significant increase in AUC for both HU-values (both p<0.001).

The optimal predictive cut-off values for a persistent occlusion were an absolute HU of <56.5 (sensitivity 71.0%, specificity 73.7%, positive predictive value 90.7%, negative predictive value 41.2%) and a relative HU of <1.38 (sensitivity 70.0%, specificity 73.7%, positive predictive value 90.6%, negative predictive value 40.0%).

DISCUSSION

This study shows that thrombus density in acute ischemic stroke patients is related to the likelihood of recanalization and that HU-measurements on NCCT can help to predict persistent occlusion after IV-rtPA treatment. Lower absolute and relative HU-values are associated with a greater likelihood of a persistent occlusion after IV-rtPA.

Our study is in good agreement with the four previous studies investigating the HU-measurements and rate of recanalization [8, 9, 25, 26]. In these studies the investigators also found that high HU-values of thrombi on NCCT are associated with successful recanalization after IV-rtPA. Although Nam *et al*. did not find a significant relation between the HU-values and successful recanalization on thin-slices in a population of 100 patients: higher thrombus HU was significantly associated with a greater degree of thrombus resolution (18% resolution increase per 10 HU) [8]. In a study of 34 patients Kim *et al*. investigated 8 IV-rtPA treated patients and found a corrected HU (mean HU of contralateral vessel x relative HU) of 55.0 on 0.6 mm slices in thrombi of patients in which recanalization was achieved and 48.4 in thrombi that showed persistent occlusion [9]. Puig *et al*. described mean absolute HU-values of respectively 49.3 and 42.1 and relative HU-values of respectively 1.57 and

1.11 of recanalized and persistent thrombi on 3 mm thick slices in 45 IV-rtPA treated patients. They found a similar cut-off value of relative HU <1.382 to predict persistent occlusion [25]. Moftakhar *et al*. found a mean relative HU of 1.58 in thrombi of IV-rtPA treated patients (n=45) with successful recanalization and 1.39 with a persistent occlusion. Measurements were performed on 2.5 mm slices and cut-off values were not calculated [26]. They also found that high HU-values of thrombi are associated with successful recanalization after mechanical thrombectomy, although this relationship has been questioned more recently [27]. Overall we found similar relative HU-values and somewhat higher absolute thrombus density in both recanalized thrombi and persistent occlusions compared to other articles in which either absolute or relative HU was calculated. The higher absolute HU values might be explained by the fact that we used 1 mm thin slices and thus incorporated less partial volume effects compared to the other articles.

Our study is the first in which both the absolute and relative HU were measured and cut-off values were calculated on 1 mm slice thickness in a large group of patients. Furthermore, we are the first to show that HU-measurements are independently associated with the likelihood of recanalization and significantly increase discriminative performance over known predictors for recanalization. The attenuation of thrombi on NCCT has a linear correlation with the amount of haemoglobin. Since lysability seems to increase with increasing haematocrit levels, thrombi with lower HU are likely to consist out of components that are more resistant to fibrinolytic agents than thrombi with higher HU [4, 5, 11]. Our study shows that HU-measurements of thrombi on thin-slices can help to identify patients who are likely or unlikely to respond to IV-rtPA. In our study we found a higher rate of recanalization (78%) than the other four previous studies in which it varied from 33-71%. This might be explained by the timing of our follow-up scans (1-4 days) which was relatively late compared to two studies in which follow-up imaging was done immediately (the two other studies do not mention the time of follow-up imaging). As the occurrence of spontaneous recanalization is known to increase within time [1], part of the recanalizations might be described to spontaneous recanalization and not due to IV-rtPA. Furthermore, although every patient, independent of clinical development, is prospectively being asked on admission to allow follow-up angiography, in practice not every patient included in the main study undergoes follow-up imaging. A number of patients deceases before follow-up takes place. The percentage of patients that decease within the first days after an ischemic stroke is in the order of 12% [28]. As this group is likely to have persistent occlusions after IV-rtPA, the absence of follow-up imaging in these patients could also partly explain the high percentage of full recanalizations on follow-up.
However, as the clinical outcome is significantly better in patients who show recanalization on late follow-up compared to patients with persistent occlusion at the same time, our findings are clinically important [29].
The most important determinants which have been described as being related

to recanalization are the stroke subtype, extent of the occlusion (clot burden score), site of occlusion and time to thrombolysis, all of which we included in our multivariate analyses.

Niesten et al. recently found that thrombus density on thin-slice NCCT could be related to stroke subtype [30]. Moreover, some studies found that cardioembolic thrombi have a higher likelihood to recanalize after treatment than large artery atherosclerosis thrombi [31, 32] although other studies found no relation between stroke aetiology and recanalization [33, 34]. Riedel *et al*. described thrombus volume as an important predictor for successful recanalization [35] while other investigators did not find a significant relationship [8, 9]. However, the clot burden score [1, 15, 18] and the site of occlusion [19-21], which are both related to the thrombus volume [36, 37], have more often been described as being associated with recanalization rate. IV-rtPA may be more effective in fresh than old thrombi and a recent study found that early recanalization depends on time from stroke onset to IV-rtPA treatment [22]. Although some investigators describe the presence of a dense vessel sign as a predictor for severe brain ischemia, its value in predicting the efficacy of IV-rtPA and its impact on functional outcome is controversial [38-40]. Therefore we did not include the presence of a dense vessel sign in our multivariate analyses.

Although in our population differences in the above mentioned determinants between patients with a persistent occlusion and with a successful recanalization were small on average, we adjusted our analyses for these important predictors to investigate the independent relationship between thrombus attenuation and the rate of recanalization.

In conclusion, thrombus density on thin-slice NCCT is related to the likelihood of recanalization in patients treated with IV-rtPA. Lower absolute HU and relative HU are independently related to persistent occlusion and HU-measurements significantly increase discriminative performance in a multivariate model with other known predictors for recanalization. Cut-off values of <56.5 absolute HU and relative HU of <1.38 showed the most optimal predictive values for persistent occlusion and may help to select IV-rtPA treated stroke patients who may benefit from (additional) intra-arterial treatment.

REFERENCES

1. Rha JH, Saver JL. The impact of recanalization on ischemic stroke outcome: A meta-analysis. *Stroke*. 2007;38:967-973
2. Saver JL. Time is brain - quantified. *Neurology*. 2005;64:A295-A295
3. Mazighi M, Serfaty JM, Labreuche J, Laissy JP, Meseguer E, Lavallee PC, Cabrejo L, Slaoui T, Guidoux C, Lapergue B, Klein IF, Olivot JM, Abboud H, Simon O, Niclot P, Nifle C, Touboul PJ, Raphaeli G, Gohin C, Claeys ES, Amarenco P. Comparison of intravenous alteplase with a combined intravenous-endovascular approach in patients with stroke and confirmed arterial occlusion (recanalise study): A prospective cohort study. *Lancet neurology*. 2009;8:802-809
4. Jang IK, Gold HK, Ziskind AA, Fallon JT, Holt RE, Leinbach RC, May JW, Collen D. Differential sensitivity of erythrocyte-rich and platelet-rich arterial thrombi to lysis with recombinant tissue-type plasminogen activator. A possible explanation for resistance to coronary thrombolysis. *Circulation*. 1989;79:920-928
5. Caplan LR. Antiplatelet therapy in stroke prevention: Present and future. *Cerebrovasc Dis*. 2006;21 Suppl 1:1-6
6. Kim EY, Lee SK, Kim DJ, Suh SH, Kim J, Heo JH, Kim DI. Detection of thrombus in acute ischemic stroke: Value of thin-section noncontrast-computed tomography. *Stroke*. 2005;36:2745-2747
7. Riedel CH, Zoubie J, Ulmer S, Gierthmuehlen J, Jansen O. Thin-slice reconstructions of nonenhanced ct images allow for detection of thrombus in acute stroke. *Stroke*. 2012;43:2319-2323
8. Nam HS, Kim EY, Kim SH, Kim YD, Kim J, Lee HS, Nam CM, Heo JH. Prediction of thrombus resolution after intravenous thrombolysis assessed by ct-based thrombus imaging. *Thrombosis and haemostasis*. 2012;107:786-794
9. Kim EY, Heo JH, Lee SK, Kim DJ, Suh SH, Kim J, Kim DI. Prediction of thrombolytic efficacy in acute ischemic stroke using thin-section noncontrast ct. *Neurology*. 2006;67:1846-1848
10. Moulin T, Tatu L, Vuillier F, Cattin F. [brain ct scan for acute cerebral infarction: Early signs of ischemia]. *Revue neurologique*. 1999;155:649-655
11. Kirchhof K, Welzel T, Mecke C, Zoubaa S, Sartor K. Differentiation of white, mixed, and red thrombi: Value of ct in estimation of the prognosis of thrombolysis phantom study. *Radiology*. 2003;228:126-130
12. Adams HP, Jr., Bendixen BH, Kappelle LJ, Biller J, Love BB, Gordon DL, Marsh EE, 3rd. Classification of subtype of acute ischemic stroke. Definitions for use in a multicenter clinical trial. Toast. Trial of org 10172 in acute stroke treatment. *Stroke*. 1993;24:35-41
13. Chen CJ, Tseng YC, Lee TH, Hsu HL, See LC. Multisection ct angiography compared with catheter angiography in diagnosing vertebral artery dissection. *AJNR Am J Neuroradiol*. 2004;25:769-774
14. Kim YK, Schulman S. Cervical artery dissection: Pathology, epidemiology and management. *Thrombosis research*. 2009;123:810-821
15. Puetz V, Dzialowski I, Hill MD, Subramaniam S, Sylaja PN, Krol A, O'Reilly C, Hudon ME, Hu WY, Coutts SB, Barber PA, Watson T, Roy J, Demchuk AM. Intracranial thrombus extent predicts clinical outcome, final infarct size and hemorrhagic transformation in ischemic stroke: The clot burden score. *International journal of stroke : official journal of the International Stroke Society*. 2008;3:230-236
16. Tomsick T, Broderick J, Carrozella J, Khatri P, Hill M, Palesch Y, Khoury J. Revascularization results in the interventional management of stroke ii trial. *AJNR Am J Neuroradiol*. 2008;29:582-587
17. Yoo AJ, Simonsen CZ, Prabhakaran S, Chaudhry ZA, Issa MA, Fugate JE, Linfante I, Liebeskind DS, Khatri P, Jovin TG, Kallmes DF, Dabus G, Zaidat OO. Refining angiographic biomarkers of revascularization: Improving outcome prediction after intra-arterial therapy. *Stroke*. 2013
18. Barreto AD, Albright KC, Hallevi H, Grotta JC, Noser EA, Khaja AM, Shaltoni HM, Gonzales NR, Illoh K, Martin-Schild S, Campbell MS, 3rd, Weir RU, Savitz SI. Thrombus burden is associated with clinical outcome after intra-arterial therapy for acute ischemic stroke. *Stroke*. 2008;39:3231-3235
19. Saqqur M, Uchino K, Demchuk AM, Molina CA, Garami Z, Calleja S, Akhtar N, Orouk FO, Salam A, Shuaib A, Alexandrov AV. Site of arterial occlusion identified by transcranial doppler predicts the response to intravenous thrombolysis for stroke. *Stroke*. 2007;38:948-954
20. Murphy A, Symons SP, Hopyan J, Aviv RI. Factors influencing clinically meaningful recanalization after iv-rtpa in acute ischemic stroke. *AJNR Am J Neuroradiol*. 2013;34:146-152
21. Molina CA, Alexandrov AV, Demchuk AM, Saqqur M, Uchino K, Alvarez-Sabin J. Improving the predictive accuracy of recanalization on stroke outcome in patients treated with tissue plasminogen activator. *Stroke*. 2004;35:151-156
22. Kimura K, Iguchi Y, Shibazaki K, Aoki J, Watanabe M, Matsumoto N, Yamashita S. Early stroke treatment with iv t-pa associated with early recanalization. *Journal of the neurological sciences*. 2010;295:53-57
23. Swets JA. Measuring the accuracy of diagnostic systems. *Science*. 1988;240:1285-1293
24. DeLong ER, DeLong DM, Clarke-Pearson DL. Comparing the areas under two or more correlated receiver operating characteristic curves: A nonparametric approach. *Biometrics*. 1988;44:837-845

25. Puig J, Pedraza S, Demchuk A, Daunis IEJ, Termes H, Blasco G, Soria G, Boada I, Remollo S, Banos J, Serena J, Castellanos M. Quantification of thrombus hounsfield units on noncontrast ct predicts stroke subtype and early recanalization after intravenous recombinant tissue plasminogen activator. *AJNR Am J Neuroradiol*. 2012;33:90-96

26. Moftakhar P, English JD, Cooke DL, Kim WT, Stout C, Smith WS, Dowd CF, Higashida RT, Halbach VV, Hetts SW. Density of thrombus on admission ct predicts revascularization efficacy in large vessel occlusion acute ischemic stroke. *Stroke*. 2013;44:243-245

27. Yilmaz U, Roth C, Reith W, Papanagiotou P. Thrombus attenuation does not predict angiographic results of mechanical thrombectomy with stent retrievers. *AJNR Am J Neuroradiol*. 2013

28. Ahmed N, Wahlgren N, Grond M, Hennerici M, Lees KR, Mikulik R, Parsons M, Roine RO, Toni D, Ringleb P. Implementation and outcome of thrombolysis with alteplase 3-4.5 h after an acute stroke: An updated analysis from sits-istr. *Lancet neurology*. 2010;9:866-874

29. Yeo LL, Paliwal P, Teoh HL, Seet RC, Chan BP, Liang S, Venketasubramanian N, Rathakrishnan R, Ahmad A, Ng KW, Loh PK, Ong JJ, Wakerley BR, Chong VF, Bathla G, Sharma VK. Timing of recanalization after intravenous thrombolysis and functional outcomes after acute ischemic stroke. *JAMA neurology*. 2013;70:353-358

30. Niesten JM, van der Schaaf IC, Biessels GJ, van Otterloo AE, van Seeters T, Horsch AD, Luitse MJ, van der Graaf Y, Kappelle LJ, Mali WP, Velthuis BK. Relationship between thrombus attenuation and different stroke subtypes. *Neuroradiology*. 2013;55:1071-1079

31. Cho KH, Lee DH, Kwon SU, Choi CG, Kim SJ, Suh DC, Kim JS, Kang DW. Factors and outcomes associated with recanalization timing after thrombolysis. *Cerebrovasc Dis*. 2012;33:255-261

32. Molina CA, Montaner J, Arenillas JF, Ribo M, Rubiera M, Alvarez-Sabin J. Differential pattern of tissue plasminogen activator-induced proximal middle cerebral artery recanalization among stroke subtypes. *Stroke*. 2004;35:486-490

33. Rocha S, Pires A, Gomes J, Rocha J, Sousa F, Pinho J, Rodrigues M, Ferreira C, Machado A, Mare R, Fontes JR. Intravenous thrombolysis is more effective in ischemic cardioembolic strokes than in non-cardioembolic? *Arquivos de neuro-psiquiatria*. 2011;69:905-909

34. Hsia AW, Sachdev HS, Tomlinson J, Hamilton SA, Tong DC. Efficacy of iv tissue plasminogen activator in acute stroke: Does stroke subtype really matter? *Neurology*. 2003;61:71-75

35. Riedel CH, Zimmermann P, Jensen-Kondering U, Stingele R, Deuschl G, Jansen O. The importance of size: Successful recanalization by intravenous thrombolysis in acute anterior stroke depends on thrombus length. *Stroke*. 2011;42:1775-1777

36. Ernst R, Pancioli A, Tomsick T, Kissela B, Woo D, Kanter D, Jauch E, Carrozzella J, Spilker J, Broderick J. Combined intravenous and intra-arterial recombinant tissue plasminogen activator in acute ischemic stroke. *Stroke*. 2000;31:2552-2557

37. Tandberg Askevold E, Naess H, Thomassen L. Predictors for recanalization after intravenous thrombolysis in acute ischemic stroke. *Journal of stroke and cerebrovascular diseases : the official journal of National Stroke Association*. 2007;16:21-24

38. Roberts HC, Dillon WP, Furlan AJ, Wechsler LR, Rowley HA, Fischbein NJ, Higashida RT, Kase C, Schulz GA, Lu Y, Firszt CM. Computed tomographic findings in patients undergoing intra-arterial thrombolysis for acute ischemic stroke due to middle cerebral artery occlusion - results from the proact ii trial. *Stroke*. 2002;33:1557-1565

39. Manelfe C, Larrue V, von Kummer R, Bozzao L, Ringleb P, Bastianello S, Iweins F, Lesaffre E. Association of hyperdense middle cerebral artery sign with clinical outcome in patients treated with tissue plasminogen activator. *Stroke*. 1999;30:769-772

40. Fitzsimmons PR, Biswas S, Hill AM, Kumar R, Cullen C, White RP, Sharma AK, Durairaj R. The hyperdense internal carotid artery sign: Prevalence and prognostic relevance in stroke thrombolysis. *Stroke research and treatment*. 2011;2011:843607

PART 2

CT-imaging in Acute Ischemic Stroke: Technique Optimization

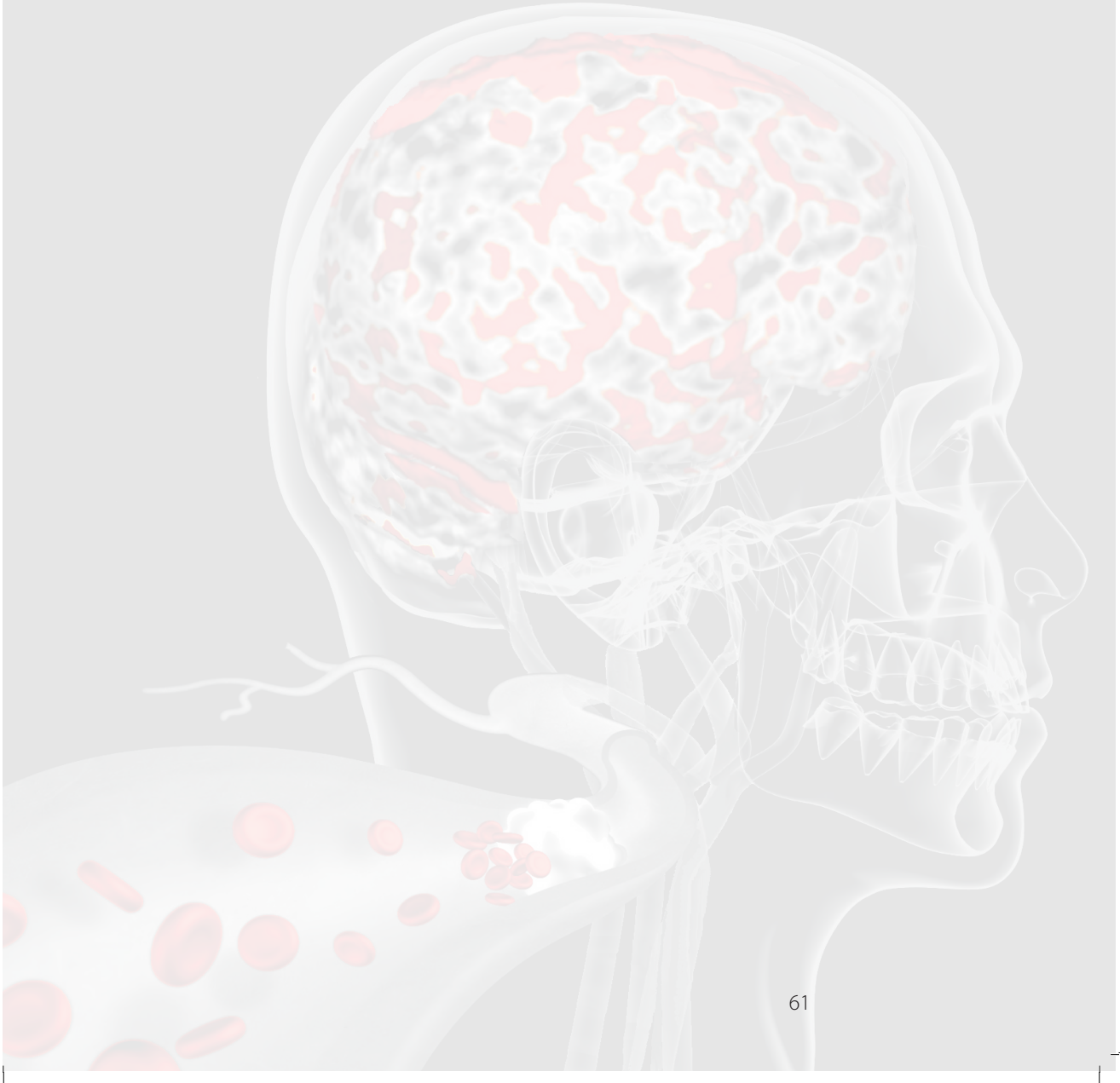

Diagnostic accuracy of CT-perfusion imaging for detecting acute ischemic stroke: a systematic review and meta-analysis

JM Niesten*, JM Biesbroek*, JW Dankbaar, GJ Biessels, BK Velthuis, JB Reitsma, IC van der Schaaf

*Shared first authors

Cerebrovascular Diseases, 2013

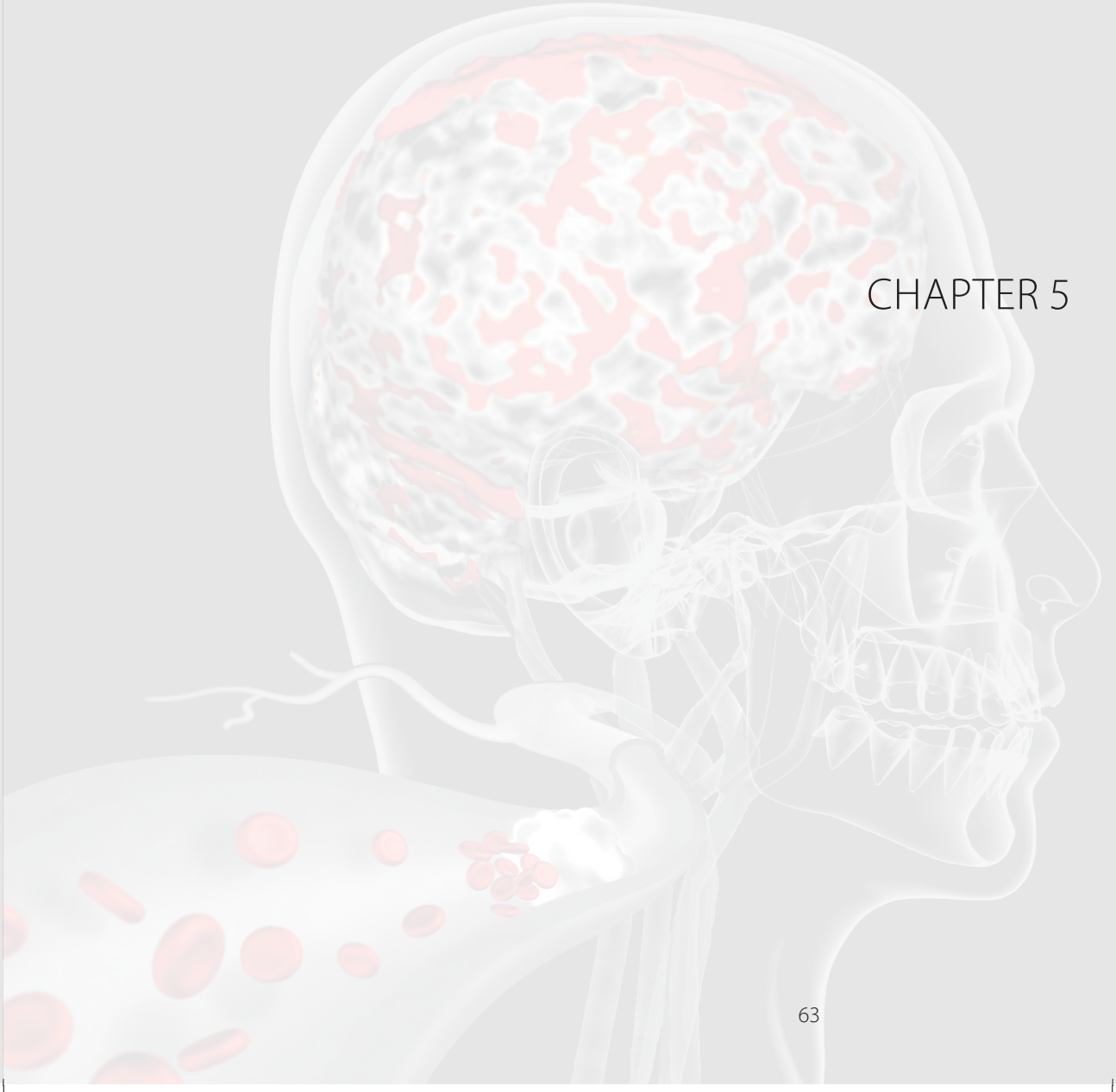

CHAPTER 5

ABSTRACT

Background

The aim of the current study was to determine the sensitivity and specificity of CT-perfusion for the detection of ischemic stroke by performing a systematic review and meta-analysis of published reports.

Methods

We searched Pubmed, Embase and the Cochrane library using the terms "perfusion computed tomography", "ischemic stroke" and synonyms. We included studies that: 1) reported original data; 2) studied the diagnostic value of CT-perfusion for detecting ischemic stroke 3) used MRI-DWI or follow-up MRI or follow-up CT as the reference standard; 4) included at least 10 patients who were suspected of ischemic stroke; and 5) reported the number of true positives, true negatives, false positives and false negatives for the diagnosis of ischemic stroke.

Results

Fifteen studies were finally included in the current review with a total of 1107 patients. A pooled analysis resulted in a sensitivity of 80% (95% CI 72-86%) and a specificity of 95% (95% CI 86-98%). Almost two-thirds of the false negatives were due to small lacunar infarcts; the remaining false negatives were mostly due to limited coverage.

Conclusion

The current systematic review shows that CT-perfusion has a high sensitivity and a very high specificity for detecting infarcts.

INTRODUCTION

On arrival to the emergency department patients with symptoms of acute ischemic stroke are currently often evaluated with CT-perfusion (CTP). Adding CTP to non-contrast CT has been shown to increase the diagnostic accuracy for the detection of ischemia [1]. Furthermore, CTP can be used to determine the extent and potential reversibility of ischemia. This may be helpful in selecting patients who are likely to benefit from thrombolytic therapy [2-6].

Although promising, CTP does not always accurately predict the presence or absence of ischemic stroke. An ischemic lesion may not be detected, leading to a false negative evaluation of the CTP images. In addition, several diseases such as extracranial carotid artery stenosis and proximal intracranial stenosis can mimic perfusion patterns seen in acute cerebral ischemia, leading to a false positive evaluation [7-10].

Since its introduction, the accuracy of CTP for detecting ischemic stroke has been the subject of several studies. To date, a systematic review comparing these studies has not been performed. The purpose of our study is to systematically review published reports to determine the sensitivity and specificity of CTP for the detection of ischemic stroke.

METHODS

Search strategy

We searched Pubmed, Embase and the Cochrane library using the terms "perfusion computed tomography", "ischemic stroke" and synonyms (the complete search syntax is provided in supplemental table 1). All papers published until May 5, 2012 were included. Titles and abstracts of the obtained articles were screened for relevance. The full text of articles that were eligible for inclusion based on the title and abstract were read and assessed for inclusion independently by two authors (J.M.B. and J.M.N.). Disagreements were resolved by consensus. The bibliographies of the included articles were screened to find additional eligible reports.

Inclusion and exclusion criteria

We included studies that: 1) reported original data; 2) studied the diagnostic value of CTP for detecting ischemic stroke; 3) used MRI-DWI, follow-up MRI or follow-up CT as the reference standard; 4) included at least 10 patients who were suspected of ischemic stroke; and 5) reported the number of true positives, true negatives, false positives and false negatives for the diagnosis of ischemic stroke. All study designs (prospective and retrospective) were included. Studies that used duplicate data were excluded. If a study supplied insufficient data to meet the inclusion criteria, an effort was made to contact the study authors to request additional information; if there was no response, the study was excluded.

Data extraction

Data was extracted from all included articles by two authors (J.M.B. and J.M.N.) Disagreements were resolved by consensus. Extracted data included study population characteristics, technical information regarding the CTP acquisition, the proportion of patients with ischemic stroke as determined by the reference standard and the accuracy of CTP (number of true and false positives and true and false negatives) for the diagnosis of ischemic stroke. The methodological quality of each study was assessed using the QUADAS criteria, with a maximum score of 13 points (supplemental table 2) [11]. Specific guidance for scoring the items was developed acknowledging the specific characteristics of the current review.

Statistical and Data Analysis

We used a bivariate, random effects model to meta-analyze the pairs of sensitivity and specificity calculated from each study in order to obtain summary estimates with corresponding 95% confidence intervals. The bivariate approach simultaneously models the logit transformed sensitivity and specificity from studies, thereby incorporating any correlation that might exist between these measures. The model uses a random effects approach for both sensitivity and specificity, allowing for heterogeneity beyond chance due to clinical and methodological differences between studies. Forest plots of sensitivity and specificity with their corresponding 95% confidence intervals (CI) using the Wilson method were generated.

Covariates were added to the bivariate model to examine whether sensitivity and/or specificity were different depending on specific study characteristics. These subgroup analyses were performed on: 1) only studies with a prospective design (8 studies); 2) only studies in which patients were scanned within six hours of the onset of symptoms (8 studies) and 3) including only patients in which the false negative findings were not due to limited brain coverage (536 patients).

The non-linear mixed models procedure (PROC NLMIXED) of SAS (version 9.2, SAS Institute, Cary, N.C., USA) was used to estimate the parameters of the bivariate models. Other analyses were performed with StatXact (version 6.0, Cytel Software Corporation,Cambridge, Mass., USA). In the subgroup analyses, P-values below 0.05 were considered statistically significant.

RESULTS

Our search yielded 1768 unique results. After screening title and abstract, 60 papers were selected for full text screening. The bibliographies of the included articles did not result in the inclusion of additional studies, thereby validating the applied search string. After screening the full text of these 60 articles, 15 articles [1, 12-25] were finally included in the current study. A flow chart of the inclusion of studies is provided in figure 1.

Figure 1 *Flowchart of the search strategy and the selection of reports. The search was conducted on May 5, 2012*

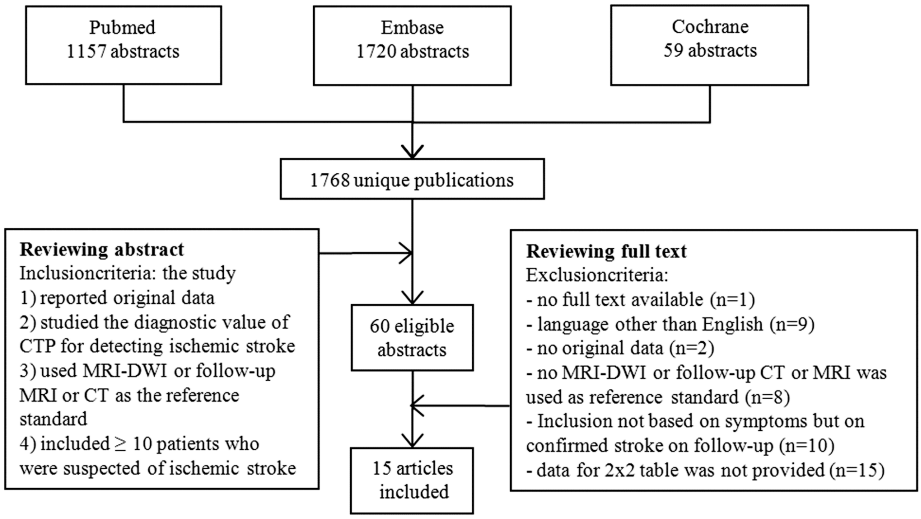

Study characteristics

The patient characteristics, the proportion of patients with a final diagnosis of stroke, and the QUADAS score of the included studies are summarised in table 1. The 15 included studies totalled 1107 patients with a median of 42 patients per study (range 12 to 422). Eight studies had a prospective design and 5 studies a retrospective design (not specified in 2 studies). None of the studies excluded patients with a lacunar syndrome. The maximum time between the onset of clinical symptoms and CTP acquisition ranged from 3 hours to 24 hours; mean time from symptom onset (provided by 9 out of 15 studies) ranged from 2.3 to 5.5 hours. Two studies excluded patients who received thrombolytic therapy; for the remaining studies the proportion of treated patients ranged from 17% to 59% (not specified in 4 studies). The proportion of patients with a final diagnosis of ischemic stroke ranged from 37% to 100% (median 76%). The quality of the included studies as assessed by the QUADAS tool varied considerably (median QUADAS score 11; range 5-13).

Data regarding the acquisition, postprocessing and review methods of CTP are summarised in table 2. Brain coverage ranged from 5-10 mm to 80 mm (median 20 mm) and the slice thickness was either 5 mm or 10 mm in all studies (not specified in 1 study). Temporal resolution varied from 500 ms to 5000 ms (median 1000 ms). Four studies used postprocessing software that was based on the maximum-slope model compared to 11 studies that used deconvolution-based software. The CTP color maps were reviewed by 'visual assessment' in 13 studies; two studies used thresholds for defining infarcted tissue.

Table 1 *Characteristics of included studies*

Study	*Year*	*Study design*	*Patients, n*	*NIHSS, mean (SD)*	*Time to CTP, maximum (mean) †*	*Patients thrombolysed, n (%)*	*Reference standard*	*Time to reference standard‡*	*Stroke, n (%)*	*QUADAS score*
Eckert	2010	P	107	8.3 (NS)	6 (NS)	51 (48)	FU MR or CT	2-5 days	76 (71)	11
Lin	2009	R	100	12 (4-28)§	3 (NS)	25 (25)	DWI	< 7 days	65 (65)	11
Rai	2008	R	422	NS	15 (3.9)	0 (0)||	DWI	< 7 days	157 (37)	12
Youn	2008	R	58	NS	24 (3.4)	14 (24)	DWI	< 27 hours	51 (88)	12
Langer	2007	P	50	6 (0-28)§	8 (NS)	NS	FU CT	> 48 hours	38 (76)	8
Suzuki	2005	NS	118	NS	10 (NS)	20 (17)	FU MR or CT	NS	110 (93)	5
Wintermark	2005	R	46	NS	12 (5.5)	0 (0)||	FU MR or CT	2-18 days	26 (57)	13
Esteban	2004	R	42	NS	6 (NS)	NS	FU MR or CT	1-2 days	29 (69)	10
Kloska	2004	P	41	10.5(NS)#	8 (3.1)	NS	FU MR or CT	1-11 days	38 (93)	11
Schramm	2004	P	22	10 (4-28)§	6 (2.3)	13 (59)	FU CT	5 days	13 (59)	11
Eastwood	2003	P	15	12.6 (5.9)	8 (3.1)	3 (20)	DWI	<11 hours	14 (93)	11
Roberts	2001	NS	12	NS	6 (NS)	NS	FU MR or CT	> 1 day	9 (75)	7
Rother	2000	P	22	13.2 (5.2)	6 (2.4)	6 (27)	FU CT	NS	20 (91)	9
Reichenbach	1999	P	20	NS	6 (2.8)	7 (35)	FU MR or CT	NS	20 (100)	7
Koenig	1998	P	32	NS	6 (2.7)	10 (31)	FU MR or CT	NS	28 (88)	7

R: retrospective; P: prospective; NS: not stated. †Time from the onset of symptoms to CTP acquisition in hours. ‡Time from the onset of symptoms to reference standard acquisition. §Median with range provided instead of mean. ||Patients who were treated with thrombolysis were excluded. #Mean NIHSS provided for 44 patients, three of whom were excluded from the analysis because they suffered infratentorial stroke.

Table 2 *Perfusion CT acquisition and review methods of the included studies*

Study	*CT-scanner used*	*Brain coverage (mm)*	*Slice thickness (mm)*	*Temporal resolution (ms)*	*Software used*	*Color maps used*	*Review method*
Eckert	Philips 40-slice	40	10	1500	Deconvolution	CBV, MTT	Visual assessment
Lin	Siemens 16-slice	24	12	1000	Maximum slope	TTP, CBV, CBF	Visual assessment
Rai	GE Multislice#	20	10	500	Deconvolution	CBV, CBF, MTT	Visual assessment
Youn	Philips 64-slice	80	10	4000	Deconvolution	TTP, CBV, CBF, MTT	Visual assessment
Langer	GE Multislice#	NS	NS	800	Deconvolution	CBV, CBF, MTT	Visual assessment
Suzuki	GE 64-slice	30	10	2000	Deconvolution	CBV, CBF, MTT	Visual assessment
Wintermark	Philips Multislice#	40	10	1000	Deconvolution	TTP, CBV, CBF, MTT	Visual assessment
Esteban	GE 16-slice	20	5-10	1000	Deconvolution	CBV, CBF, MTT	Visual assessment
Kloska	Siemens 4-slice	20	10	1000	Maximum slope	TTP, CBV, CBF	Visual assessment
Schramm	Siemens Multislice#	20	10	1000	Maximum slope	TTP, CBV, CBF	Visual assessment
Eastwood	GE 1-slice	5-10	5-10	500-1000	Deconvolution	CBV, CBF, MTT	Threshold*
Roberts	GE Multislice#	40	10	5000	Deconvolution	TTP, CBV, CBF, MTT	Visual assessment
Rother	Siemens Slip-Ring	10	10	1000-1600	Deconvolution	TTP	Threshold †
Reichenbach	Siemens Slip-Ring	10	10	1000	Deconvolution	TTP	Visual assessment
Koenig	Siemens Slip-Ring	10	10	1000	Maximum slope	CBF	Visual assessment

TTP: time to peak; CBV: cerebral blood volume; CBF: cerebral blood flow; MTT: mean transit time. *Defined thresholds: CBV <1.5 mL/100g; CBF <10 mL/100g/min; MTT >6 seconds. †Defined threshold: TTP > 6 seconds delay. #Only information about CT vendor provided.

Diagnostic accuracy

The sensitivity and specificity of CTP for diagnosing ischemic stroke as reported by the 15 included studies are shown in figure 2. A pooled analysis resulted in a sensitivity of 80% (95% CI 72-86%) and a specificity of 95% (95% CI 86-98%). The pooled sensitivity and specificity are presented in figure 3.

Figure 2 *Left: sensitivity of CTP for detecting ischemic stroke. n=number of true positives, N= number of true positives + number of false negatives. Right: specificity of CTP for detecting ischemic stroke. n=number of true negatives, N= number of true negatives + number of false positives.*

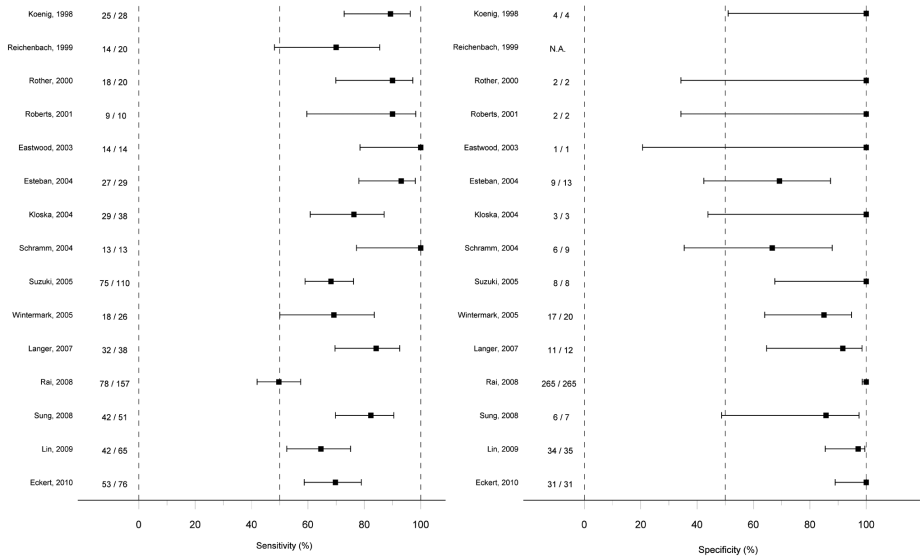

CHAPTER 5

Figure 3 *Left: Diagnostic accuracy of the included studies for detecting ischemic stroke. The circle size represents the sample size of the corresponding study. Right: 95% confidence ellips around mean sensitivity and specificity, which is represented by the square. The triangles represent the sensitivity and specificity of each included study.*

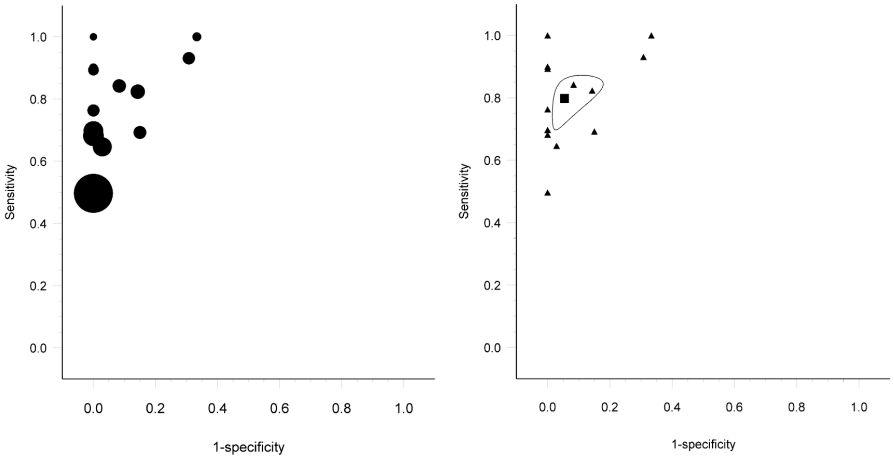

False negatives and false positives

Thirteen studies specified the false negative findings. In these 92 false negative CTP findings the missed infarcts were located outside the CTP covered brain area in 31 patients (supplemental table 3). In 61 patients the missed infarct was located within the covered brain area; five of these were missed due to motion artefacts; 54 patients had a lacunar infarct and 2 had a territorial infarct. Rai et al. [13] and Suzuki et al. [16] did not specify the location and type of infarct for all false negative findings. In all 15 studies combined false positive findings (i.e. perfusion deficits without an ischemic lesion on follow-up imaging) were reported in 13 patients. Seven of these patients were diagnosed with transient ischemic attack which might have resulted in a transient perfusion deficit; in 1 patient the false positive finding was due to a chronic ischemic lesion; the cause was not specified in 5 patients.

Subgroup analyses

The results of the subgroup analyses are summarized in table 3. In the first subgroup analysis, including only studies (n=8) with a prospective design, the sensitivity increased to 85% (95%CI 75-92%) and specificity increased slightly to 97% (95%CI 77-100%). There were no statistically significant differences in sensitivity (P=0.11) and specificity (P=0.73) between prospective and retrospective studies. In the second subgroup analysis, including only studies (n=8) that stated that all patients underwent CTP within 6 hours of symptom onset, sensitivity increased slightly to 83% (95%CI 73-90) and specificity decreased slightly to 94% (95%CI 76-99). The increase in sensitivity (P=0.29) and decrease in specificity (P=0.73) were not statistically significant. In the third subgroup analysis, including only the 13 studies that specified the false negative findings and excluding 31 false negative findings due to limited brain coverage, sensitivity increased to 89% (95%CI 81-94%) and specificity decreased to 90% (95%CI 78-96).

Table 3 *Pooled analyses*

	Studies, n	*Patients, n*	*Sensitivity, % (95% CI)*	*Specificity, % (95%CI)*
All studies	15	1107	80 (72-86)	95 (86-98)
Prospective study design	8	309	85 (75-92)	97 (77-100)
< 6 hours between symptom onset and CTP acquisition	8	357	83 (73-90)	94 (76-99)
After exclusion FN due to limited coverage	13	536	89 (81-94)	90 (79-96)

FN: false negatives

DISCUSSION

The findings of the current systematic review show that CT perfusion has a very high specificity, and a high sensitivity for the diagnosis of ischemic stroke. False negatives mainly occurred in case of small lacunar infarcts. Other causes for false negatives were limited brain coverage and motion artefacts.

The sensitivity of CTP varied considerably between studies, which is probably due to heterogeneity in patient characteristics, CTP spatial and temporal resolution and postprocessing methods. Therefore, the point estimates for sensitivity and specificity from our meta-analysis should be interpreted with some caution. We identified several potential sources of heterogeneity. Firstly, the proportion of patients with lacunar infarcts varied between studies. Patients with lacunar infarcts should not be excluded when studying the diagnostic accuracy of CTP because in the acute phase lacunar syndromes cannot always be distinguished clinically from non-lacunar infarcts and both groups are likely to benefit from thrombolytic therapy [26]. Secondly, the maximum time between symptom onset and CTP scan acquisition varied between studies. Larger time interval between symptom onset and CTP acquisition might be expected to increase sensitivity because after 6-12 hours ischemia can also be visible on unenhanced CT. To assess this, a subgroup analysis was performed including only studies that stated that all patients underwent CTP within 6 hours of the onset of symptoms. This time window was chosen because intra-arterial thrombolysis in patients with anterior circulation ischemic stroke is recommended and generally performed within 6 hours [27-29]. In this analysis sensitivity and specificity remained essentially the same. Thirdly, the proportion of patients with a confirmed diagnosis of ischemic stroke ranged from 37 to 100%, which may reflect differences in patient selection. Fourthly, coverage and temporal resolution of CT perfusion imaging varied between studies. The oldest studies used only one CTP slice of 5-10 mm width, whereas more recent studies used CTP with up to 8 slices of 10 mm width. In the past few years, CT scanners that allow CTP imaging of the entire brain with good temporal resolution have been introduced and are likely to improve the sensitivity of CTP. In the subgroup analysis in which 31 false negative findings due to limited brain coverage were excluded, sensitivity increased from 80% to 89%. However, many institutions still use CT scanners without full brain coverage. Youn et al. [14] and Roberts et al. [22] used the "toggling table" technique which results in a doubled volume coverage at the cost of decreased temporal resolution which may decrease spatial resolution if the arterial curves are undersampled. Fifthly, postprocessing of the raw CTP data differed between studies. Eleven studies used deconvolution-based software to calculate the CTP color maps, whereas four studies used maximum-slope-based software. However, these two different types of software have been shown to yield comparable qualitative and quantitative results [30]. None of the studies used tracer delay insensitive perfusion algorithms in their software. It has recently been shown that using tracer-delay sensitive methods will result in an overestimation of the perfusion abnormalities in stroke patients [31]. This may have contributed to false positive evaluation of CTP maps. However, this occurred only in a total of 13 patients in the studies analyzed in this review. Another potential cause of false positive findings is transient ischemia that might have resulted in a perfusion deficit that did not correspond with an ischemic lesion on follow-up. Sixthly, 8 studies had a prospective design, 5 studies had a retrospective design and 2 studies did not specify their design. We performed a subgroup

analysis including only the 8 prospective studies which showed a slight, but statistically insignificant increase in sensitivity (80% to 85%) and specificity (95% to 97%). Therefore, the impact of differences in study design of the included studies on diagnostic accuracy appears to be small. Finally, the CTP color maps review methods varied between studies. In 13 studies the CTP color maps were subjectively reviewed by "visual assessment", whereas two studies applied thresholds. Currently, no consensus exists regarding optimal thresholds to distinguish infarct core and penumbra from well-perfused brain tissue [32]. The 2 studies using thresholds showed similar sensitivity and specificity compared to the other 13 studies. Currently, most postprocessing software packages provide a summary map in addition to the color maps. This summary map estimates the size and location of the infarct core and penumbra and enables quick interpretation by neurologists and radiologists in both academic and non-academic centers. The summary map results from software-dependent thresholds of quantitative perfusion values. Frequently used thresholds to calculate summary maps are a prolonged MTT of more than 145% compared to the non-ischemic hemisphere to identify the whole ischemic region in combination with absolute CBV values to differentiate infarct core (CBV < 2.0 mL/100g) from potentially salvageable penumbra (CBV ≥ 2.0 mL/100g) [33]. However, some software packages apply other thresholds or use other perfusion parameters (for example CBF) to estimate the infarct core and penumbra. Using different thresholds or perfusion parameters to estimate penumbra and infarct core can result in large differences in summary maps [34]. These findings emphasize the need for standardization of CTP analysis algorithms and software.

Since CTP has improved in the last decade, the reported diagnostic accuracy might be an underestimation of the accuracy that may be achieved using contemporary software and full brain coverage. New postprocessing techniques have been developed to improve the detection of lacunar infarcts [35] and full coverage has been shown to improve the detection of ischemic lesions [36]. Since the current review, based on relatively older studies, shows that CTP has a high sensitivity and very high specificity for detecting ischemic stroke, diagnostic accuracy will only increase with newer software and full brain coverage.

The use of CTP has some considerations that need to be addressed. Firstly, acute CT stroke protocols (with CTP and CTA arch to vertex) require more time than NCCT alone, although only in the order of minutes [35, 37]. Secondly, due to iodinated contrast administration around 2-3% of patients develop a contrast-induced nephropathy, however the risk for developing long-term renal sequelae is negligible [36-39]. Thirdly, CTA and CTP increase the radiation dose with around 4-6 times on average compared to the dose of an unenhanced CT scan of the head, depending on the scan parameters used [38-41]. The results of our review suggest that increased brain coverage might increase the accuracy of CTP. However, a 14 cm full brain coverage scan with a 320-detector row CT

increases the effective radiation doses with around 40% when compared to 3.2 cm coverage with a 64-row CT [40, 42]. Several new technical modifications and recently introduced reduction techniques like iterative reconstruction can help to reduce radiation exposure [41, 43]. Therefore, a combination of newer scanners with new technical modifications and reduction techniques might lead to improved diagnostic accuracy at an acceptable radiation dose. CTP has been shown to be at least two times more sensitive than NCCT alone for detecting acute ischemic stroke and can facilitate in the clinical treatment decision making [1, 5]. Diffusion weighted MRI is considered the most accurate imaging modality for detecting acute ischemic stroke, with a very high sensitivity (88 to 100%) and specificity (95 to 100%) [27]. Furthermore, in multimodal MR including perfusion-weighted imaging the penumbra can be estimated as regions of perfusion change without a corresponding diffusion abnormality (diffusion-perfusion mismatch) [27]. Advantages of the multimodal CT approach over MRI include wider availability of emergency CT imaging, rapid imaging, and fewer contraindications to CT versus MRI [27]. Current treatment protocols for the emergency management (i.e. thrombolysis and thrombectomy) of patients with acute ischemic stroke are not yet based on perfusion imaging [27]. A number of studies have provided support for perfusion imaging-based selection for the treatment of acute ischemic stroke [44-47]. However, there is currently insufficient evidence that perfusion imaging-based treatment protocols result in improved clinical outcome [48].

The current systematic review shows that CT perfusion has a high sensitivity and a very high specificity for detecting infarcts. Spatial resolution remains an important limitation of CTP since almost two-thirds of the false negatives were due to small lacunar infarcts. Another drawback in CTP until recently has been the limited brain coverage. However, recently introduced CT systems that are equipped with new postprocessing techniques and allow full brain CT perfusion could resolve these issues, and will likely further improve the diagnostic accuracy of CTP. Therefore, future studies should focus on increasing sensitivity for the detection of lacunar infarcts by optimizing CTP techniques.

REFERENCES

1. Lin K, Do KG, Ong P, Shapiro M, Babb JS, Siller KA, Pramanik BK. Perfusion CT improves diagnostic accuracy for hyperacute ischemic stroke in the 3-hour window: study of 100 patients with diffusion MRI confirmation. Cerebrovasc Dis 2009;28:72-79.
2. Barber PA, Demchuk AM, Hudon ME, Pexman JH, Hill MD, Buchan AM. Hyperdense sylvian fissure MCA "dot" sign: A CT marker of acute ischemia. Stroke. 2001;32(1):84-8.
3. Wintermark M. Brain perfusion-CT in acute stroke patients. Eur Radiol 2005;15 Suppl 4:D28-31.
4. Parsons MW, Pepper EM, Bateman GA, Wang Y, Levi CR. Identification of the penumbra and infarct core on hyperacute noncontrast and perfusion CT. Neurology 2007;68:730-736.
5. Bivard A, Spratt N, Levi C, Parsons M. Perfusion computer tomography: imaging and clinical validation in acute ischaemic stroke. Brain 2011;134:3408-3416.
6. Agarwal S, Jones PS, Alawneh JA, Antoun NM, Barry PJ; Carrera E, Cotter PE, O`Brien EW, Salih I, Scoffings DJ, Baron JC, Warburton EA. Does perfusion computed tomography facilitate clinical decision making for thrombolysis in unselected acute patients with suspected ischaemic stroke? Cerebrovasc Dis 2011;32:227-233.
7. Eastwood JD, Lev MH, Azhari T, Lee TY, Baboriak DP; Delong DM, Fitzek C, Herzau M, Wintermark M, Meuli R, Brazier D, Provenzale JM. CT perfusion scanning with deconvolution analysis: pilot study in patients with acute middle cerebral artery stroke. Radiology 2002;222:227-236.
8. Waaijer A, van der Schaaf IC, Velthuis BK, Quist M, van Osch MJ, Vonken EP, van Leeuwen MS, Prokop M. Reproducibility of quantitative CT brain perfusion measurements in patients with symptomatic unilateral carotid artery stenosis. AJNR Am J Neuroradiol 2007;28:927-932.
9. Jongen LM, van der Worp HB, Waaijer A, van der Graaf Y, Mali WP. Interrelation between the degree of carotid stenosis, collateral circulation and cerebral perfusion. Cerebrovasc Dis 2010;30:277-284.
10. Waaijer A, van Leeuwen MS, van Osch MJ, van der Worp BH, Moll FH, Lo RT, Mali WP, Prokop M. Changes in cerebral perfusion after revascularization of symptomatic carotid artery stenosis: CT measurement. Radiology 2007;245:541-548.
11. Whiting P, Rutjes AW, Reitsma JB, Bossuyt PM, Kleijnen J. The development of QUADAS: a tool for the quality assessment of studies of diagnostic accuracy included in systematic reviews. BMC Med Res Methodol 2003;3:25.
12. Eckert B, Kusel T, Leppien A, Michels P, Muller-Jensen A, Fiehler J. Clinical outcome and imaging follow-up in acute stroke patients with normal perfusion CT and normal CT angiography. Neuroradiology 2011;53:79-88.
13. Rai AT, Carpenter JS, Peykanu JA, Popovich T, Hobbs GR, Riggs JE. The role of CT perfusion imaging in acute stroke diagnosis: a large single-center experience. J Emerg Med 2008;35:287-292.
14. Youn SW, Kim JH, Weon YC, Kim SH, Han MK, Bae HJ. Perfusion CT of the brain using 40-mm-wide detector and toggling table technique for initial imaging of acute stroke. AJR Am J Roentgenol 2008;191:W120-126.
15. Langer RD, Neidl van Gorkom K, Al Kaabi HO, Torab F, Czechowski J, Nagi M, Ashish GM. Comparison of two imaging protocols for acute stroke: unenhanced cranial CT versus a multimodality cranial CT protocol with perfusion imaging. Australas Radiol 2007;51:532-537.
16. Suzuki Y, Nakajima M, Ikeda H, Abe T. Evaluation of hyperacute stroke using perfusion computed tomography. Neurol Med Chir (Tokyo) 2005;45:333-343;discussion 341-343.
17. Wintermark M, Fischbein NJ, Smith WS, Ko NU, Quist M, Dillon WP. Accuracy of dynamic perfusion CT with deconvolution in detecting acute hemispheric stroke. AJNR Am J Neuroradiol 2005;26:104-112.
18. Esteban JM, Cervera V. Perfusion CT and angio CT in the assessment of acute stroke. Neuroradiology 2004;46:705-715.
19. Kloska SP, Nabavi DG, Gaus C, Nam EM, Klotz E, Ringelstein EB, Heindel W. Acute stroke assessment with CT: do we need multimodal evaluation? Radiology 2004;233:79-86.
20. Schramm P, Schellinger PD, Klotz E, Kallenberg K, Fiebach JB, Kulkens S, Heiland S, Knauth M, Sartor K. Comparison of perfusion computed tomography and computed tomography angiography source images with perfusion-weighted imaging and diffusion-weighted imaging in patients with acute stroke of less than 6 hours' duration. Stroke 2004;35:1652-1658.
21. Eastwood JD, Lev MH, Wintermark M, Fitzek C, Barboriak DP, Delong DM, Lee TY, Azhari T, Herzau M, Chilukuri VR, Provenzale JM. Correlation of early dynamic CT perfusion imaging with whole-brain MR diffusion and perfusion imaging in acute hemispheric stroke. AJNR Am J Neuroradiol 2003;24:1869-1875.
22. Roberts HC, Roberts TP, Smith WS, Lee TJ, Fischbein NJ, Dillon WP. Multisection dynamic CT perfusion for acute cerebral ischemia: the "toggling-table" technique. AJNR Am J Neuroradiol 2001;22:1077-1080.
23. Rother J, Jonetz-Mentzel L, Fiala A, Reichenbach JR, Herzau M, Kaiser WA, Weiller C. Hemodynamic assessment of acute stroke using dynamic single-slice computed tomographic perfusion imaging. Arch Neurol 2000;57:1161-1166.

24. Reichenbach JR, Rother J, Jonetz-Mentzel L, Herzau M, Fiala A, Weiller C, Kaiser WA. Acute stroke evaluated by time-to-peak mapping during initial and early follow-up perfusion CT studies. AJNR Am J Neuroradiol 1999;20:1842-1850.
25. Koenig M, Klotz E, Luka B, Venderink DJ, Spittler JF, Heuser L. Perfusion CT of the brain: diagnostic approach for early detection of ischemic stroke. Radiology 1998;209:85-93.
26. Cocho D, Belvis R, Marti-Fabregas J, Bravo Y, Aleu A, Pagonabarraga J, Molina-Porcel L, Diaz-Manera J, San Roman L, Martinez-Lage M, Martinez A, Moreno M, Marti-Vilalta JL.. Does thrombolysis benefit patients with lacunar syndrome? European neurology 2006;55:70-73.
27. Jauch EC, Saver JL, Adams HP Jr, Bruno A, Connors JJ, Demaerschalk BM, Khatri P, McMullan PW Jr, Qureshi AI, Rosenfield K, Scott PA, Summers DR, Wang DZ, Wintermark M, Yonas H; American Heart Association Stroke Council; Council on Cardiovascular Nursing; Council on Peripheral Vascular Disease; Council on Clinical Cardiology. Guidelines for the Early Management of Patients With Acute Ischemic Stroke: A Guideline for Healthcare Professionals From the American Heart Association/American Stroke Association. Stroke 2013;44:870-947.
28. Mullen MT, Pisapia JM, Tilwa S, Messe SR, Stein SC. Systematic review of outcome after ischemic stroke due to anterior circulation occlusion treated with intravenous, intra-arterial, or combined intravenous+intra-arterial thrombolysis. Stroke 2012;43:2350-2355.
29. Mono ML, Romagna L, Jung S, Arnold M, Galimanis A, Fischer U, Kohler A, Ballinari P, Brekenfeld C, Gralla J, Schroth G, Mattle HP, Nedeltchev K. Intra-arterial thrombolysis for acute ischemic stroke in octogenarians. Cerebrovasc Dis 2012;33:116-122.
30. Abels B, Klotz E, Tomandl BF, Kloska SP, Lell MM. Perfusion CT in acute ischemic stroke: a qualitative and quantitative comparison of deconvolution and maximum slope approach. AJNR Am J Neuroradiol 2010;31:1690-1698.
31. Kudo K, Sasaki M, Yamada K, Momoshima S, Utsunomiya H, Shirato H, Ogasawara K. Differences in CT perfusion maps generated by different commercial software: quantitative analysis by using identical source data of acute stroke patients. Radiology 2010;254:200-209.
32. Dani KA, Thomas RG, Chappell FM, Shuler K, Muir KW, Wardlaw JM. Systematic review of perfusion imaging with computed tomography and magnetic resonance in acute ischemic stroke: heterogeneity of acquisition and postprocessing parameters: a translational medicine research collaboration multicentre acute stroke imaging study. Stroke 2012;43:563-566.
33. Wintermark M, Flanders AE, Velthuis B, Meuli R, van Leeuwen M, Goldsher D, Pineda C, Serena J, van der Schaaf I, Waaijer A, Anderson J, Nesbit G, Gabriely I, Medina V, Quiles A, Pohlman S, Quist M, Schnyder P, Bogousslavsky J, Dillon WP, Pedraza S. Perfusion-CT assessment of infarct core and penumbra: receiver operating characteristic curve analysis in 130 patients suspected of acute hemispheric stroke. Stroke 2006;37:979-985.
34. Fahmi F, Marquering HA, Streekstra GJ, Beenen LF, Velthuis BK, VanBavel E, Majoie, CB. Differences in CT perfusion summary maps for patients with acute ischemic stroke generated by 2 software packages. AJNR Am J Neuroradiol 2012;33:2074-2080.
35. Mendrik AM, Vonken EJ, van Ginneken B, de Jong HW, Riordan A, van Seeters T, Smit EJ, Viergever MA, Prokop M. TIPS bilateral noise reduction in 4D CT perfusion scans produces high-quality cerebral blood flow maps. Phys Med Biol 2011;56:3857-3872.
36. Dorn F, Muenzel D, Meier R, Poppert H, Rummeny EJ, Huber A. Brain perfusion CT for acute stroke using a 256-slice CT: improvement of diagnostic information by large volume coverage. Eur Radiol 2011;21:1803-1810.
37. Fox AJ, Symons SP, Howard P, Yeung R, Aviv RI. Acute stroke imaging: CT with CT angiography and CT perfusion before management decisions. AJNR Am J Neuroradiol 2012;33:792-794.
38. Krol AL, Dzialowski I, Roy J, Puetz V, Subramaniam S, Coutts, SB, Demchuk, AM. Incidence of radiocontrast nephropathy in patients undergoing acute stroke computed tomography angiography. Stroke 2007;38:2364-2366.
39. Hopyan JJ, Gladstone DJ, Mallia G, Schiff J, Fox AJ, Symons SP, Buck BH, Black SE, Aviv RI. Renal safety of CT angiography and perfusion imaging in the emergency evaluation of acute stroke. AJNR Am J Neuroradiol 2008;29:1826-1830.
40. Cohnen M, Wittsack HJ, Assadi S, Muskalla K, Ringelstein A, Poll LW, Saleh A, Modder U. Radiation exposure of patients in comprehensive computed tomography of the head in acute stroke. AJNR Am J Neuroradiol 2006;27:1741-1745.
41. Mnyusiwalla A, Aviv RI, Symons SP. Radiation dose from multidetector row CT imaging for acute stroke. Neuroradiology 2009;51:635-640.
42. Diekmann S, Siebert E, Juran R, Roll M, Deeg W, Bauknecht HC, Diekmann F, Klingebiel R, Bohner Gl. Dose exposure of patients undergoing comprehensive stroke imaging by multidetector-row CT: comparison of 320-detector row and 64-detector row CT scanners. AJNR Am J Neuroradiol 2010;31:1003-1009.
43. Kilic K, Erbas G, Guryildirim M, Arac M, Ilgit E, Coskun B. Lowering the dose in head CT using adaptive statistical iterative reconstruction. AJNR Am J Neuroradiol 2011;32:1578-1582.
44. Garcia-Bermejo P, Calleja AI, Perez-Fernandez S, Cortijo E, del Monte JM, Garcia-Porrero M, Fe Munoz M, Fernandez-Herranz R, Arenillas JF. Perfusion computed tomography-guided intravenous thrombolysis for acute ischemic stroke beyond 4.5 hours: a case-control study. Cerebrovasc Dis 2012;34:31-37.
45. Albers GW, Thijs VN, Wechsler L, Kemp S, Schlaug G, Skalabrin E, Bammer R, Kakuda W, Lansberg MG, Shuaib A, Coplin W, Hamilton S, Moseley M, Marks MP. Magnetic resonance imaging profiles predict clinical response to early reperfusion: the diffusion and perfusion imaging evaluation for understanding stroke evolution (DEFUSE) study. Ann Neurol 2006;60:508-517.

46. Davis SM, Donnan GA, Parsons MW, Levi C, Butcher KS, Peeters A, Barber PA, Bladin C, De Silva DA, Byrnes G, Chalk JB, Fink JN, Kimber TE, Schultz D, Hand PJ, Frayne J, Hankey G, Muir K, Gerraty R, Tress BM. Desmond, P. M.. Effects of alteplase beyond 3 h after stroke in the Echoplanar Imaging Thrombolytic Evaluation Trial (EPITHET): a placebo-controlled randomised trial. Lancet neurol 2008;7:299-309.

47. Parsons M, Spratt N, Bivard A, Campbell B, Chung K, Miteff F, O'Brien B, Bladin C, McElduff P, Allen C, Bateman G, Donnan G, Davis S, Levi Cl. A randomized trial of tenecteplase versus alteplase for acute ischemic stroke. New Engl J Med 2012;366:1099-1107.

48. Yoo AJ, Pulli B, Gonzalez RG. Imaging-based treatment selection for intravenous and intra-arterial stroke therapies: a comprehensive review. Expert Rev Cardiovasc Ther 2011;9:857-876.

Supplemental table 1 *Search syntax*

Database	*Search*
PubMed	1. CT perfusion and synonyms: "**Perfusion CT**"[Title/Abstract] OR "**CT Perfusion**"[Title/Abstract] OR "**perfusion computed tomography**"[Title/Abstract] OR "**computed tomography perfusion**" [Title/Abstract] OR "**dynamic CT**"[Title/Abstract] OR "**dynamic computed tomography**"[Title/Abstract] OR "**perfusion imaging**"[Title/Abstract] OR "**perfusion parameter**"[Title/Abstract] OR "**perfusion parameters**"[Title/Abstract] OR "**cerebrovascular hemodynamics**"[Title/Abstract] OR (**CT**[Title/Abstract] AND "**quantitative assessment**"[Title/Abstract]) OR (**CT**[Title/Abstract] AND "**mean transit time**"[Title/Abstract]) OR (**CT**[Title/Abstract] AND "**time to peak**"[Title/Abstract]) OR (**CT**[Title/Abstract] AND "**cerebral blood volume**"[Title/Abstract]) OR (**CT**[Title/Abstract] AND "**cerebral blood flow**"[Title/Abstract])) AND 2. ischemic stroke and synonyms: "**stroke**" [Title/Abstract] OR "**cerebral ischaemia**"[Title/Abstract] OR "**cerebral ischemia**" [Title/Abstract] OR "**brain ischaemia**" [Title/Abstract] OR "**brain ischemia**"[Title/Abstract] OR "**cerebral infarction**"[Title/Abstract] OR "**brain infarction**" [Title/Abstract] OR "**brain hypoxia**"[Title/Abstract] OR "**cerebral hypoxia**"[Title/Abstract] OR "**cerebrovascular disease**"[Title/Abstract] 3. 1 AND 2
Embase	1. CT perfusion and synonyms "**Perfusion CT**":ab:ti OR "**CT perfusion**":ab:ti OR "**perfusion computed tomography**":ab:ti OR "**computed tomography perfusion**":ab:ti OR "**dynamic CT**":ab:ti OR "**dynamic computed tomography**":ab:ti OR "**perfusion imaging**":ab:ti OR "**perfusion parameter**":ab:ti OR "**perfusion parameters**":ab:ti OR "**cerebrovascular hemodynamics**":ab:ti OR (**CT**:ab:ti AND "**quantitative assessment**":ab:ti) OR (**CT**:ab:ti AND "**mean transit time**":ab:ti) OR (**CT**:ab:ti AND "**time to peak**":ab:ti) OR (**CT**:ab:ti AND "**cerebral blood volume**":ab:ti) OR (**CT**:ab:ti AND "**cerebral blood flow**":ab:ti) 2. Ischemic stroke and synonyms "**stroke**":ab:ti OR "**cerebral ischaemia**":ab:ti OR "**cerebral ischemia**":ab:ti OR "**brain ischaemia**":ab:ti OR "**brain ischemia**":ab:ti OR "**cerebral infarction**":ab:ti OR "**brain infarction**":ab:ti OR "**brain hypoxia**":ab:ti OR "**cerebral hypoxia**":ab:ti OR "**cerebrovascular disease**":ab:ti 3) 1 AND 2
Cochrane	1. CT perfusion and synonyms "**Perfusion CT**":ti,ab,kw OR "**CT perfusion**":ti,ab,kw OR "**perfusion computed tomography**":ti,ab,kw OR "**computed tomography perfusion**":ti,ab,kw OR "**dynamic CT**":ti,ab,kw OR "**dynamic computed tomography**":ti,ab,kw OR "**perfusion imaging**":ti,ab,kw OR "**perfusion parameter**":ti,ab,kw OR "**perfusion parameters**":ti,ab,kw OR "**cerebrovascular hemodynamics**":ti,ab,kw OR (**CT**:ti,ab,kw AND "**quantitative assessment**":ti,ab,kw) OR (**CT**:ti,ab,kw AND "**mean transit time**":ti,ab,kw) OR (**CT**:ti,ab,kw AND "**time to peak**":ti,ab,kw) OR (**CT**:ti,ab,kw AND "**cerebral blood volume**":ti,ab,kw) OR (**CT**:ti,ab,kw AND "**cerebral blood flow**":ti,ab,kw) 2) ischemic stroke and synonyms "**stroke**":ti,ab,kw OR "**cerebral ischaemia**":ti,ab,kw OR "**cerebral ischemia**":ti,ab,kw OR "**brain ischaemia**":ti,ab,kw OR "**brain ischemia**":ti,ab,kw OR "**cerebral infarction**":ti,ab,kw OR "**brain infarction**":ti,ab,kw OR "**brain hypoxia**":ti,ab,kw OR "**cerebral hypoxia**":ti,ab,kw OR "**cerebrovascular disease**":ti,ab,kw 3) 1 AND 2

Supplemental table 2 *Methodological quality scoring*

Quality Item	*Positive Score*
1. Was the spectrum of patients representative of the patients who will receive the test in practice?	Only patients suspected of ischemic stroke were included
2. Were selection criteria clearly described?	It was clear how patients were selected to undergo CTP scan
3. Is the reference standard likely to enable correct classification of the target condition?	Follow-up MRI/CT or early MRI DWI was used as the reference standard.
4. Is the time period between reference standard and Index test short enough to be reasonably sure that the target condition did not change between the two tests?	Time period between CTP and reference standard was short enough.
5. Did the whole sample or a random selection of the sample receive verification with a reference standard?	All patients or a random selection of the patients received verification with the reference standard.
6. Did patients receive the same reference standard regardless of the index test result?	All patients received the same reference standard regardless of the CTP result
7. Was the execution of the index test described insufficient detail to permit replication of the test	The CTP scan protocol (scanner type, acquisition mode, reconstruction method, brain coverage, slice thickness) and interpreter(s) were described.
8. Was the execution of the reference standard described insufficient detail to permit its replication?	Sufficient details or citations were reported to permit replication of the reference standard.
9. Were the index test results interpreted without knowledge of the results of the reference standard?	Interpretation of CTP findings was performed without knowledge of MRI DWI findings.
10. Were the reference standard results interpreted without knowledge of the results of the index test?	Interpretation of the reference standard results was performed without knowledge of the CTP findings.
11. Were the same clinical data available when test results were interpreted as would be available when the test is used in practice?	The observer was aware that the patient was suspected of ischemic stroke and of the side of symptoms when CT results were interpreted.
12. Were uninterpretable and/or intermediate test results reported?	All CTP results, including uninterpretable and/ or intermediate results, were reported.
13. Were withdrawals from the study explained?	It was clear what happened to all patients who entered the study.

Supplemental table 3 *Confirmed infarcts on follow-up that were not detected with perfusion CT*

Study	*Number of FN (% of TP+ FN)*	*Specification of false negatives*			
		Infarct outside CTP coverage (n)	*Infarct within CTP coverage*		
			Motion artefacts	*Lacunar infarcts (n (definition used))*	*Territorial infarcts (n)*
Eckert	23 (30)	7	None	16 (NS)	None
Lin	23 (35)	10	None	13 (≤15 mm in size)	None
Youn	9 (18)	None	None	7 (NS)	2
Langer	6 (16)	None	None	6 (NS)	None
Wintermark	8 (31)	1	4	3 (NS)	None
Esteban	2 (7)	2	None	None	None
Kloska	9 (24)	5	None	4 (<3 cc)	None
Schramm	0 (0)	None	None	None	None
Eastwood	0 (0)	None	None	None	None
Roberts	1 (10)	None	None	1 (NS)	None
Rother	2 (10)	1	None	1 (NS)	None
Reichenbach	6 (40)	2	1	3 (<10 mm width)	None
Koenig	3 (11)	3	None	None	None
Subtotal	92	31	5	54	2
Rai	79 (50)	Not stated	Not stated	Not stated	Not stated
Suzuki	35 (32)	Not stated	Not stated	Not stated	Not stated

FN: false negatives; TP: true positives; CTP: computed tomography perfusion; NS: not specified.

Optimization of vascular input and output functions in CT-perfusion imaging using 256-(or more-)slice multidetector CT

JM Niesten, IC van der Schaaf, AJ Riordan, HWAM de Jong, WPTM Mali, BK Velthuis

European Radiology, 2013

CHAPTER 6

ABSTRACT

Background

To evaluate the accuracy and reproducibility of CT-perfusion (CTP) by finding the optimal artery for the Arterial Input Function (AIF) and re-evaluating the necessity of the Venous Output Function (VOF).

Methods

Forty-four acute ischemic stroke patients who underwent non-enhanced CT, CTP and CT-angiography using 256-slice MDCT were evaluated. The ACA, MCA, ICA and basilar artery were selected as the AIF. Subsequently the resulting area under the time-enhancement curve of the AIF (AUC_{AIF}) and quantitative perfusion measurements were analysed by repeated Measures ANOVA and subsequently the paired t-test. To evaluate reproducibility we examined if the VOF could be deleted by comparing the perfusion measurements using versus not using the VOF (paired t-test).

Results

The AUC_{AIF} and perfusion measurements resulting from the different AIFs showed significant group differences (all $P<0.0001$). The ICA had the largest AUC_{AIF} and resulted in the highest MTT and lowest CBF, while the basilar artery showed the lowest CBV. Not using the VOF showed significantly higher CBV and CBF in 66% of patients on the ipsilateral ($P<0.0001$ and $P=0.007$, respectively) and contralateral hemisphere ($P<0.0001$ and $P=0.019$, respectively).

Conclusion

Selecting the ICA as the AIF and continuing the use of the VOF would improve the accuracy of CTP.

INTRODUCTION

CT-perfusion (CTP) is used worldwide to assess cerebrovascular diseases including ischemic stroke, for the assessment of tumour vascular support and for guiding reperfusion therapy [1-5]. CTP offers rapid assessment, low costs and continuous availability in most clinical facilities [6,7], but also has some limitations concerning the validity of the quantitative perfusion values.
An important problem resulting in reduced accuracy and reproducibility is the selection of the Arterial Input Function (AIF) and Venous Output Function (VOF)[8, 9] with a reported variability in inter-observer agreement between 10 and 27% [10]. Since definitions of salvageable and irreversible tissue, the vascular support of tumours and delayed cerebral ischemia are based on absolute perfusion values [11 12], the pursuit of quantitative CTP remains relevant.

The selection of an AIF and a VOF in CTP using a deconvolution algorithm is necessary to create quantitative maps of CBV, CBF and MTT [7, 13]. The CBV is calculated as the ratio of the area under the time-enhancement curve (AUC) of the first passage through the tissue (AUC_{Tissue}) to the AUC of the first passage of contrast through the artery selected as AIF(AUC_{AIF}) with a hematocrit correction factor H to account for differences in small and large vessels (CBV = H x AUC_{Tissue} / AUC_{AIF}) [14, 15]. Selection of smaller intracranial arteries as the AIF is hampered by partial volume effects, potentially underestimating the AUC_{AIF} [15]. To correct for these partial volume effects a VOF is selected as measured in a venous sinus. Effectively this means that the CBV is inversely related to the AUC_{VOF} (CBV = H x AUC_{Tissue} / AUC_{VOF}) . Subsequently, a noniterative deconvolution method is then applied to calculate the MTT map [16]. The CBF is then calculated according to the central volume principle (CBF=CBV / MTT).
The selection of different vessels as the AIF and VOF can result in different estimations of quantitative perfusion maps and subsequently diverging predictions of the final infarct volume[13, 17].

The accuracy of the quantitative perfusion maps can be improved by selecting an artery with the least partial volume effects as the AIF. Partial volume effects in arteries selected as the AIF result in a decreased signal-to-noise ratio and poorly defined time-attenuation curves. As a result, the curve becomes less precise, leading to an underestimation of the MTT and, following the central volume principle, also to an overestimation of the CBF [15, 17]. As this underestimation of MTT and overestimation of CBF lead to underestimation of the ischemic area, the AIF showing the lowest perfusion can be defined as being most valid in this particular CTP algorithm [15]. The introduction of the 256-(or more-)MDCT systems, with larger perfusion slab coverage [18], provides the opportunity to select the ICAs and basilar artery as the AIF. The influence of partial volume effects in these large and perpendicular arteries will be a lot smaller and the selection of these arteries could therefore result in the most valid quantitative perfusion values. Theoretically, it may even be unnecessary to use the VOF any longer for partial volume correction.

The purpose of this study was to evaluate the accuracy and reproducibility of quantitative perfusion by the assessment of the optimal artery for the AIF and re-evaluating the necessity of the VOF.

MATERIAL AND METHODS

Patients

We reviewed a consecutive series of 58 patients between May 2009 and February 2011, who were diagnosed with an acute ischemic stroke due to an M1 or M2 segment occlusion in the MCA. All patients were derived from a large prospective multicentre observational cohort study. The study was approved by the institutional medical ethics committee. The diagnosis of an infarct due to an occlusion in the MCA was based on the final discharge diagnosis made by experienced stroke-neurologists, based on all clinical and radiological information. On admission, all patients underwent neurological examination, non-enhanced CT, CTP and CT-angiography (CTA). Inclusion criteria were: age ≥ 18 years, onset of stroke symptoms < 9 hours, NIHSS ≥ 2, and informed consent from patient or family, a visible occlusion in the MCA on CTA without a significant carotid artery stenosis (>50%) and CTP performed using 256-slice MDCT. Exclusion criteria were: therapy before neuroimaging and insufficient quality of the CTP to perform adequate measurements.

Imaging

All imaging studies were performed using 256 MDCT (Philips Brilliance iCT, Philips Healthcare, Best, The Netherlands). CT parameters of the non-enhanced CT were: 120 kVp, 300 mAs, and 5 mm reconstructed slice thickness. The collimation width was set to 128x0.625. For CTP 40 mL of contrast agent (300mg I/mL) was injected into the cubital vein (18-gauge needle) at a rate of 6 mL/s followed by a 40 mL saline flush at a rate of 6 mL/s by using a dual power injector (Stellant Dual CT injector; Medrad Europe, Beek, the Netherlands). CTP data acquisition was initiated at the start of the contrast bolus injection. Images were acquired at a temporal sampling rate of 1 image/ 2 sec. The following acquisition and reconstruction parameters were used for the CTP: 80 kVp, 150 mAs, 5 mm reconstructed slice thickness and UB image filter. The CTP slab was performed 4 mm above the sella turcica, assessing twelve 5mm-thick sections.

For CTA 65 mL of contrast agent (300mg I/mL) was injected into the cubital vein (18-gauge needle) at a rate of 6 mL/s followed by a 40 mL saline flush at a rate of 6 mL/s. The following parameters were used for the CTA: 120 kVp, 150 mAs, 0.45-mm reconstruction increment with a 512 x 512 matrix and the standard reconstruction kernel with 1 mm reconstructed slice thickness. The mean total effective dose for the three CT data acquisitions was 6.09 mSv.

Perfusion data was analysed using commercially available software on an Extended Brilliance Workstation (Philips Medical Systems Nederland B.V., PC Best, The Netherlands). The software, which has been validated previously [19],

applied Gaussian curve fitting by least mean squares to obtain mathematical descriptions of the time-enhancement curves, describing the wash-in and the wash-out of the contrast material in these voxels [10, 18, 20], For perfusion measurements motion correction was applied, vascular voxel elimination was done and the edge-preserving spatial filter was disabled to eliminate the influences of spatial blurring on the vessels and ensure that any partial volume effects are not dependent on post-processing steps. After calculation of the CBV map, the MTT was calculated by using a deconvolution operation (as described by Axel [16]), and subsequently CBF was computed according to the central volume principle (CBF=CBV / MTT).

Measurements

For evaluation of the presence of a thrombus in the MCA and significant carotid stenosis, the CTA images were evaluated separately by two observers of which at least one had experience for 5 or more years in neurovascular imaging. Discrepant readings were solved by a third reader. The observers were blinded for all other radiologic, neurologic and clinical data, except for side of symptoms.

Optimizing accuracy

We studied the effect of selecting the AIF in different intracranial arteries without an upstream occlusion on the AUC_{AIF}. Small ROIs in circles of 4mm^2 were placed in the 1) ACA, 2) MCA contralateral to the thrombosed MCA, 3) intracranial ICA contralateral to the thrombosed MCA and 4) the basilar artery (Fig**.** 1).

Figure 1 *Selecting different arteries as the AIF in the axial CTP*

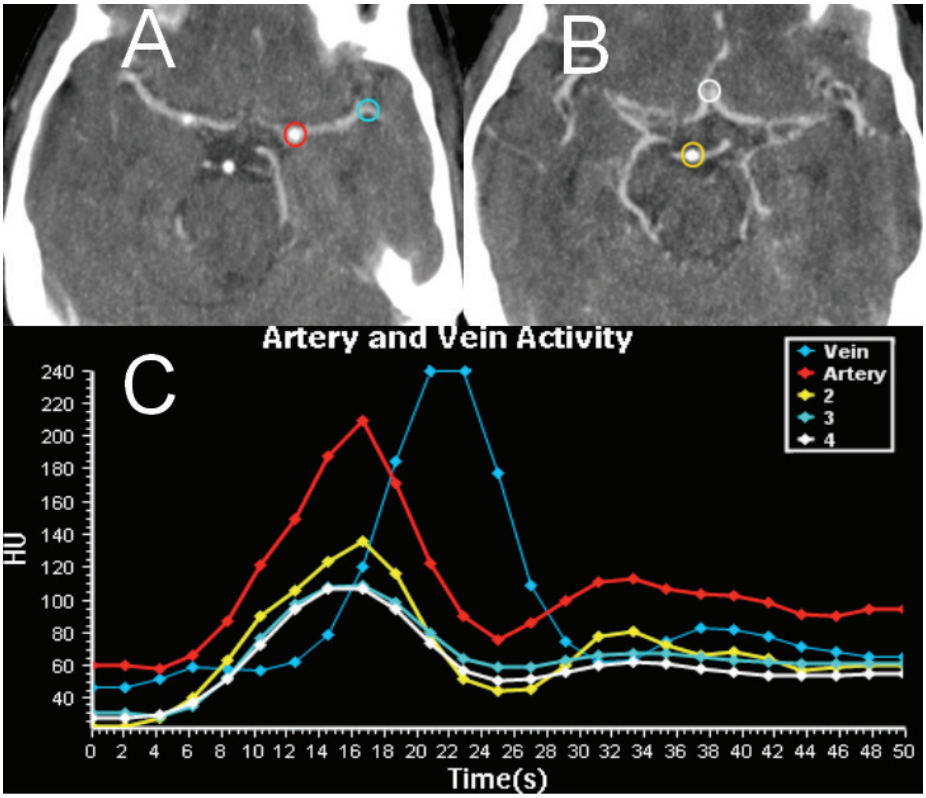

A. Selection of the carotid internal artery (red) and the middle cerebral artery (blue) as the AIF B. Selection of the basilar artery (yellow) and the anterior cerebral artery (white) as the AIF. C Associated curves of the reference voxel with highest AUC (with the VOF, selected on a different slice, in darker blue).

The software then identified the one most appropriate reference voxel (i.e. with the highest AUC) within these ROIs. To find the optimal location for the AIF in the different arteries the ROIs were moved by hand along the arteries while examining the resulting time-attenuation curve that was displayed simultaneously on the monitor and the time-attenuation curve with the largest AUC was chosen. The AUC was measured in the resulting AIF curves using a Gaussian-fit to separate the first pass bolus from the recirculation. For the selection of the VOF we used the same technique as for the selection of the AIF. Second, quantitative perfusion values (CBV, CBF, MTT) were evaluated in ROIs drawn manually in a single representative slice, including white matter and grey matter, in the MCA territory at the level of the lateral ventricles in the slice just above the body of the caudate nucleus, as previously described by Soares et al. [10]The ROI in one hemisphere was mirrored to the contralateral hemisphere and the ROIs remained unchanged with selection of different AIF and VOF locations to ensure valid comparison of CTP values.

Reducing operator dependent post-processing steps

To evaluate the effect of removing the VOF, we placed the VOF in the exact same location as the AIF (in the ICA). In patients in whom the AUC_{AIF} is larger than the AUC_{VOF}, which can be the case in large arteries with none or little partial volume effects, the perfusion software automatically chooses the larger AUC_{AIF} as the baseline value to calculate the CBV. This effectively means that in those cases that the VOF is not used by the software, exactly the same perfusion values were seen when we placed ROI of the VOF from the superior sagittal sinus to the same location as the AIF in the ICA. To analyse the effect of removing the VOF on the perfusion values we therefore only performed analysis in those cases where the AUC_{VOF} was larger than the AUC_{AIF}.

Analysis

Optimizing accuracy

By means of the repeated Measures ANOVA test (comparing paired data between more than two groups) we investigated if differences in the AUC_{AIF} of the ACA, MCA, ICA and basilar artery and the quantitative perfusion measurements resulting from these different arteries were present. Significant group differences were further analysed by the paired t-test to determine individual differences between the artery showing most valid values and the other arteries. The artery with the largest AUC and showing lowest perfusion was defined as being most valid. For all values 95%-confidence intervals are also presented. The analyses for the quantitative perfusion values were performed for the hemisphere ipsi- as well as contralateral to the thrombus.

Reducing operator dependent post-processing steps.

By means of the paired t-test we compared the quantitative perfusion values resulting from the conventionally placed VOF in the venous sinus and the VOF placed in the ICA (i.e. deleting the VOF). For all values 95%-confidence intervals are presented. Analyses were performed for the hemisphere ipsi- as well as contralateral to the thrombus. For all analyses a *P* -value of <0.05 was considered statistical significant.

RESULTS

Of the total of 58 patients, 9 were excluded because they had severe carotid stenosis and 5 patients were excluded because the CTP was of insufficient quality, resulting in a total of 44 patients. The mean age of these patients was 71 years (ranging from 45 to 97 years), 57% were women and twenty thrombi (45%) were located in the right MCA.

Optimizing accuracy

The AUC_{AIF} (in mean Hus) with 95%-confidence intervals (95%CI) of all investigated arteries are shown in Fig**.** 2. Significant group differences were present (*P*<0.001). The ICA showed the largest AUC_{AIF} (mean 1156.3 Hus, 95%CI

1036.2-1276.4) followed by the basilar artery (mean 1075.3 Hus, 95%CI 973.3-1177.3), the MCA (mean 778.1 Hus, 95%CI 709.1-847.1) and the ACA (mean 698.7 Hus, 95%CI 639.0-758.3). The individual differences in AUC_{AIF} were statistically significant between the ICA and the ACA (P<0.0001) and the ICA and MCA (P<0.0001) but not between the ICA and basilar artery (P=0.138).

Figure 2 *AUC_{AIF} of different cerebral arteries (in HUs with 95%CI)*

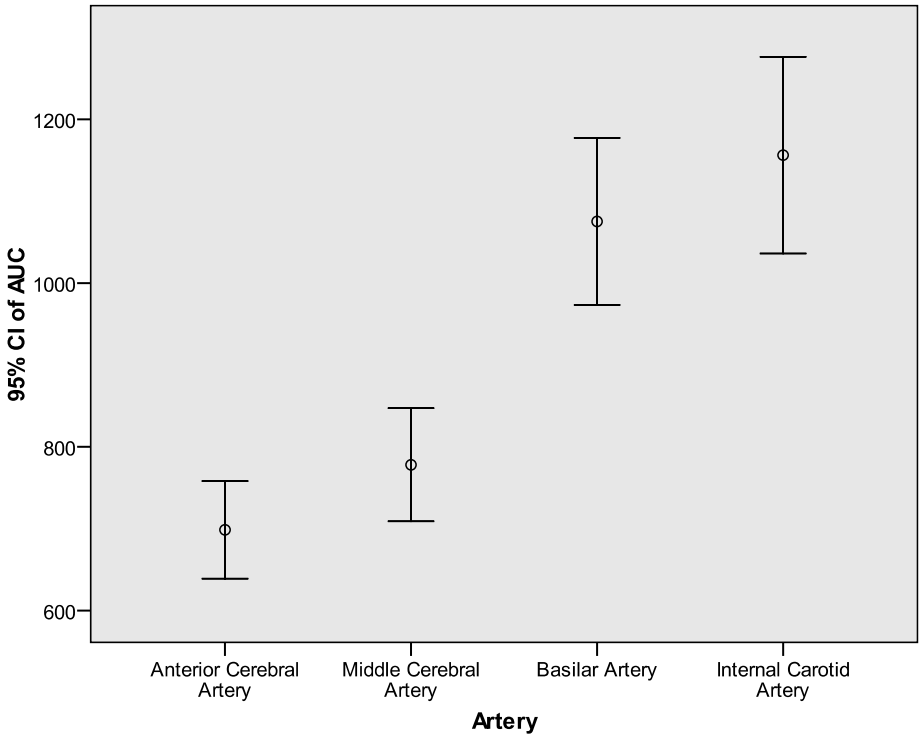

The quantitative perfusion measurements resulting from selecting the different arteries as the AIF are shown in table 1. Significant group differences in CBV, CBF and MTT were seen in both hemispheres (P<0.0001). In the ipsilateral hemisphere selecting the basilar artery as the AIF resulted in the lowest mean CBV (4.5 mL/100g), followed by the ICA (4.6 mL/100g), the MCA (5.0 mL/100g), and ending with the highest mean CBV value (5.1 mL/100g) in the ACA. The CBF showed the lowest mean value when the AIF was placed in the ICA (23.0 mL/100g/min), followed by the basilar artery (24.8 mL/100g/min), the ACA (28.5 mL/100g/min), and highest in the MCA (28.7 mL/100g/min). Accordingly, the MTT showed an inversed relation, and was longest in the ICA (15.3 s), shorter in the basilar artery (14.3 s), followed by the MCA (13.9 s) and shortest for the ACA (13.8 s). Table 1 shows the significant individual differences between the most valid perfusion values and the values resulting from other arteries.

The perfusion values in the contralateral hemisphere had the same distribution as in the ipsilateral hemisphere; the AIF placed in the ICA (along with the basilar artery) resulted in the most valid perfusion values with the lowest CBV and CBF and longest MTT (Table 1).

Table 1 *Comparison of perfusion measurements resulting from AIF in different cerebral arteries in the hemisphere ipsi- and contralateral to thrombus*

	Mean value (95%CI)		
Artery		*Ipsilateral Side*	
	CBV (mL/100g)	*CBF (mL/100g/min)*	*MTT (s)*
ACA	5.1 (4.5-5.6)*	28.5 (23.5-33.5)*	13.8 (11.1-16.5)*
MCA	5.0 (4.5-5.6)*	28.7 (22.8-34.5)*	13.9 (11.3-16.5)*
BAS	4.5 (4.0-5.0)	24.8 (20.3-29.3)	14.3 (11.6-17.0)*
ICA	4.6 (4.1-5.1)	23.0 (18.7-27.3)	15.3 (12.7-17.9)
Average	4.8 (4.5-5.1)	26.3 (23.8-28.7)	14.3 (13.0-15.6)
		Contralateral side	
	CBV (mL/100g)	*CBF (mL/100g/min)*	*MTT (s)*
ACA	5.7 (5.1-6.2)*	84.0 (68.7-100.2)*	4.9 (4.2-5.5)*
MCA	5.5 (5.1-6.0)*	81.7 (66.6-98.6)*	4.9 (4.3-5.6)*
BAS	5.0 (4.6-5.5)	67.3 (57.5-78.2)*	5.3 (4.5-5.9)*
ICA	5.1 (4.7-5.5)	54.9 (47.1-63.6)	6.2 (5.6-6.8)
Average	5.3 (5.1-5.6)	72.0 (65.7-78.7)	5.3 (5.0-5.6)

BAS = Basilar artery * Statistically different from most valid value (in grey)

Reducing operator dependent post-processing steps

In 15 patients (34%) the AUC_{AIF} exceeded the AUC_{VOF}, these patients were excluded from this analysis. In 29 patients (66%) the AUC of the ICA was lower than the AUC of the sinus with mean HUs values of 1059.3 versus 1347.2 respectively (paired t-test, $P<0.0001$). Table 2 shows the differences in these 29 patients in quantitative perfusion parameters resulting from using the VOF versus not using the VOF.

Not using the VOF as correction resulted in the hemisphere ipsilateral to the thrombus in significantly higher mean CBV (6.0 vs. 4.9 mL/100g) and mean CBF (34.8 vs. 25.2 mL/100g/min) compared to the situation in which we did use the VOF ($P<0.0001$ and $P=0.007$, respectively). The same significant differences were found for CBV (6.2 vs. 5.1 mL/100g) and CBF (68.1 vs. 53.0 mL/100g/min) in the contralateral hemisphere ($P<0.0001$ and $P=0.019$, respectively).

Table 2 *Comparison of perfusion measurements with correction and without correcting with the VOF in the hemisphere ipsi- and contralateral to thrombus in patients with the AUC_{VOF} larger than the AUC_{AIF}.*

Correction with VOF?	***Mean value (95%CI)***		
	Ipsilateral Side		
	CBV (mL/100g)	*CBF (mL/100g/min)*	*MTT (s)*
Yes	4.9 (4.1-5.6)	25.2 (19.1-31.2)	13.7 (11.5-15.9)
No	6.0 (4.9-7.1)	34.8 (25.0-44.6)	13.7 (11.5-15.9)
	Contralateral side		
	CBV (mL/100g)	*CBF (mL/100g/min)*	*MTT (s)*
Yes	5.1 (4.5-5.6)	53.0 (43.6-62.4)	6.4 (5.6-7.2)
No	6.2 (5.3-7.0)	68.1 (51.2-85.1)	6.4 (5.6-7.2)

DISCUSSION

Our study shows that the choice which artery to select as the AIF has significant effects on the accuracy of quantitative perfusion measurements, leading to significant and major differences (up to 13% for the MTT, 25% for the CBV and more than 50% for CBF). Selecting the ICA as the AIF resulted in the most accurate perfusion values. Reducing post-processing steps by deleting the VOF decreases the validity of perfusion values since even the largest artery available (ICA) is still hampered by more partial volume effects than the VOF in two-thirds of the patients.

Few previous studies have investigated the effect of selecting different arteries as the AIF in CTP. Most of them focus on the difference in perfusion measurements between an artery with or without an upstream occlusion and advise to use the artery without an occlusion. Some investigators advise to select the artery as close as possible to the ROI of the tissue [10, 21], while other studies recommend to use the ACA[20, 22] or even an extracranial vessel [23] as AIF. Consequently no consensus has been reached as to which artery should be selected as the AIF[24]. Four studies describe the influence on perfusion measurements of selecting different cerebral arteries without an upstream occlusion as the AIF in one CT data-acquisition [20, 25-27] Three of them investigated only the ACA and MCA and did not include the ICA and/or basilar artery as the AIF in their analyses [20, 26, 27]. In concordance with our results they found only little differences in quantitative perfusion measurements between the ACA and MCA as the AIF. One study compared the selection of one of the ICAs, the MCA and the ACA as the AIF with each other and found no significant difference in mean CBF, CBV and MTT. However, they only included three patients, did not use a 256-slice MDCT and investigated the MCA with occlusion [25].

Increased z-coverage with 256-slice MDCT has been shown to provide additional diagnostic CTP information [18]. Our study shows that with the increased z-coverage the ICA is the most appropriate AIF compared to other intracranial arteries.

Because the CBV is calculated with the AUC_{VOF} of a large venous sinus, one would not expect any differences in this perfusion parameter when selecting different arteries as AIF. However, in accordance with other studies[17, 26], we did find significant differences. One explanation may be that if the AUC_{AIF} exceeds the AUC_{VOF}, which was the case in 15 patients (34%), the AUC_{AIF} is automatically chosen as the baseline value to calculate the CBV. One possible reason for the fact that the AUC_{AIF} exceeded the AUC_{VOF} in these patients, is that the VOF, even when placed correctly, is still not partial volume free in relative thick 5-mm slices [15].

The major differences we revealed for the quantitative MTT values (up to 1.5 seconds) cannot just be explained by the different locations of the arteries compared to the tissue but is also due to the stronger partial volume effects in smaller vessels.[13] As explained, these partial volume effects (with a corresponding decrease in signal-to-noise ratio of the first pass bolus) affect the accuracy of the curves of the AIFs from smaller vessel, resulting in less valid MTT values.

Reproducibility of CTP can be optimized by reducing operator dependent post-processing steps. The selection of a venous sinus as the VOF is required to correct for partial volumes in the AIF. Theoretically this VOF selection would be obsolete if the AIF was less hampered by partial volume effects than the VOF. This was true for one third of patients. However in 66% of patients even a large artery as the ICA still suffers from more partial volume effects, since in these patients we found a significant lower AUC of the ICA compared to the AUC of the venous sinus with accompanying significantly higher mean CBV and mean CBF in both hemispheres. As deleting the VOF will be detrimental for validity in these patients, we recommend continuing the use of the VOF. However, if the venous curve is incomplete, which can happen if time to peak enhancement is slower due to cardiac dysfunction, the VOF can be best replaced by the ICA, as this is the artery with the largest AUC.

Some limitations of our study need to be addressed and may require further investigation. First, absolute quantitative CTP values vary considerably with the type of vendor software package and algorithm used. We used a commercially available time-sensitive algorithm (Philips Medical Systems), while most systems also offer a delay-insensitive algorithm to avoid overestimation of MTT and underestimation of CBF [22, 28-31]. To mitigate effects of delay, we took care to select only vessels without upstream thrombi, excluded patients with a significant (>50%) carotid artery stenosis, and compared measurements in both the hemisphere ipsi- and contralateral to the thrombus. Although we assume that our results are also valid for other algorithms, the effect that selection of different AIFs has on perfusion values when using different vendor software and algorithms requires further investigation. The effect of a downstream carotid artery stenosis on the perfusion values should also be explored. Second, variation in quantitative perfusion values may also cause variation in threshold-based infarct core/penumbra maps. This effect on infarct core/penumbra maps and subsequently on clinical decision making needs to be studied further [31]. Third, although the 5-mm CTP slice thickness will

increase partial volume effects, we deliberately performed our measurements on the 5-mm thick slices as it is the most common choice in clinical protocols to reduce noise and enable rapid post-processing.

In conclusion, in 256-slice MDCT selecting the ICA as the AIF and continuing the use of a venous sinus as the VOF will improve the accuracy of CTP. With the increased CTP coverage selection of the ICA instead of the ACA, MCA or basilar artery as the AIF will improve the accuracy of absolute quantitative values in CTP. Deleting the VOF will be detrimental for the validity of perfusion results in the majority of patients.

REFERENCES

1. Wintermark M, Reichhart M, Thiran JP, Maeder P, Chalaron M, Schnyder P, Bogousslavsky J, Meuli R. Prognostic accuracy of cerebral blood flow measurement by perfusion computed tomography, at the time of emergency room admission, in acute stroke patients. *Ann Neurol*. 2002;51:417-432
2. Miles KA, Lee TY, Goh V, Klotz E, Cuenod C, Bisdas S, Groves AM, Hayball MP, Alonzi R, Brunner T. Current status and guidelines for the assessment of tumour vascular support with dynamic contrast-enhanced computed tomography. *Eur Radiol*.22:1430-1441
3. Bisdas S, Donnerstag F, Ahl B, Bohrer I, Weissenborn K, Becker H. Comparison of perfusion computed tomography with diffusion-weighted magnetic resonance imaging in hyperacute ischemic stroke. *J Comput Assist Tomogr*. 2004;28:747-755
4. Nabavi DG, Cenic A, Henderson S, Gelb AW, Lee TY. Perfusion mapping using computed tomography allows accurate prediction of cerebral infarction in experimental brain ischemia. *Stroke*. 2001;32:175-183
5. Rother J, Jonetz-Mentzel L, Fiala A, Reichenbach JR, Herzau M, Kaiser WA, Weiller C. Hemodynamic assessment of acute stroke using dynamic single-slice computed tomographic perfusion imaging. *Arch Neurol*. 2000;57:1161-1166
6. Wintermark M, Meuli R, Browaeys P, Reichhart M, Bogousslavsky J, Schnyder P, Michel P. Comparison of ct perfusion and angiography and mri in selecting stroke patients for acute treatment. *Neurology*. 2007;68:694-697
7. Eastwood JD, Lev MH, Azhari T, Lee TY, Barboriak DP, Delong DM, Fitzek C, Herzau M, Wintermark M, Meuli R, Brazier D, Provenzale JM. Ct perfusion scanning with deconvolution analysis: Pilot study in patients with acute middle cerebral artery stroke. *Radiology*. 2002;222:227-236
8. Turk AS, Grayev A, Rowley HA, Field AS, Turski P, Pulfer K, Mukherjee R, Haughton V. Variability of clinical ct perfusion measurements in patients with carotid stenosis. *Neuroradiology*. 2007;49:955-961
9. Zussman B, Jabbour P, Talekar K, Gorniak R, Flanders AE. Sources of variability in computed tomography perfusion: Implications for acute stroke management. *Neurosurg Focus*.30:E8
10. Soares BP, Dankbaar JW, Bredno J, Cheng S, Bhogal S, Dillon WP, Wintermark M. Automated versus manual post-processing of perfusion-ct data in patients with acute cerebral ischemia: Influence on interobserver variability. *Neuroradiology*. 2009;51:445-451
11. Wintermark M, Ko NU, Smith WS, Liu S, Higashida RT, Dillon WP. Vasospasm after subarachnoid hemorrhage: Utility of perfusion ct and ct angiography on diagnosis and management. *AJNR Am J Neuroradiol*. 2006;27:26-34
12. Dankbaar JW, de Rooij NK, Rijsdijk M, Velthuis BK, Frijns CJ, Rinkel GJ, van der Schaaf IC. Diagnostic threshold values of cerebral perfusion measured with computed tomography for delayed cerebral ischemia after aneurysmal subarachnoid hemorrhage. *Stroke*. 2010;41:1927-1932
13. Kealey SM, Loving VA, Delong DM, Eastwood JD. User-defined vascular input function curves: Influence on mean perfusion parameter values and signal-to-noise ratio. *Radiology*. 2004;231:587-593
14. Sakai F, Nakazawa K, Tazaki Y, Ishii K, Hino H, Igarashi H, Kanda T. Regional cerebral blood volume and hematocrit measured in normal human volunteers by single-photon emission computed tomography. *J Cereb Blood Flow Metab*. 1985;5:207-213
15. van der Schaaf I, Vonken EJ, Waaijer A, Velthuis B, Quist M, van Osch T. Influence of partial volume on venous output and arterial input function. *AJNR Am J Neuroradiol*. 2006;27:46-50
16. Axel L. Tissue mean transit time from dynamic computed tomography by a simple deconvolution technique. *Invest Radiol*. 1983;18:94-99
17. Ferreira RM, Lev MH, Goldmakher GV, Kamalian S, Schaefer PW, Furie KL, Gonzalez RG, Sanelli PC. Arterial input function placement for accurate ct perfusion map construction in acute stroke. *AJR Am J Roentgenol*.194:1330-1336
18. Dorn F, Muenzel D, Meier R, Poppert H, Rummeny EJ, Huber A. Brain perfusion ct for acute stroke using a 256-slice ct: Improvement of diagnostic information by large volume coverage. *Eur Radiol*. 2011;21:1803-1810
19. Wintermark M, Flanders AE, Velthuis B, Meuli R, van Leeuwen M, Goldsher D, Pineda C, Serena J, van der Schaaf I, Waaijer A, Anderson J, Nesbit G, Gabriely I, Medina V, Quiles A, Pohlman S, Quist M, Schnyder P, Bogousslavsky J, Dillon WP, Pedraza S. Perfusion-ct assessment of infarct core and penumbra: Receiver operating characteristic curve analysis in 130 patients suspected of acute hemispheric stroke. *Stroke*. 2006;37:979-985
20. Wintermark M, Lau BC, Chien J, Arora S. The anterior cerebral artery is an appropriate arterial input function for perfusion-ct processing in patients with acute stroke. *Neuroradiology*. 2008;50:227-236
21. Kamath A, Smith WS, Powers WJ, Cianfoni A, Chien JD, Videen T, Lawton MT, Finley B, Dillon WP, Wintermark M. Perfusion ct compared to h(2) (15)o/o (15)o pet in patients with chronic cervical carotid artery occlusion. *Neuroradiology*. 2008;50:745-751
22. Calamante F, Morup M, Hansen LK. Defining a local arterial input function for perfusion mri using independent component analysis. *Magn Reson Med*. 2004;52:789-797
23. Sheikh K, Schipper MJ, Hoeffner EG. Feasibility of superficial temporal artery as the input artery for cerebral perfusion ct. *AJR Am J Roentgenol*. 2009;192:W321-329

24. Lee TY. Functional ct: Psychological models. . *Trends in Biotechnology*. 2002;20:s3-s10

25. Sanelli PC, Lev MH, Eastwood JD, Gonzalez RG, Lee TY. The effect of varying user-selected input parameters on quantitative values in ct perfusion maps. *Acad Radiol*. 2004;11:1085-1092

26. Bisdas S, Konstantinou GN, Gurung J, Lehnert T, Donnerstag F, Becker H, Vogl TJ, Koh TS. Effect of the arterial input function on the measured perfusion values and infarct volumetric in acute cerebral ischemia evaluated by perfusion computed tomography. *Invest Radiol*. 2007;42:147-156

27. Chiu FY, Teng MM, Kao YH, Chen YD, Luo CB, Chang FC, Guo WY, Chang CY. Selection of arterial input function for postprocessing of cerebral ct perfusion in chronic unilateral high-grade stenosis or occlusion of the carotid or middle cerebral artery. *Acad Radiol*. 2012;19:8-16

28. Wu O, Ostergaard L, Weisskoff RM, Benner T, Rosen BR, Sorensen AG. Tracer arrival timing-insensitive technique for estimating flow in mr perfusion-weighted imaging using singular value decomposition with a block-circulant deconvolution matrix. *Magn Reson Med*. 2003;50:164-174

29. Sasaki M, Kudo K, Ogasawara K, Fujiwara S. Tracer delay-insensitive algorithm can improve reliability of ct perfusion imaging for cerebrovascular steno-occlusive disease: Comparison with quantitative single-photon emission ct. *AJNR Am J Neuroradiol*. 2009;30:188-193

30. Smith MR, Lu H, Trochet S, Frayne R. Removing the effect of svd algorithmic artifacts present in quantitative mr perfusion studies. *Magn Reson Med*. 2004;51:631-634

31. Abels B, Villablanca JP, Tomandl BF, Uder M, Lell MM. Acute stroke: A comparison of different ct perfusion algorithms and validation of ischaemic lesions by follow-up imaging. *Eur Radiol*. 2012;22:2559-2567

Radiation dose reduction in cerebral CT-perfusion imaging using iterative reconstruction

JM Niesten, IC van der Schaaf, AJ Riordan, HWAM de Jong, AD Horsch, D Eijspaart, EJ Smit, WPTM Mali, BK Velthuis

European Radiology, 2013

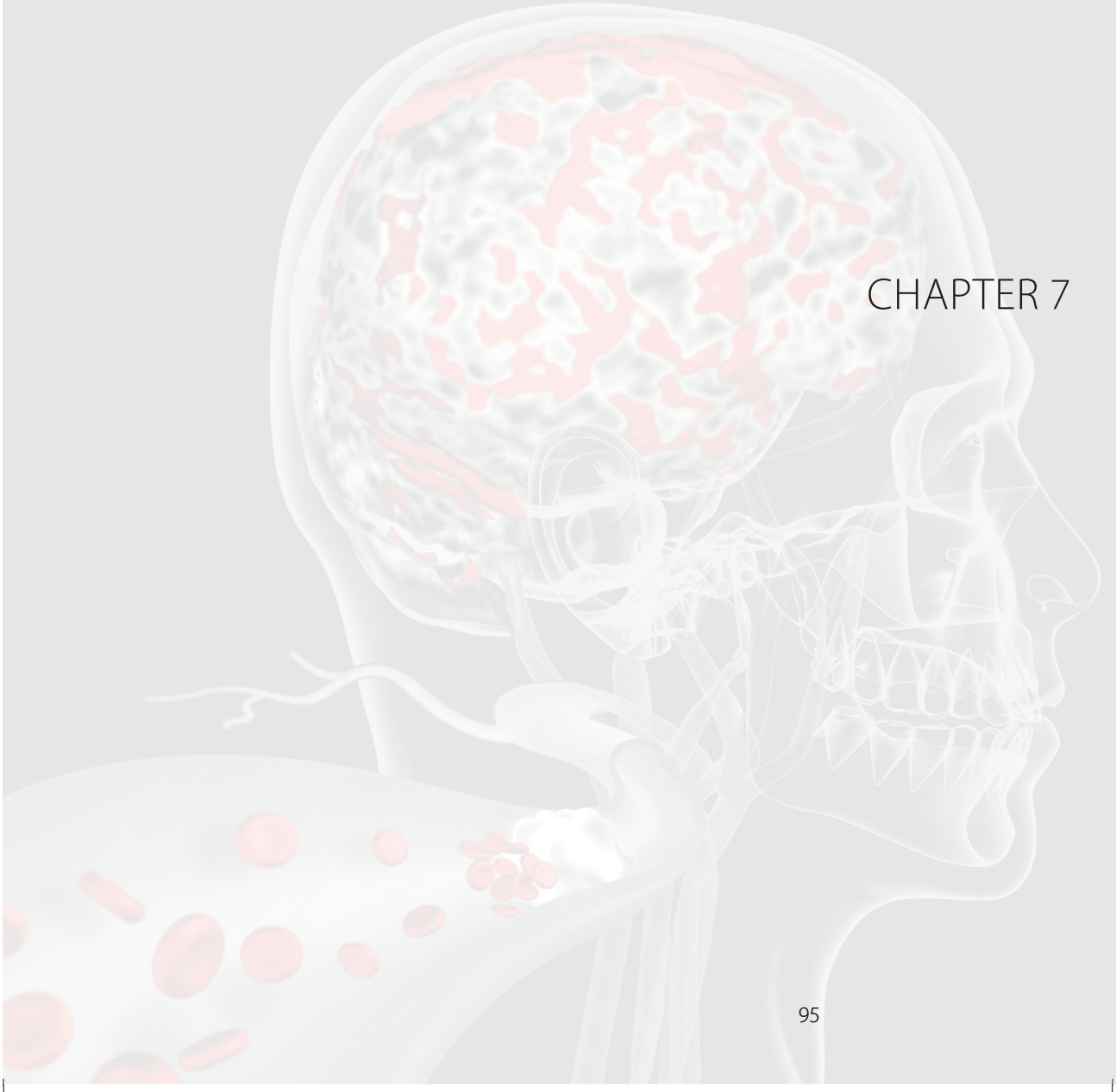

CHAPTER 7

ABSTRACT

Purpose

To investigate whether iterative reconstruction (IR) in cerebral CT perfusion (CTP) allows for 50% dose reduction while maintaining image quality (IQ).

Methods

A total of 48 CTP examinations were reconstructed into a standard dose (150 mAs) with Filtered Back Projection (FBP) and half-dose (75 mAs) with two strengths of IR (middle and high). Objective IQ (quantitative perfusion values, contrast-to-noise ratio (CNR), penumbra, infarct area and penumbra/infarct (P/I) index) and subjective IQ (diagnostic IQ on a four-point Likert-scale and overall IQ binomial) were compared among the reconstructions.

Results

Half-dose CTP with high IR level had, compared with standard dose with FBP, similar objective (grey matter Cerebral blood volume (CBV) 4.4 versus 4.3 mL/100g, CNR 1.59 versus 1.64 and P/I index 0.74 versus 0.73, respectively) and subjective diagnostic IQ (mean Likert-scale: 1.42 versus 1.49, respectively). The overall IQ in half-dose with high IR level was scored lower in 26-31%. Half-dose with FBP and with the middle IR level were inferior to standard dose with FBP.

Conclusion

With the use of IR in CTP imaging it is possible to examine patients with a half dose without significantly altering the objective and diagnostic IQ. The standard dose with FBP is still preferable in terms of subjective overall IQ in about one quarter of patients.

INTRODUCTION

In patients with symptoms of stroke the combination of an unenhanced CT followed by CT perfusion (CTP) and CT angiography (CTA) is one possible algorithm for the assessment of stroke patients. Unenhanced CT is performed to exclude haemorrhage, to detect old infarction and to evaluate classic signs of ischemia. CTA is used to detect and evaluate intracranial and extracranial vascular disease whereas CTP has been shown to increase the diagnostic accuracy for the detection, localisation and assessment of potentially reversible ischemia [1]. The increased diagnostic information gained by adding CTA and CTP is, however, at the expense of increased ionising radiation dose, as it will on average triple the radiation dose as compared to unenhanced CT alone [2]. With the ongoing introduction of full-brain CTP in many centres, the radiation exposure of the CTP will increase even further [2, 3]. Recently iterative reconstruction (IR) algorithms have been introduced with the aim to improve CT image quality (IQ) with the same radiation dose. These algorithms optimize the data iteratively on the basis of a noise- and artefact-reducing model resulting in an improvement of IQ [4]. It has also been demonstrated that it is possible to significantly reduce radiation dose while maintaining IQ in various CT applications. The purpose of this study was to assess whether IR in cerebral CTP imaging enables a 50% dose reduction while maintaining IQ.

METHODS

We prospectively enrolled patients with less than 24-h onset of neurological stroke symptoms between July 2011 and June 2012. All patients were referred from the emergency department of the university hospital by a neurologist for CT imaging (unenhanced CT, CTP and CTA). Inclusion criteria were: age at least 18 years, and CTP performed using 256-slice multidetector CT (MDCT). Exclusion criteria were: therapy before neuroimaging, haemorrhage on unenhanced CT, and insufficient quality of the CTP to perform adequate measurements. The study was approved by the local institutional reviewboard. The need for informed consent was waived as anonymous data were obtained from routine care CTP image acquisitions and patients were not exposed to additional radiation doses.

CTP post-processing

CTP protocol

All imaging studies were performed using 256 MDCT (Philips Brilliance iCT, Philips Healthcare, Best, The Netherlands). Standard CTP acquisition parameters in our hospital were normally 80 kVp, 150 mAs per image with temporal sampling rate of 1 image/2 s (150 mAs/2 s) for the whole examination without an initial delay and with a rotation time of 0.33 s, 5-mm reconstructed slice thickness with 60-mm coverage, 512x512 image matrix, collimation width of

128x0.625, a 200-mm field of view, reconstruction with Filtered Back Projection (FBP) and a smoothing (UB) image filter, with an image resolution filter of the source images of 1.46 mm, resulting in an effective dose of 3.0 mSv. A total of 40 mL of contrast agent (300 mg I/mL) injected intravenously at a rate of 6 mL/s followed by a 40-mL saline flush at a rate of 6 mL/s. CTP data acquisition was initiated at the start of the contrast bolus injection.

For this study we compared a standard CTP data set (3.0 mSv) with three half-dose CTP datasets (50% dose reduction), all reconstructed to a temporal resolution of 1 image/2 s. Because of ethical reasons we could not perform a CTP twice in the same patient using different CT protocols; we therefore reconstructed both the standard dose CTP and half-dose CTP images from the same raw CTP acquisition data. For this purpose, the CTP protocol was temporarily changed and CTP data were acquired at 75 mAs per image with a temporal sampling rate of 1 image/1 s (75 mAs/1 s, also with a resulting effective dose of 3.0 mSv) with the other CTP-parameters remaining the same. Subsequently, the raw data of the CTP examinations were converted by physicists into a standard protocol data set reconstructed with FBP (150 mAs/2 s) and in three data sets with 50% dose reduction (75 mAs/2 s), of which one was reconstructed with FBP and two were reconstructed with IR. The standard protocol data set (150 mAs/2 s) was created by averaging FBP reconstructed images from two sequencing frames of the acquired 75 mAs/1 s data. This created data set was validated as being equivalent to CTP images obtained from imaging with the original standard protocol in both the noise level (which abides by the equation $\sqrt{(mAs\_original)/(mAs\_new)}$[5], Fig. 1) and the shape of the attenuation curve (Fig. 2). The half-dose CTP datasets (75 mAs/2 s) were created from the acquired 75 mAs/1 s data by removing every second frame. The half-dose raw data CTP were reconstructed with FBP, with the highest possible IR level (IRhigh) and with middle IR level (IRmid).

Figure 1 *Noise levels between various computed tomography perfusion (CTP) reconstructions in background frames expressed as standard deviation in Hounsfield Units (HU).*

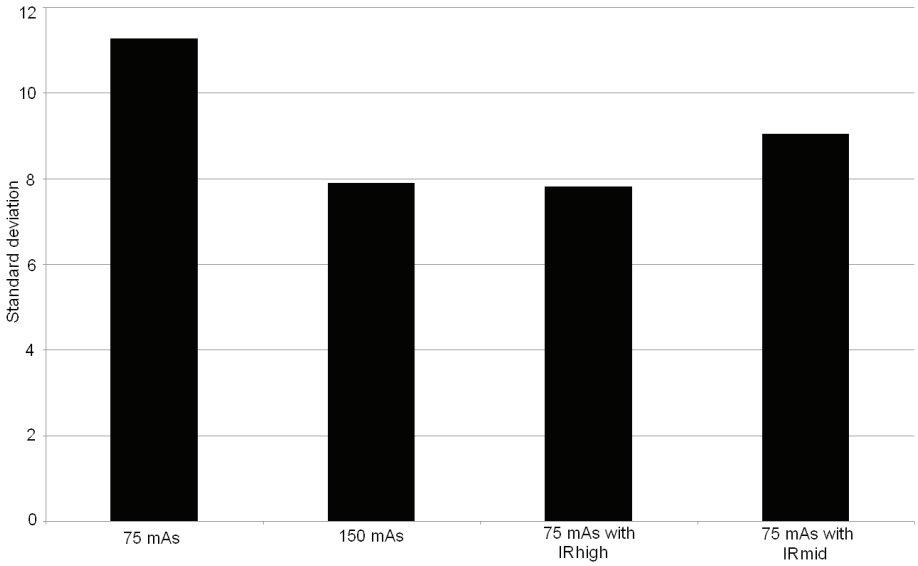

Noise levels in pre-bolus CT slices were measured using ROI analyses (white matter). The 150-mAs frame had approximately √2 (1.4) times lower noise compared with the 750mAs original data, as expected from a frame with twice the dose. The 75-mAs data reconstructed with highest IR level have a noise level comparable to 150 mAs

Figure 2 *Time-attenuation curves in HU for the various CTP reconstructions. Example arterial time-attenuation curves of the middle cerebral artery (MCA) are shown from the same patient.*

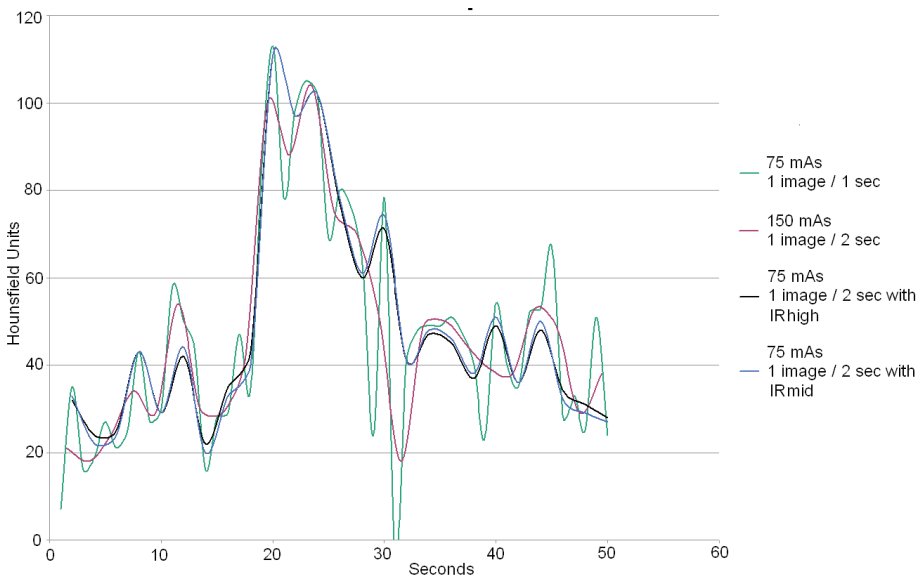

The shape of the time-attenuation curves proved to be similar to the 75 mAs/2 s data albeit at lower noise because of the higher dose. All curves have the same shape and the original 75-mAs acquisition has much higher noise content per frame than the 150-mAs acquisition, as expected with half the dose

Perfusion Analysis

Perfusion data were analysed using commercially available software (Extended Brilliance Workstation 4.5, Philips Healthcare). Cerebral Blood Volume (CBV, in millilitres per 100g) and Mean Transit Time (MTT, in seconds) were calculated using a deconvolution operation and Cerebral Blood Flow (CBF, in millilitres per 100g per minute) was derived from CBV/MTT. Subsequently, penumbra and infarct maps and penumbra/infarct index (total penumbra area divided by total infarct + penumbra area) were obtained automatically, whereby MTT > 145% compared with the contralateral side defined the total ischemic area, divided by CBV in the infarct core (CBV < 2.0 mL/100g) and penumbra (CBV ≥ 2.0 mL/100g) [6]. The Region of Interest (ROI) for the selection of the arterial input function (AIF) was set in the internal carotid artery of the non-affected hemisphere and for the venous output function (VOF) in the posterior part of the superior sagittal sinus [7]. In each patient the AIF and VOF were replicated for each reconstruction by placing the arterial and venous ROIs in the same vessel location. Concurrently, the software guaranteed the selection of the voxel with the highest area under the curve (AUC) within this ROI.

Image quality

First, objective IQ was assessed for the four CTP reconstructions (standard dose with FBP, half-dose with FBP, half-dose IRhigh and half-dose IRmid) by comparing quantitative perfusion values, image noise and the penumbra/infarct index. Second, to assess subjective IQ, the overall IQ and the diagnostic IQ of three different sets of CTP reconstructions (standard dose with FBP, half-dose IRhigh and half-dose IRmid) were investigated.

Objective image quality

For the four CTP reconstruction a total of four identical circular ROIs of 100 mm^2 were placed; one ROI in the white matter (WM) and one in the grey matter (GM) in both hemispheres in the middle cerebral artery (MCA) territory at ASPECTS level 2 (at the level of the most superior margin of the ganglionic structures) [8]. These ROI positions were saved for each patient so that the placement of the ROIs was identical in the different CTP reconstructions. Quantitative perfusion parameters (CBV, CBF, MTT), the average attenuation (in Hounsfield Units, HU) and the noise (standard deviation) were measured in each ROI. For the HU measurements the CTP reconstructions were set on so-called temporal maximum intensity projection (tMIP). A tMIP shows, for each voxel, the highest attenuation in the time-attenuation curve and is the application used in the clinical setting. Subsequently, for the different CTP reconstructions the mean quantitative perfusion parameters, the signal-to-noise ratio and contrast-to-noise were calculated and compared. The signal-to-noise ratio was used to measure the quality of the signal density and was defined as the mean attenuation (in HU) in the tMIP divided by the standard deviation. The contrast-to-noise ratio was defined as the difference in mean attenuation (in HU) between the ROI in the GM and the ROI in the WM divided

by the square root of the sum of their variance [9]. For each CTP reconstruction we compared the total area of penumbra and infarct of all slices (in square centimetres) and the penumbra/infarct index of the ischemic hemisphere.

Subjective image quality

The subjective IQ was assessed by two observers (one Neuroradiologist and one experienced Radiology resident) for three reconstructions. The observers were blinded to the type of CTP reconstruction. Two different grading systems were used, one designed to evaluate overall IQ (binomial scale) and one specifically for the assessment of diagnostic IQ (four-point Likert scale).

First, overall IQ was assessed. For all patients colour maps of the three perfusion parameters CBF, CBV and MTT on ASPECTS levels 1 (at the level of basal ganglia and thalamus) and 2 were randomly presented pairwise (either standard with FBP vs. half-dose IRhigh, standard with FBP vs. half-dose IRmid or half-dose IRhigh vs. half-dose IRmid) to the observers. The observers scored which of the two CTP reconstructions was superior, or equal if no differences were seen, on each of the following three points: (a) GM-WM differentiation of CBF and CBV maps and grading of the MTT and TTP maps, (b) homogeneity (contrast, contours, coherency/dissemination) and (c) compensation for artefacts, based on an adapted version of Abels et al.'s scoring system [2]. Second, we performed an analysis of the diagnostic quality of the different CTP reconstructions using a four-point Likert scale: 0, non-diagnostic; 1, moderate; 2, good; 3, excellent. A score from 0 to 3 was given by both blinded observers for each of the three CTP reconstructions on the basis of how confident the observers were in including or excluding the presence of an ischemic lesion and, if a lesion was present, the differentiation between ischemic and normal tissue.
To minimise potential sources of bias, there was a time interval of at least 6 weeks between the assessment of the overall IQ and diagnostic IQ.

Statistical analysis

Data were assessed for normality using the Shapiro-Wilk test. Differences in the objective parameters (quantitative perfusion values, attenuation, image noise, total area of penumbra and infarct and the penumbra/infarct index) among the four CTP reconstructions were tested by means of the ANOVA with repeated measures test. If statistical differences among the four CTP reconstructions were present, individual CTP reconstructions were compared pairwise using paired *t*-tests with Bonferroni-correction.
Subsequently, ischemic lesion size (the total area of penumbra and infarct of all slices and the penumbra/infarct index) obtained with the four reconstructions were compared using Pearson's correlation coefficients (*r*) to test the similarity in ischemic lesion sizes among the different CTP reconstructions with *r* indicating the strength of the relationship: 0.90–1, very strong; 0.70–0.89, strong; 0.40–0.69, moderate; 0.20–0.39, weak and 0.01–0.19, negligible relationship.

For the evaluation of subjective overall IQ, the overall proportions of cases in which one CTP reconstruction was found to be superior, equal, or inferior to another technique was calculated and compared using the Chi-square test. For the evaluation of subjective diagnostic IQ the scores on the Likert scale of both observers and the average scores for each CTP reconstruction technique were compared using the Wilcoxon signed-rank test.

For the subjective IQ Cohen's kappa (κ) values with correction of change were used to assess the interobserver agreement [10]. Statistical analysis was performed using SPSS, version 19.0 (SPSS Inc., Chicago, IL, USA). A *P* value of less than 0.05 was considered to indicate a statistically significant difference.

RESULTS

Patients

Two of the 50 patients who met the inclusion criteria were excluded because of movement artefacts. Of the remaining 48 patients that were included in this study 16 were women (33%) and the average age was 64.2 years (95% CI 36.2–92.2). The mean National Institutes of Health Stroke Scale (NIHSS) on admission was 4.2 (95%CI 3.3–5.2) and the mean onset time to imaging was 425 min (95 % CI 285–565). A total of 34 (71%) patients had cerebral ischemia: 18 owing to a transient ischemic attack and 16 with a confirmed infarct on follow-up imaging. The remaining 14 patients were diagnosed with functional symptoms (*n*=5), space-occupying lesions (*n*=4), intoxications (*n*=2) or other neurological diseases (*n*=3).

Quantitative Analyses

Perfusion parameters

Table 1 shows the average values of CBV, CBF and MTT measurements in the GM and WM for the four different sets of CTP reconstructions. No significant differences were seen in the MTT in both the GM and WM. The half-dose with FBP showed significant lower CBV compared to the three other reconstructions in GM (all $P < 0.001$), higher CBV and CBF in WM compared to the standard dose with FBP (p=0.044 and 0.028, respectively) and compared to half-dose IRmid (p=0.009 and 0.002, respectively) and higher CBF in WM compared to the half-dose IRhigh (p=0.002). No significant differences in CBV and CBF were present in either GM or WM among standard dose with FBP and half-dose IRhigh and IRmid with the exception of significantly lower CBF in WM at the half-dose IRmid compared with the standard dose with FBP (*P*=0.005).

Table 1 *Cerebral blood volume (CBV), cerebral blood flow (CBF), mean transit time (MTT) values for the various computed tomography perfusion (CTP) reconstructions*

	Mean (95% Confidence Interval)				
	Standard dose with FBP	*Half-dose IRhigh*	*Half-dose IRmid*	*Half-dose with FBP*	***P-value***
CBV					
Grey Matter	4.3 (4.0-4.6)	4.4 (4.0-4.7)	4.4 (4.1-4.7)	3.5 (3.2-3.9)[abc]	<0.001
White Matter	2.6 (2.4-2.7)	2.6 (2.4-2.8)	2.4 (2.3-2.6)	2.9 (2.6-3.3)[ac]	0.022
CBF					
Grey Matter	59.8 (54.0-65.7)	57.1 (52.1-62.0)	57.3 (52.5-62.2)	53.7 (43.4-64.1)	0.40
White Matter	28.4 (25.1-31.8)	26.3 (23.8-28.8)	24.7 (22.3-27.2)[a]	37.3 (30.0-44.7)[abc]	0.004
MTT					
Grey matter	4.8 (4.3-5.3)	5.0 (4.5-5.5)	4.9 (4.4-5.4)	5.2 (4.5-5.9)	0.36
White matter	6.0 (5.4-6.6)	6.3 (5.7-6.9)	6.3 (5.8-6.8)	6.5 (4.6-8.3)	0.71

[a] Significantly different from the standard dose with FBP
[b] Significantly different from half-dose IRhigh
[c] Significantly different from half-dose IRmid

Image noise, area of penumbra and infarct and the penumbra/infarct index

Table 2 shows the quantitative measurements of the mean attenuation, noise, the signal-to-noise ratio in the GM and WM, and the contrast-to-noise for all four sets of CTP reconstructions. The attenuation ranged from 49.3 to 52.9 HU in GM and from 37.7 to 41.9 in WM and was significantly lower in the standard dose with FBP compared to IRmid (P<0.001 and P<0.001, respectively) and to the half-dose with FBP (P=0.005 and P<0.001, respectively).

The noise of the half-dose with FBP in the GM and WM was higher compared to standard dose with FBP (P=0.019 and p<0.001, respectively), half-dose IRhigh (P=0.005 and P<0.001, respectively) and half-dose IRmid (P=0.151 and P<0.001, respectively). The noise values between all other reconstructions were comparable with the exception of a lower noise in the WM of the standard dose with FBP compared with the half-dose IRmid (P=0.007). The signal-to-noise ratio was significantly lower in the half-dose with FBP compared to the half-dose IRhigh in the GM (P=0.020) and to all other reconstructions in the WM (all P<0.001). The contrast-to-noise ratio was significantly the lowest in the half-dose with FBP compared to standard dose with FBP, half-dose IRhigh and half-dose IRmid (P=0.018, 0.008 and 0.048, respectively). There were no statistically significant differences in the contrast-to-noise ratio among the other three sets of CTP reconstructions (Table 2).

Table 2 *Attenuation and signal-to-noise ratio of the grey matter and white matter and contrast-to-noise ratio on tMIP and total area of penumbra, infarct and the penumbra/infarct*

	Mean (95% Confidence Interval)				
	Standard dose with FBP	*Half-dose IRhigh*	*Half-dose IRmid*	*Half-dose with FBP*	***P-value***
Attenuation (HU)					
Grey Matter	49.3 (47.5-51.0)	50.2 (48.7-51.8)	52.4 (50.7-54.1)[a]	52.9 (51.0-54.8)[a]	<0.001
White Matter	37.7 (36.4-39.1)	39.1 (37.6-40.6)	40.5 (39.2-41.9)[a]	41.9 (40.6-43.3)[a]	<0.001
Noise (HU)					
Grey Matter	6.3 (5.7-6.9)	6.0 (5.6-6.4)	6.5 (6.0-7.1)	7.7 (6.8-8.6)[ab]	0.001
White Matter	4.0 (3.7-4.4)	4.2 (3.9-4.6)	4.5 (4.2-4.8)[a]	5.4 (5.1-5.6)[abc]	<0.001
Signal-to-noise ratio	8.5 (7.9-9.2)	8.9 (8.2-9.5)	8.6 (7.9-9.3)	7.5 (6.9-8.0)[b]	0.004
Grey matter White matter	10.0 (9.4-10.0)	9.7 (9.2-10.3)	9.3 (8.8-9.8	7.9 (7.5-8.3)[abc]	<0.001
Contrast-to-noise ratio	1.64 (1.35-1.92)	1.59 (1.32-1.87)	1.57 (1.36-1.78)	1.19 (1.03-1.35)[abc]	0.004
Total penumbra (cm^2)	98 (33-164)	93 (28-157)	92 (27-157)	104 (40-169)	0.58
Total infarct (cm^2)	21 (5-364)	18 (2-335)	18 (3-336)	17 (4-332)	0.41
Penumbra/ Infarct index	0.73 (0.60-86)	0.74 (0.63-0.86)	0.75 (0.65-0.85)	0.78 (0.68-0.88)	0.37

[a] Significantly different from the standard dose with FBP
[b] Significantly different from half-dose IRhigh
[c] Significantly different from half-dose IRmid

Comparing the mean total area of penumbra and infarct, and the penumbra/infarct index, there were no significant differences among all reconstructions (Table 1). The correlation of these parameters between half-dose with FBP and the standard dose with FBP was strong (R^2= 0.82, 0.87 and 0.72, respectively, all *P*<0.01), between half-dose with FBP and half-dose IRhigh very strong to weak (R^2= 0.81, 0.94 and 0.36, and *P*<0.01, <0.001 and 0.023, respectively) and very strong to moderate between half-dose with FBP and half-dose IRmid (R^2= 0.81, 0.95 and 0.65, all *P*<0.01). The correlation was strong to very strong between standard with FBP versus half-dose with highest IR level (R^2=0.89, 0.91 and 0.89, respectively, all *P*<0.001), very strong to moderate between standard with FBP versus half-dose IRmid (R^2=0.89, 0.91 and 0.64, respectively, all *P*<0.01) and very strong to strong between half-dose IRhigh versus half-dose IRmid (R^2=0.99, 0.99 and 0.82, respectively, all *P*<0.001).

Qualitative Analyses

Overall image quality

Figure 3 displays the visual assessment of each of the three imaging parameters of the overall IQ: GW/WM differentiation and grading; homogeneity; and compensation for artefacts. Examples of the comparison are shown in Figs. 4 and 5.The average interobserver agreement was 0.57. Comparing standard dose with FBP and half-dose IRhigh, the overall IQ was most often scored as equal for the three parameters. However, the standard dose with FBP was rated as being superior to half-dose IRhigh in about 25% and inferior in about

15% (p<0.001, Fig. 3a). When comparing the standard dose with FBP and the half-dose IRmid, the overall IQ was scored equal in about half of the patients. The standard dose with FBP was rated superior in around 40 %, and only rarely as inferior (*P*<0.001, Fig. 3b). Half-dose IRhigh versus half-dose IRmid showed equal scores in most cases while half-dose IRhigh was rated superior more often than IRmid (*P*<0.001, Fig. 3c).

Diagnostic image quality

Examples of the comparison are shown in Figs. 4 and 5. The average interobserver agreement was 0.88. For both observers the standard dose with FBP was comparable to the half-dose IRhigh (*P*=0.10 and *P*=0.26) and significantly superior to half-dose IRmid (*P*<0.001 and *P*=0.005). The diagnostic quality of the half-dose IRhigh was significantly superior to the half-dose IRmid for both observers (*P*=0.002 and *P*=0.034).

The average Likert scale points for the standard dose with FBP (1.49 (95%CI 1.22–1.76)), was not significantly different (*P*=0.11) to half-dose IRhigh (1.42 (95%CI 1.13–1.71)) but was significantly different (*P*<0.001) to half-dose IRmid (1.25 (95%CI 0.99–1.51)). The difference in average Likert-points between half-dose IRhigh and IRmid was also significant (*P*=0.003).

Figure 3 *Comparison of subjective overall image quality among various CTP reconstructions.*

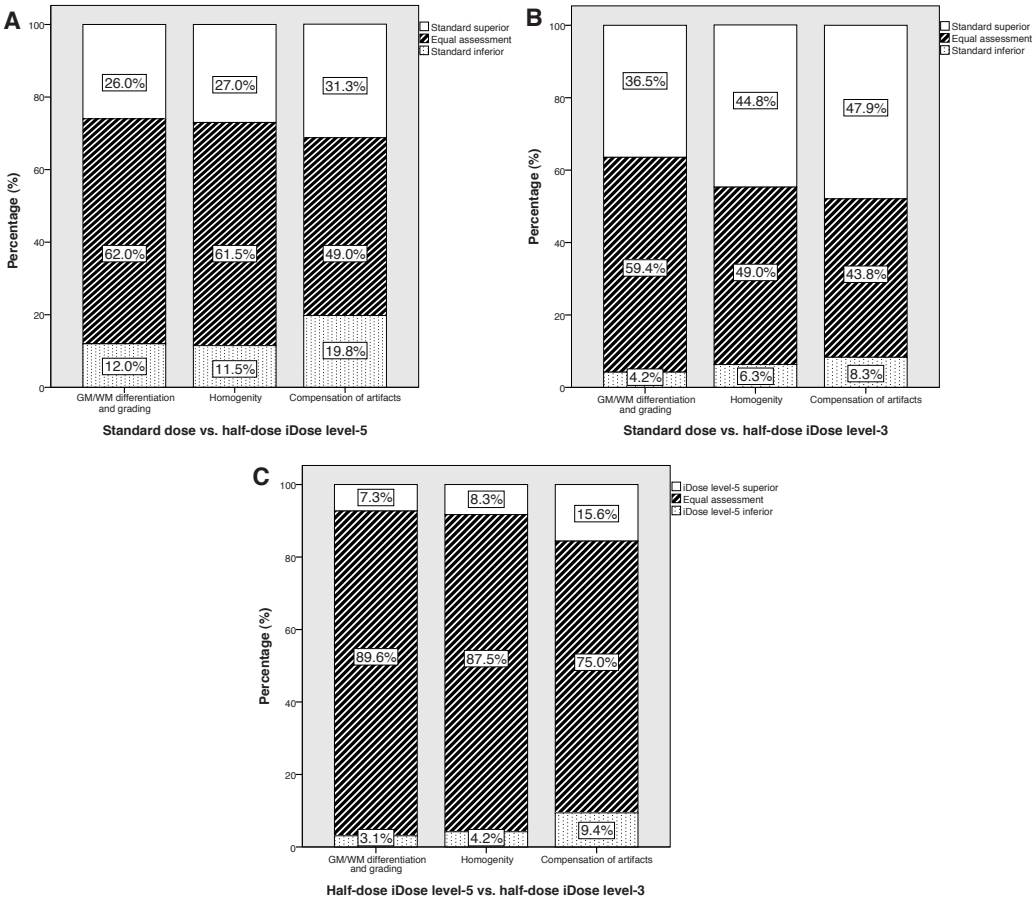

Proportions of superiority, equal assessment or inferiority of the standard dose with FBP compared with ***A*** half-dose IRhigh and ***B*** half-dose IRmid. ***C*** Proportions of superiority, equal assessment or inferiority of half-dose IRhigh compared with half-dose IRmid.

Figure 4 *Example of CTP images of standard dose with FBP (A) and half-dose IRhigh (B) and IRmid (C).*

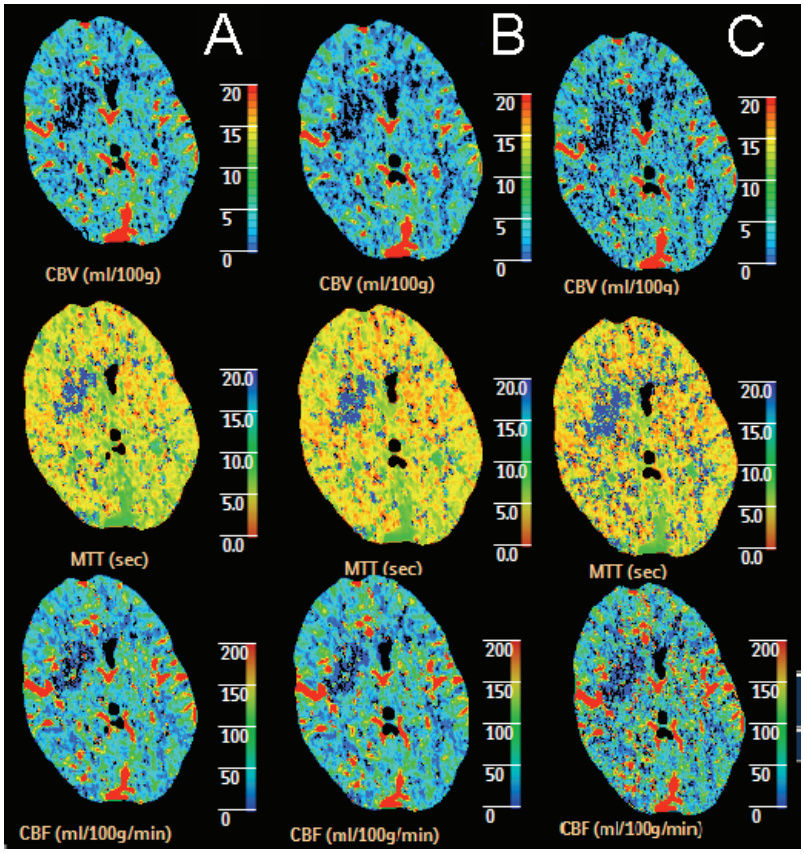

This image was scored as superior on WM/GM differentiation and grading and compensation of artefacts for the standard CTP with FBP compared to half-dose IRhigh and IRmid, whereas IRhigh was scored as superior to IRmid for grading and compensation for artefacts. The average diagnostic image quality points were 1.5, 1.5 and 1.0 respectively.

Figure 5 *Example of CTP images of standard dose with FBP (A) and half-dose IRhigh (B) and IRmid (C).*

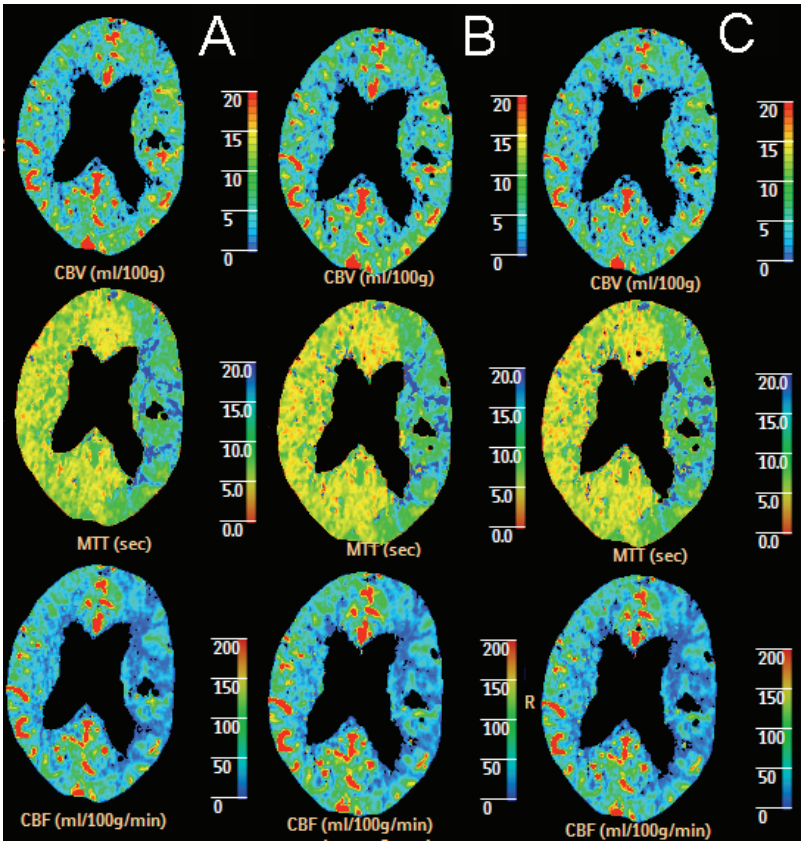

This image was scored as superior only on compensation of artefacts for the standard CTP with FBP compared with IRhigh and IRmid. The average diagnostic image quality points were 2.0, 2.0 and 2.0, respectively.

DISCUSSION

The main finding of this study is that in CTP imaging it is possible to image patients with half of the usual dose when it is reconstructed with IR without altering the objective IQ (quantitative perfusion parameters, image noise, penumbra and infarct) and diagnostic IQ. The overall IQ still remains higher in the standard dose with FBP in a quarter of patients.

Although additional CTP imaging in acute stroke patients has several advantages for the diagnostic process, a major drawback is the considerable increase in radiation dose compared to the unenhanced CT or MRI. This is particularly important in younger patients

and in the large number of patients who turn out not to have an ischemic stroke but a transient ischemic attack (TIA) or a stroke mimic. CTP of the brain should be performed with the lowest acceptable dose but also requires good IQ because the attenuation differences between WM and GM and of perfusion

deficits can be very small. The possibilities for achieving dose reduction in brain CT are therefore limited [11].

Many parameters influence the quality of CTP and affect the accuracy of perfusion values, the spatial coverage and the radiation dose [12]. Strategies that have been proposed to lower the radiation dose are the use of 80 kVp instead of 120 kVp [13], lowering the tube current and increasing the temporal interval. Lowering the tube current resulted in a deterioration of the accuracy of cerebral perfusion parameters [14]. Different conclusions concerning the maximal temporal interval have been drawn, ranging up to 1 image every 3 s [2, 3, 12, 15, 16]. Therefore, the utility of reducing radiation dose by decreasing the temporal interval still needs further investigation [17]. Up till now, dose reduction has been limited as the standard algorithm reconstruction FBP does not produce images of consistent quality if there is a substantial decrease in the dose.

The recently introduced IR algorithm provides an alternative for FBP in decreasing the radiation dose[18]. Goals of these algorithms include improvement of IQ at a constant radiation dose and radiation dose reduction with similar IQ. In head CT the use of IR algorithms has been shown to be beneficial to low-dose CT of the paranasal sinuses [19], paediatric head CT [20] and adult unenhanced CT. In the unenhanced CT of the adult head the use of IR algorithms is associated with a dose reduction of 20–30% with similar IQ [9, 11, 18, 21]. In head CTA IR has been shown to be beneficial in measuring the diameter of arteries in vitro and to improve the delineation of arteries in the posterior fossa [22, 23].

To our knowledge, only two scientific papers have been published about the use of IR in CTP imaging in which in-house developed iterative image reconstruction algorithms were tested on digital phantoms only, yielding good performing results [24, 25]. Our study is the first clinical CTP study investigating the use of a commercially available IR of a major CT vendor in patients.

For the reconstructions we used the IR algorithm called iDose^4 (Philips Healthcare, Best, The Netherlands). The half-dose raw data CTP were reconstructed with iDose^4 level 5 (the highest possible level for CTP) and iDose^4 level 3 (middle level) which corresponds to a noise reduction of 37% and 23%, respectively, according to the manufacturer's instructions [26]. The iDose^4 algorithm is a recently introduced hybrid IR algorithm by Philips Healthcare. This algorithm filters in the projection data domain as well as the image domain following two de-noising components: first, this algorithm identifies low intensity streaks and pixel-to-pixel noise and corrects this by comparing it with the ideal value of a generated noise map using an iterative maximum likelihood-type sinogram restoration method based on Poisson noise distribution. Second, local structure model fitting is performed on image data that iteratively decreases the image domain uncorrelated noise [17, 27]. The dose reduction can be adjusted with different levels (so-called iDose levels) [4, 26, 28]. These different levels of iDose^4 are used to define the strength of the IR technique in reducing image quantum mottle noise. The desired level can be set

independent of the radiation dose of the acquisition and allows targeting the application of iDose^4 to a clinical target (dose reduction, IQ improvement, or combined dose-reduction with IQ improvement). Parameter improvements can occur if higher iDose^4 levels are used than required as compensation for the noise from dose reduction. The choice of the appropriate iDose^4 level depends on the clinical goal: dose reduction, IQ improvement or a combination of both [26].

For the aim of our study we chose to construct the standard and half-dose data sets from one single-dose acquisition. Ideally, a comparison between reconstruction methods is based on a half-dose acquisition, independently acquired from the standard-dose acquisition but this would require unethical higher dose exposure. Furthermore, two separate acquisitions may differ because of motion and other influencing factors. Alternatively, it would be easier to use full- versus half-rotation reconstructions. However, such an implementation was not possible on our scanner and therefore one data set was artificially constructed by combining two consecutive frames. Comparison showed that this had no effect on the shape of contrast in- and outflow of time-attenuation curves and, in addition, that the noise level of the reconstructed data set was equal to the data acquired with the standard-dose protocol. This demonstrated that our methods could be used to compare equivalent CTP data with different doses.

The strength of an IR algorithm can influence both the objective and subjective IQ. In our study, the CTP images reconstructed with half-dose IRhigh were superior to half-dose IRmid in attenuation, image noise and in the overall and diagnostic IQ. Half-dose IRmid was inferior in both objective and subjective IQ compared with the standard with FBP and is therefore less suitable when CTP imaging is performed with half the dose.

The results of this study are promising, suggesting that a significant dose reduction in head CTP can be achieved when using IR, without affecting the objective IQ and the subjective diagnostic quality. For future use in clinical practice it is important that diagnostic conclusions are consistent despite dose reduction. As both the objective and diagnostic IQ were comparable despite a 50% dose reduction when using IRhigh, it is unlikely that dose reduction in combination with the use of IRhigh algorithms will influence diagnostic conclusions and therapeutic decisions. However, as the subjective overall IQ was still scored inferiorly in about one quarter of patients with a 50% dose reduction using IR, the effect of the decreased overall IQ on the clinical decisions should be further examined.

The subjective IQ assessment was performed without the half-dose with FBP because most objective measurements were already significantly inferior. To assess the subjective IQ we used an adapted version of Abels' scoring system because we wanted to make a distinction between the overall and diagnostic IQ. The assessment of overall IQ was based on three of the four parameters of the Abels system (GM/WM differentiation or grading; homogeneity; and compensation of artefacts) . As we expected only minor differences between the reconstructions (as the aim was to maintain IQ despite dose reduction)

we chose a pairwise ranking, which is more sensitive for detection of small differences, instead of the three-point scale of the Abels system. However, the results of this one-to-one comparison do not necessarily reflect the diagnostic IQ e.g. the overall IQ of two reconstructions could be scored equally despite both reconstructions having very low diagnostic value. Furthermore, the ranking of scans as inferior or superior does also not allow estimation of the order of magnitude of the differences. Therefore we added a second scale for assessment of diagnostic IQ which we scored on a four-point Likert scale.

The subjective IQ (visual assessment) of the half-dose IRhigh was scored lower than standard dose with FBP, although in the objective IQ (means in 100 mm^2 ROIs) only small and non-significant differences were seen. Possibly slight differences are visually detectable but do not reach significance in 100 mm^2 ROIs.

This study has some limitations. First, the image acquisition, the IR algorithm and the software package were from the same single vendor and therefore we cannot comment on those of other vendors. However, it has been shown that different CT perfusion post-processing algorithms usually lead to the same clinical decision [29]. Second, as mentioned, we did not investigate the possible differences in therapeutic decisions between the different reconstructions. As still in one quarter of patients the half-dose scans with IR was scored inferior, they could be interpreted differently. As a result of these limitations, a final large study on diagnostic conclusions and therapeutic decisions, based on CTP acquisitions with a standard dose and dose reduction with the use of different IR algorithms needs to be performed.

In conclusion, with the use of IR in CTP imaging it is possible to image patients with half of the dose without significantly altering the objective and diagnostic IQ. As the subjective overall IQ is still inferior in about a quarter of the patients, a smaller dose reduction than 50% may be required. This should be studied further.

REFERENCES

1. Lin K, Do KG, Ong P, Shapiro M, Babb JS, Siller KA, Pramanik BK. Perfusion ct improves diagnostic accuracy for hyperacute ischemic stroke in the 3-hour window: Study of 100 patients with diffusion mri confirmation. *Cerebrovasc Dis*. 2009;28:72-79
2. Abels B, Klotz E, Tomandl BF, Villablanca JP, Kloska SP, Lell MM. Ct perfusion in acute ischemic stroke: A comparison of 2-second and 1-second temporal resolution. *AJNR Am J Neuroradiol*. 2011;32:1632-1639
3. Kloska SP, Fischer T, Sauerland C, Buerke B, Dziewas R, Fischbach R, Heindel W. Increasing sampling interval in cerebral perfusion ct: Limitation for the maximum slope model. *Acad Radiol*. 2010;17:61-66
4. Willemink MJ, de Jong PA, Leiner T, de Heer LM, Nievelstein RA, Budde RP, Schilham AM. Iterative reconstruction techniques for computed tomography part 1: Technical principles. *Eur Radiol*. 2013;23:1623-1631
5. Primak AN, McCollough CH, Bruesewitz MR, Zhang J, Fletcher JG. Relationship between noise, dose, and pitch in cardiac multi-detector row ct. *Radiographics*. 2006;26:1785-1794
6. Wintermark M, Flanders AE, Velthuis B, Meuli R, van Leeuwen M, Goldsher D, Pineda C, Serena J, van der Schaaf I, Waaijer A, Anderson J, Nesbit G, Gabriely I, Medina V, Quiles A, Pohlman S, Quist M, Schnyder P, Bogousslavsky J, Dillon WP, Pedraza S. Perfusion-ct assessment of infarct core and penumbra: Receiver operating characteristic curve analysis in 130 patients suspected of acute hemispheric stroke. *Stroke*. 2006;37:979-985
7. Niesten JM, van der Schaaf IC, Riordan AJ, de Jong HWAM, Mali WPTM, Velthuis BK. Optimisation of vascular input and output functions in ct-perfusion imaging using 256(or more)-slice multidetector ct. *European Radiology*. 2013;23:1242-1249
8. Pexman JH, Barber PA, Hill MD, Sevick RJ, Demchuk AM, Hudon ME, Hu WY, Buchan AM. Use of the alberta stroke program early ct score (aspects) for assessing ct scans in patients with acute stroke. *AJNR Am J Neuroradiol*. 2001;22:1534-1542
9. Rapalino O, Kamalian S, Payabvash S, Souza LC, Zhang D, Mukta J, Sahani DV, Lev MH, Pomerantz SR. Cranial ct with adaptive statistical iterative reconstruction: Improved image quality with concomitant radiation dose reduction. *AJNR Am J Neuroradiol*.33:609-615
10. Landis JR, Koch GG. The measurement of observer agreement for categorical data. *Biometrics*. 1977;33:159-174
11. Korn A, Fenchel M, Bender B, Danz S, Hauser TK, Ketelsen D, Flohr T, Claussen CD, Heuschmid M, Ernemann U, Brodoefel H. Iterative reconstruction in head ct: Image quality of routine and low-dose protocols in comparison with standard filtered back-projection. *AJNR Am J Neuroradiol*. 2012;33:218-224
12. Wintermark M, Smith WS, Ko NU, Quist M, Schnyder P, Dillon WP. Dynamic perfusion ct: Optimizing the temporal resolution and contrast volume for calculation of perfusion ct parameters in stroke patients. *AJNR Am J Neuroradiol*. 2004;25:720-729
13. Wintermark M, Maeder P, Verdun FR, Thiran JP, Valley JF, Schnyder P, Meuli R. Using 80 kvp versus 120 kvp in perfusion ct measurement of regional cerebral blood flow. *AJNR Am J Neuroradiol*. 2000;21:1881-1884
14. Murase K, Nanjo T, Ii S, Miyazaki S, Hirata M, Sugawara Y, Kudo M, Sasaki K, Mochizuki T. Effect of x-ray tube current on the accuracy of cerebral perfusion parameters obtained by ct perfusion studies. *Physics in medicine and biology*. 2005;50:5019-5029
15. Kamena A, Streitparth F, Grieser C, Lehmkuhl L, Jamil B, Wojtal K, Ricke J, Pech M. Dynamic perfusion ct: Optimizing the temporal resolution for the calculation of perfusion ct parameters in stroke patients. *Eur J Radiol*. 2007;64:111-118
16. Wiesmann M, Berg S, Bohner G, Klingebiel R, Schopf V, Stoeckelhuber BM, Yousry I, Linn J, Missler U. Dose reduction in dynamic perfusion ct of the brain: Effects of the scan frequency on measurements of cerebral blood flow, cerebral blood volume, and mean transit time. *Eur Radiol*. 2008;18:2967-2974
17. Funama Y, Taguchi K, Utsunomiya D, Oda S, Yanaga Y, Yamashita Y, Awai K. Combination of a low-tube-voltage technique with hybrid iterative reconstruction (idose) algorithm at coronary computed tomographic angiography. *J Comput Assist Tomogr*. 2011;35:480-485
18. Kilic K, Erbas G, Guryildirim M, Arac M, Ilgit E, Coskun B. Lowering the dose in head ct using adaptive statistical iterative reconstruction. *AJNR Am J Neuroradiol*. 2011;32:1578-1582
19. Bulla S, Blanke P, Hassepass F, Krauss T, Winterer JT, Breunig C, Langer M, Pache G. Reducing the radiation dose for low-dose ct of the paranasal sinuses using iterative reconstruction: Feasibility and image quality. *Eur J Radiol*. 2012;81:2246-2250
20. Vorona GA, Zuccoli G, Sutcavage T, Clayton BL, Ceschin RC, Panigrahy A. The use of adaptive statistical iterative reconstruction in pediatric head ct: A feasibility study. *AJNR Am J Neuroradiol*. 2012
21. Ren Q, Dewan SK, Li M, Li J, Mao D, Wang Z, Hua Y. Comparison of adaptive statistical iterative and filtered back projection reconstruction techniques in brain ct. *Eur J Radiol*. 2012;81:2597-2601
22. Machida H, Takeuchi H, Tanaka I, Fukui R, Shen Y, Ueno E, Suzuki S, Lin XZ. Improved delineation of arteries in the posterior fossa of the brain by model-based iterative reconstruction in volume-rendered 3d ct angiography. *AJNR Am J Neuroradiol*. 2013;34:971-975
23. Suzuki S, Machida H, Tanaka I, Ueno E. Vascular diameter measurement in ct angiography: Comparison of model-based iterative reconstruction and standard filtered back projection algorithms in vitro. *AJR Am J Roentgenol*. 2013;200:652-657
24. Ma J, Zhang H, Gao Y, Huang J, Liang Z, Feng Q, Chen W. Iterative image reconstruction for cerebral perfusion ct using a pre-contrast scan induced edge-preserving prior. *Physics in medicine and biology*. 2012;57:7519-7542

25. Manhart MT, Kowarschik M, Fieselmann A, Deuerling-Zheng Y, Royalty K, Maier AK, Hornegger J. Dynamic iterative reconstruction for interventional 4-d c-arm ct perfusion imaging. *IEEE transactions on medical imaging*. 2013;32:1336-1348

26. Scibelli A. Idose⁴ iterative reconstruction technique. Philips healthcare whitepaper. *Available via https://www.healthcare.philips.com/pwc_hc/main/shared/Assets/Documents/ct/idose_white_paper_452296267841.pdf.* 2011

27. Noel PB, Fingerle AA, Renger B, Munzel D, Rummeny EJ, Dobritz M. Initial performance characterization of a clinical noise-suppressing reconstruction algorithm for mdct. *AJR Am J Roentgenol*. 2011;197:1404-1409

28. Niu YT, Mehta D, Zhang ZR, Zhang YX, Liu YF, Kang TL, Xian JF, Wang ZC. Radiation dose reduction in temporal bone ct with iterative reconstruction technique. *AJNR Am J Neuroradiol*. 2012;33:1020-1026

29. Abels B, Villablanca JP, Tomandl BF, Uder M, Lell MM. Acute stroke: A comparison of different ct perfusion algorithms and validation of ischaemic lesions by follow-up imaging. *Eur Radiol*. 2012;22:2559-2567

Improving head and neck CTA with hybrid and model-based iterative reconstruction techniques

JM Niesten, IC van der Schaaf, PC Vos, MJ Willemink, BK Velthuis

Submitted

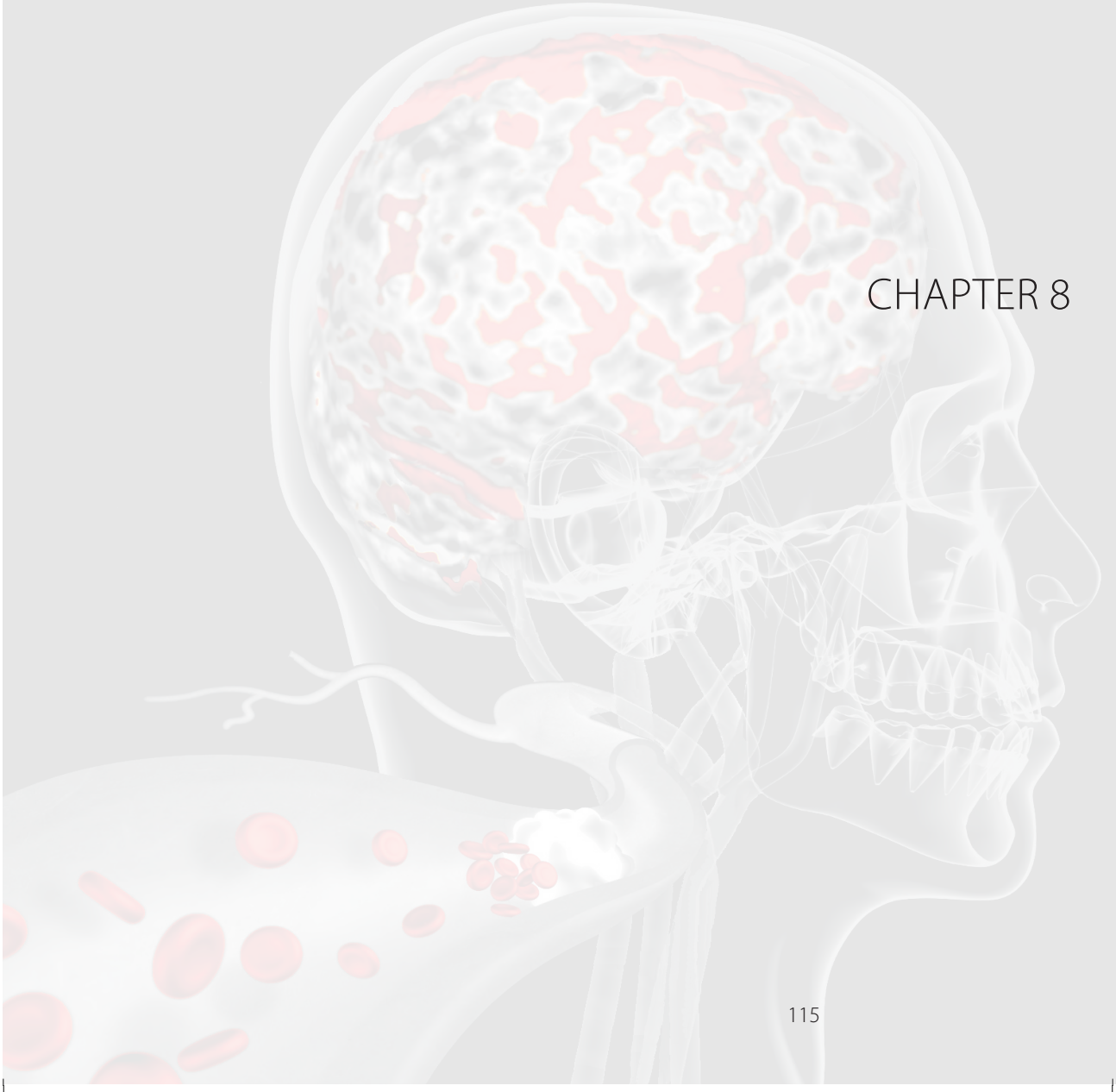

CHAPTER 8

ABSTRACT

Background

To compare image quality (IQ) of head and neck CTA reconstructed with standard filtered back projection (FBP), hybrid iterative reconstruction (HIR) and model-based iterative reconstruction (MIR) algorithms.

Methods

Thirty-four CTAs were reconstructed with FBP and two different HIR- and MIR-levels. Objective (contrast-to-noise-ratio (CNR), automatic vessel analysis (AVA), stenosis grade) and subjective IQ (ranking at level of Circle of Willis, carotid bifurcation, shoulder) of the five reconstructions were compared using repeated-measures ANOVA and post-hoc analysis.

Results

CNR was highest for high MIR, followed by low MIR, high HIR, mid HIR and FBP ($p<0.001$ except low MIR versus high HIR ($p>0.33$)).

AVA showed most complete carotids in both MIR-levels, followed by high HIR ($p>0.08$), mid HIR ($p<0.023$) and FBP ($p<0.010$), vertebral arteries completeness was similar ($p=0.40$ and $p=0.06$). Stenosis grade showed no significant differences ($p=0.16$).

High HIR showed best subjective IQ at Circle of Willis and carotid bifurcation level, followed by mid HIR. At shoulder level low MIR and high HIR were ranked best, followed by high MIR.

Conclusion

Iterative reconstruction substantially improves IQ in head and neck CTA. Both HIR and MIR improves objective IQ and AVA performance. While MIR has best objective IQ, subjective IQ is superior for HIR.

INTRODUCTION

Computed tomography angiography (CTA) of the head and neck is an integral part of assessing acute and chronic neurovascular disease. In the acute setting CTA plays an essential role in patients with acute ischemic stroke or subarachnoid hemorrhage. Head CTA is often performed in the setting of cerebral aneurysms, vascular malformations, and deep venous thrombosis. Combined head and neck CTA is performed in patients with symptoms of acute stroke to assess intracranial and extracranial vessels [1, 2]. CTA of the head is part of the routine work-up in patients with acute subarachnoid haemorrhage to detect cerebral aneurysms [3].

The standard, and most commonly used, reconstruction method for CTA is filtered back projection (FBP) [4]. The most important disadvantage of FBP is the increased amount of image noise when radiation dose is reduced. Recent developments of hardware with more computational power made it possible to replace FBP by hybrid iterative reconstruction (HIR) algorithms [5]. These HIR algorithms allow for radiation dose reduction by decreasing noise, or improve image quality with the same radiation dose [6]. All major CT vendors have now introduced their own HIR algorithms and, because these algorithms do not substantially delay CT imaging, they have been accepted as feasible and standard reconstruction algorithms in clinical routine examinations [7-9].

Recently, more advanced model-based IR algorithms (MIR) that use complex prediction models have also become available and have the potential to reduce radiation dose while maintaining image quality even further compared to HIR algorithms [4, 10]. Initial studies revealed promising results for the use of a MIR called Veo (GE Healthcare) [6, 11-18] while more recently another vendor introduced a MIR algorithm (IMR, Iterative Model Reconstruction, Philips Healthcare) [19, 20]. To our knowledge, the effects of this new IR algorithm on image quality of CTA of the head and neck have not yet been assessed.

The aim of our study was to compare the objective and subjective image quality of CTA of the head and neck arteries reconstructed with standard FBP, HIR and MIR.

MATERIALS AND METHODS

Patients

We prospectively collected consecutive CTA-scans of 34 patients who underwent a head CTA or a combined CTA of head and neck between February 2013 and March 2013. Indications for the combined CTA's were evaluation of cerebral ischemia (n=22). The head CTAs were performed for suspected sinus thrombosis (n=7) or as follow-up study of intracranial aneurysms (n=4) or arteriovenous malformation (n=1). This study was approved by the ethics committee of the University Medical Center Utrecht. The need for informed consent was waived as anonymous data were obtained from routine care CT image acquisitions and patients were not exposed to additional radiation doses.

Imaging

All imaging studies were performed on a 256-slice CT scanner (Brilliance iCT, Philips Healthcare, Best, the Netherlands). CTA was performed with 60 mL (head CTA) or 65 mL (combined CTA) of non-ionic contrast agent (Ultravist, 300 mg Iopromide/mL) injected into the antecubital vein (18 gauge needle) at a rate of 6 mL/s followed by a 40 mL saline flush at a rate of 6 mL/s.

Both CTA protocols were performed in the helical mode by using 128 x 0.625 mm collimation and a pitch of 0.30 and images were obtained by using 120 kVp, 150 mAs and a 0.4 second rotation time. Images were reconstructed with a 512 x 512 matrix and a section thickness of 0.90 mm and reconstruction increment of 0.45 mm (head CTA) or a section thickness of 0.67 mm with reconstruction increment of 0.34 mm (combined CTA).

Image reconstruction

The raw data of each study were simultaneously reconstructed with FBP, HIR (iDose^4, Philips Healthcare, Best, the Netherlands) and with a prototype version of a MIR algorithm (IMR, Philips Healthcare, Best, the Netherlands)

Unlike conventional FBP, which is based on simpler mathematical assumptions regarding the tomographic imaging system, iDose^4, which is the newest commercially available HIR technique introduced by Philips [21], filters in both the raw data and the image domain. The noisiest raw data are identified and denoised while edges are preserved using a maximum likelihood algorithm that reduces noise and artefacts based on Poisson statistics [22]. The level of noise reduction can be adjusted in six different levels, reflecting a scale of how strongly the noise reduction is performed. In this study iDose^4 levels 3 (mid HIR) and 6 (high HIR) were used, corresponding to noise reductions of 23% and 45%, respectively, according to the manufacturer's information [23].

Recently, Philips introduced a new MIR algorithm (Iterative Model Reconstruction, IMR) that models both the CT system geometry and the statistics of the X-rays [20]. Exact details are propriety and have not been published yet, however this algorithm is probably similar to Veo [19]. MIR algorithms typically use multiple forward and backward reconstruction steps and accurately model the data collection process of CT [11]. The level of noise reduction can be adjusted in three different levels; for this study IMR level 1 (low MIR) and 3 (high MIR) were used.

Quantitative assessment

To compare the objective image quality of the five different CTA reconstructions the vascular contrast and contrast-to-noise ratio (CNR) measurements as well as the ability to perform automatic vessel analysis were investigated.

For vascular contrast and CNR measurements, regions of interest (ROIs) were placed in the Circle of Willis (CoW) at the level of the middle cerebral artery (MCA) and in the carotid arteries at the level of the bifurcation. To improve reproducibility we placed five ROIs in the MCA segment 1 and segment 2 and in the carotid arteries and measured mean attenuation in Hounsfield Units (HU) and standard deviation. A large ROI of 25 x 25 mm was placed as reference in a

homogeneous region in the centre of one occipital lobe, assuring no vascular contour and no surrounding structures were included in the ROI. The exact same positions of the ROIs were copied into all reconstructions and attenuation in HU and standard deviation as a measure of noise of the ROIs were measured automatically for the five different reconstructions.
Vascular contrast was calculated as the average CT number of the vascular ROIs minus the average CT number of the reference ROI. Contrast-to-noise ratio was calculated by dividing the vascular contrast by the standard deviation of the reference ROI (i.e. image noise) and was determined separately for the MCA and carotid arteries.

Qualitative assessment

To assess the ability of automatic vessel analysis, all CTA datasets were analysed with "Advanced Vessel Analysis" software with "bone removal" in a CT workstation (Extended Brilliance Workspace; Philips Healthcare, Best, the Netherlands). No manual correction was used. All four neck arteries (carotid and vertebral arteries) were assessed for completeness of segmentation with a four point score with one point for each segment that was present by one investigator. Points were allocated for each carotid artery as follows: origin at shoulder level; common carotid artery and bifurcation; post bifurcation extracranial internal carotid artery; and intracranial level up to the top of the internal carotid artery. Points for each vertebral artery were given for: origin; proximal half and distal half of the extracranial vertebral artery; and intracranial part of the vertebral artery including the basilar artery.
Subsequently, with the use of two calipers the degree of stenosis (if present) in all five reconstructions was measured in both internal carotid arteries. One caliper was used as a stenosis marker and one caliper as a reference marker. This stenosis measurement is comparable to the original NASCET criteria [24, 25].
To assess the subjective image quality two experienced clinical radiologists (observer 1 with 10 years of experience and observer 2 with 20 years of experience in neurovascular CTA) were asked to score the quality of CTA images. The observers were blinded for all data and the different reconstructions of CTA images were presented randomly. The observers were instructed to rank the different reconstructions from best (1 point) to worst (5 points) at the level of CoW in all patients, and at the level of carotid bifurcation and the shoulder level of the origin of the carotid and vertebral arteries if the CTA scan range included the neck arteries. The observers were instructed to base their ranking on their personal preference concerning the following image quality parameters: arterial enhancement (and noise), vascular contour (sharpness of the definition of the vascular contour) and visibility of pathology (i.e. thrombus, atherosclerosis or aneurysm if present).

Statistical analysis

Data were assessed for normality using Quantile-Quantile plots and histograms. Differences in the objective parameters attenuation, image noise, CNR, means of the completeness of segmentation scores and grade of stenosis be-

tween the five CTA reconstructions were tested by means of the analysis of variance (ANOVA) with repeated measures test. In case of significant differences between the five CTA reconstructions, individual CTA reconstructions were pairwise post-hoc compared by paired t-tests with a Bonferonni correction. For the subjective image quality the interobserver agreement was estimated with the weighted Cohen's kappa (κ) and median rankings (range) were calculated for each reconstruction. Statistical analyses were performed using SPSS, version 20.0 (SPSS Inc., Chicago, USA). A P-value of <0.05 was considered to indicate a statistically significant difference.

RESULTS

Of the 34 included patients (average age of 59.6 ± 16.3 (standard deviation) years, 59% women), 22 patients underwent a combined CTA of the head and neck arteries and 12 patients underwent a CTA of the head only.

Quantitative assessment

Table 1 shows the image noise, vascular contrast and the CNR for the 5 different CTA reconstructions in the CoW and carotid arteries. The image noise was lowest in high MIR, followed by low MIR, high HIR, mid HIR and FBP, respectively. Differences were significant between all reconstructions (p<0.001), except for the difference between low MIR and high HIR (p=0.99).

Table 1 *Mean attenuation in Hounsfield Units (HU), image noise, and the contrast-to-noise ratio (CNR) for the various CT angiographic reconstructions in MCA and carotid arteries and reference region of interest*

	Reconstruction					*P-value*
	FBP	*Mid HIR*	*High HIR*	*Low MIR*	*High MIR*	
Image noise (HU)	12.7 ± 2.2*	10.2 ± 1.9[ade]	8.2 ± 1.8[abe]	8.0 ± 1.5[abe]	5.6 ± 2.0*	<0.001
Vascular territory						
Circle of Willis						
Vascular contrast (HU)	214.5 ± 57.2[de]	210.5 ± 60.1[de]	209.2 ± 61.1[de]	234.5 ± 66.0[abc]	233.9 ± 66.5[abc]	<0.001
CNR	20.4 ± 5.5*	24.9 ± 7.0*	27.2 ± 8.3[abe]	27.2 ± 9.2[abe]	41.0 ± 16.5*	<0.001
Carotid arteries						
Vascular contrast (HU)	313.5 ± 78.0[de]	312.9 ±78.3[de]	312.3 ±78.2[de]	321.1± 79.1[abc]	321.0 ± 78.5[abc]	<0.001
CNR	25.7 ± 8.5*	32.0 ± 10.5*	40.8 ± 3.1[abe]	42.7 ± 12.6[abe]	64.5 ± 24.6*	<0.001

P-values of the ANOVA with repeated measures test are shown.

[a]Significanty different from FBP [b]Significanty different from mid HIR [c]Significanty different from high HIR [d]Significanty different from low MIR [e]Significanty different from high MIR *Significant different from all other reconstructions. Data are means ± standard deviations. MCA = middle cerebral artery; FBP = filter back projection; HIR = hybrid iterative reconstruction; MIR = model-based iterative reconstruction

Vascular contrast was significantly higher in both the CoW and carotid arteries with both levels of MIR compared to the other reconstruction methods (all p<0.0001).

The CNR was highest with high MIR, followed by low MIR, high HIR, mid HIR and lowest in FBP in all vascular territories *(Figure 1,2,3).* Differences were sig-

nificant between all reconstructions in both the MCA and carotid arteries (all p<0.001) except for the differences between low MIR and high HIR (p=1.00 and p=0.33, respectively).

Figure 1 *Images of different CTA reconstructions of CoW*

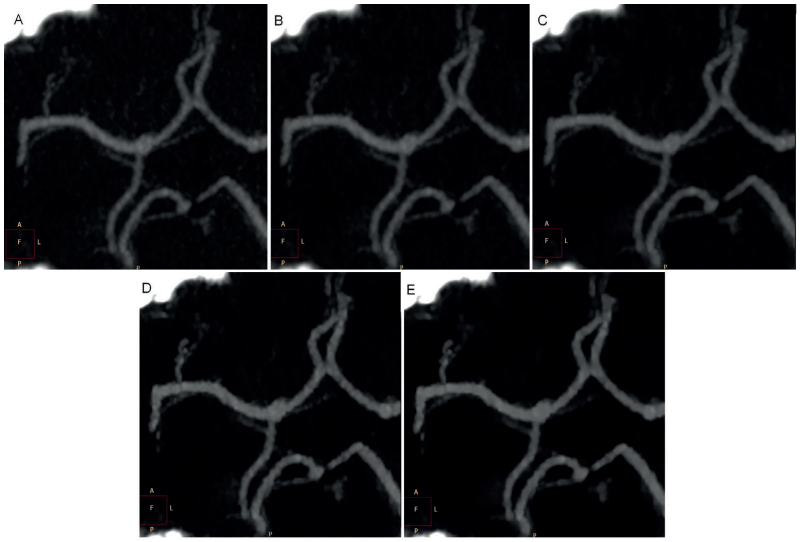

On average the highest level of model-based IR (MIR, image E) showed the best objective image quality while the subjective image quality of hybrid IR level 6 (HIR, image C) was ranked as best by both observers. A: FBP B: Mid HIR C: High HIR D: Low MIR E: High MIR

Figure 2 *Images of different CTA reconstructions of carotid arteries*

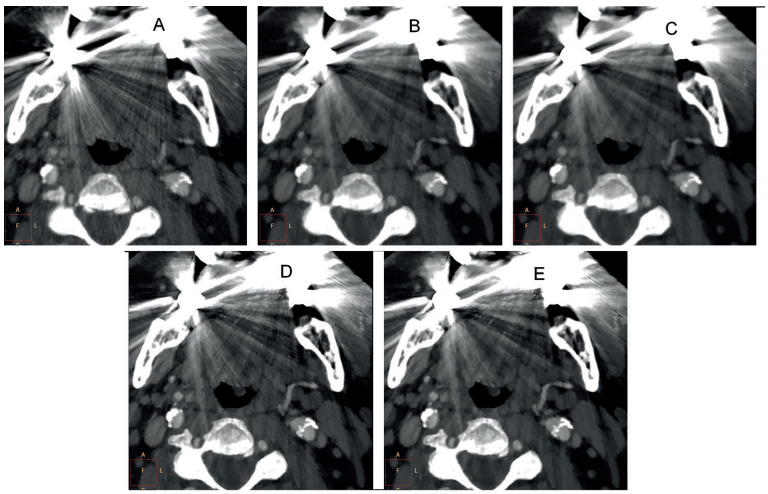

On average the highest level of model-based IR (MIR, image E) showed the best objective image quality while the subjective image quality of hybrid IR level 6 (HIR, image C) was ranked as best by both observers. A: FBP B: Mid HIR C: High HIR D: Low MIR E: High MIR

Figure 3 *Images of different CTA reconstructions of aortic arch*

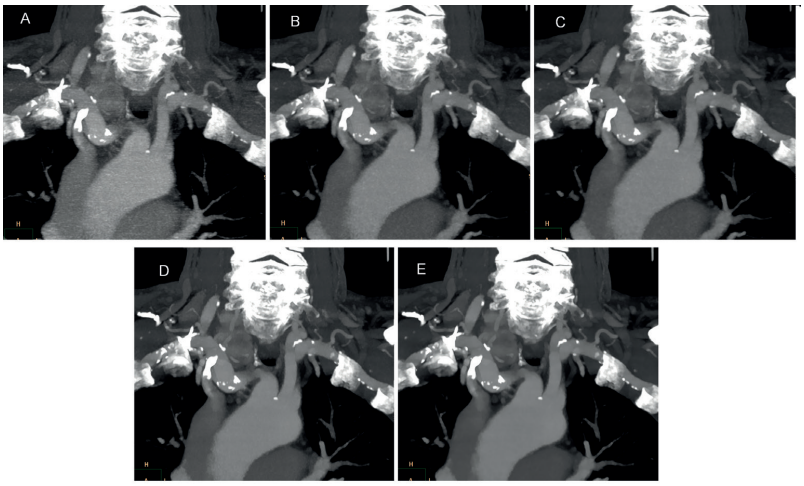

On average the highest level of model-based IR (MIR, image E) showed the best objective image quality while the subjective image quality of the lowest MIR level (observer 1, image D) and hybrid IR level 6 (HIR, observer 2, image C) were ranked as best. A: FBP B: Mid HIR C: High HIR D: Low MIR E: High MIR

Qualitative assessment

Table 2 shows the ability of automatic vessel analyses. The grade of completeness for both vertebral arteries was similar between all reconstructions (p=0.40 and p=0.06). Significant differences were found in the carotid arteries (both p<0.001). The high and low MIR showed the highest grade of completeness in these arteries, followed by high HIR, mid HIR and FBP *(Figure 4)*. Differences were significant between both MIR levels and mid HIR (all p<0.023) and FBP (all p<0.010) in both carotid arteries and between high HIR and FBP in the right carotid artery (p=0.04). The grade of stenosis showed no significant differences between the different reconstructions (p=0.16).

Table 2 *Results of the advanced vessel analyses*

Advanced Vessel Analyses	***Reconstruction***					***P-value***
	FBP	*Mid HIR*	*High HIR*	*Low MIR*	*High MIR*	
Completeness						
ICA right	2.5 ± 1.5[cde]	2.6 ± 1.5[de]	2.9 ± 1.4[a]	3.1 ± 1.3[ab]	3.1 ± 1.3[ab]	<0.001
ICA left	2.8 ± 1.3[de]	2.8 ± 1.3[de]	3.0 ± 1.2	3.2 ± 1.1[ab]	3.2 ± 1.1[ab]	<0.001
VA right	2.6 ± 1.4	2.9 ± 1.3	2.9 ± 1.3	3.1 ± 1.3	3.1 ± 1.3	0.06
VA left	2.6 ± 1.4	2.6 ± 1.3	2.6 ± 1.3	2.7 ± 1.3	2.8 ± 1.3	0.40
Grade of stenosis	23.8 ± 18.2	22.5 ± 19.9	22.6 ± 19.9	24.2 ± 18.8	26.7 ± 19.6	0.16

The degree of stenosis in all five reconstructions was determined in both internal carotid arteries and each neck artery was assessed for completeness of segmentation with a four point score.

P-values of the ANOVA with repeated measures test are shown.

[a]Significanty different from FBP [b]Significanty different from mid HIR [c]Significanty different from high HIR [d]Significanty different from low MIR [e]Significanty different from high MIR. Data are means ± standard deviations.

ICA=Internal Carotid Artery VA= Vertebral Artery

Figure 4 *Advanced vessel analysis of different reconstructions of completeness of arteries*

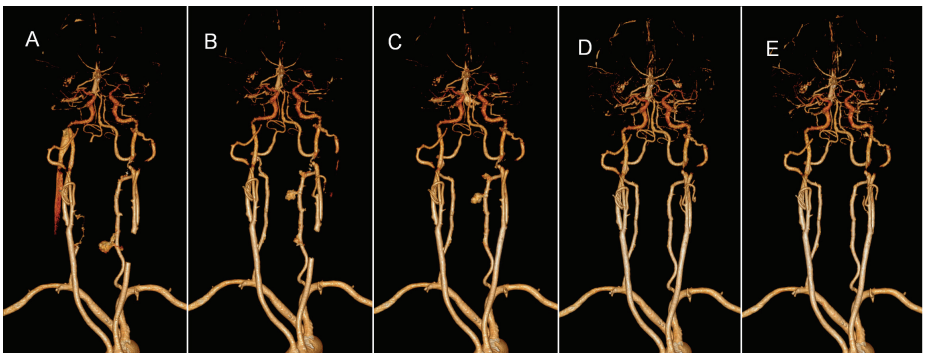

The completeness of arteries of the right and left carotid arteries and the right vertebral artery were found to increase in order from FBP (image A), middle hybrid IR (HIR) level (image B), highest HIR level (image C), lowest model-based IR (MIR, image D) to highest MIR level (image E).

Figure 5 *Scoring results of both observers for the different reconstructions showing median (± range) that reconstructions were scored as best (1 point) to worst (5 points).*

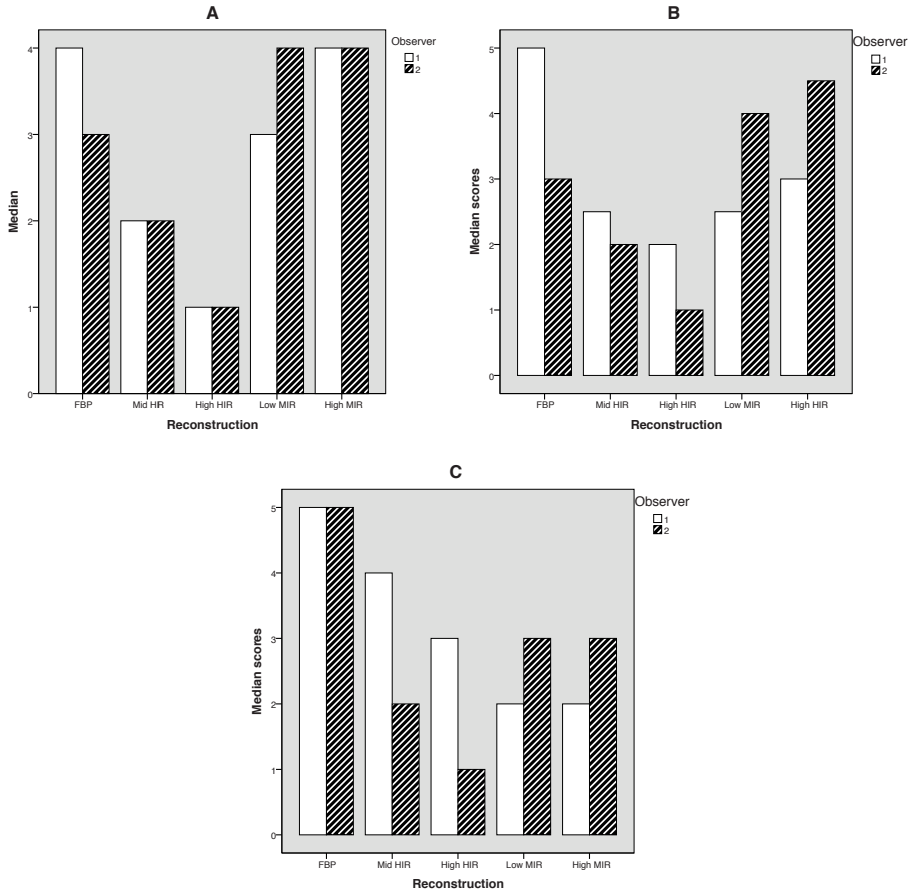

A. At the level of the Circle of Willis. B. At the level of the carotid arteries C. At the shoulder level

The average interobserver agreement for the subjective image quality scoring was fair to moderate (κ =0.40). At the level of CoW and at the level of the carotid bifurcation both observers ranked high HIR most often as having the best image quality *(Figure 1,2,5A and 5B),* followed by low MIR (observer 1) and mid HIR (observer 2) as second best.

High MIR was most often rated as worst by both observers. At shoulder level (i.e. the origin of the carotid and vertebral arteries) observer 1 ranked low MIR most often as best, followed by high HIR while observer 2 scored high HIR most often as best, followed by high MIR. In the far majority both observers scored FBP as the worst quality *(Figure 3, Figure 5C).*

DISCUSSION

This study aimed to compare the image quality of CTA of the head and neck reconstructed with standard FBP, a hybrid (HIR) and a new model-based IR (MIR) algorithm. Objectively, MIR significantly improved the overall image quality, reduced image noise and improved automated vessel analysis while FBP showed the lowest objective image quality. Subjectively, the highest level of HIR was considered superior at the level of the CoW and the carotid bifurcation, and along with the lowest level of MIR for the origins of the neck arteries at shoulder level.

Goals for obtaining good quality of head and neck CTA include correct timing of the contrast bolus to ensure adequate arterial opacification from the aortic arch to the CoW, minimising noise increase due to photon starvation at the shoulder level, avoidance of venous superimposition and blooming artifacts from calcification and minimizing vessel wall blurring along the proximal supra-aortic segments from cardiac motion [26]. Several ways have been suggested to reach some of these goals including increasing the peak voltage, the pitch and the scan speed [26-29]. However, improving the image quality is not guaranteed unless the equipment is used properly and research is an ongoing process to optimize the use of CTA techniques [30].

To our knowledge, investigations about the use of HIR and MIR algorithms in CTA of the head and neck arteries are limited. The use of HIR algorithms has increased in head CT imaging and have shown to result in significant improvements in overall image quality and noise reduction at lower radiation levels without compromising diagnostic accuracy in many clinical applications [31] including native CT of the paediatric [32] and of the adult head with a dose reduction in the range of 20 to 43% [31, 33-35].

The more recently introduced MIR algorithms have been shown to be superior over standard FBP for improving the accuracy of diameter measurement at CT angiography in vitro [12] and over both FBP and HIR in reducing image noise or decreasing radiation dose in abdominal [6], chest [13, 14], liver [11, 17] and in cervical and thoracic non-contrast CT with a reduction of streak artifacts [36].

Furthermore, MIR can improve delineation of the anterior spinal artery and arteries of the posterior fossa in CT angiography [15, 16].
Accurate measurement of the carotid stenosis is important as the benefit, or potential harm of carotid intervention (surgery or endovascular) depends on the degree of stenosis.
Automatic vessel analysis with bone subtraction can improve the detection of stenosis and aneurysms compared to conventional CTA and is approximately 1.5 times faster [25, 37].
We found no significant differences in the estimation of the grade of stenosis between the five different reconstructions. However, MIR was superior in terms of completeness of the carotid arteries compared to HIR, which was in turn superior over FBP.
Although high MIR showed the best objective image quality, high HIR was most often rated as having the best image quality at all levels of the CTA. The interobserver agreement of the subjective image quality was fair to moderate. This was due to the fact that observer 1 gave better rankings to the MIR reconstructions than observer 2. Since MIR images have substantially reduced noise, these images may appear as blotchy and pixelated [7] and, apparently, lead to differences in the subjective ranking and personal preferences of radiologists. This preferences could dependent on the experience of radiologists. Less experienced (aged) radiologists (observer 1) are potentially more open minded to work with new techniques, while more experienced radiologists (observer 2) are more used to and thus may prefer the older look of the images. Because we did not lower our CTA scan protocol, the subjective image was at least already high enough for clinical evaluation in the normal FBP reconstruction, underlined by the fact that the reconstructions preferred were dependent to personal preferences of radiologists. As IR algorithms are known to be especially effective in low-dose (with more noise) the effect of HIR and MIR can be expected to be even larger when low-dose protocols or dose reduction are applied.
There are some aspects that merit consideration. First, as our protocols are already relatively low dose we did not investigate the possibility of further dose reduction with HIR in head and neck CTA. Improvement of image quality with HIR and MIR algorithms at different radiation dose levels is a clinically relevant goal and should be the subject of future research. Second, CT data acquisition, the HIR and MIR algorithms and the software package were from the same single vendor and therefore we cannot comment on those of other vendors. Third, we used a prototype of IMR, which is still in the pre-clinical phase of research. As the clinically introduced version could be a little different, the final version of IMR could also lead to small differences in the results, although the main findings are expected to be the same.
There is a limitation concerning the automatic vessel analysis. Since some details of the vendor specific algorithm creating and displaying the rendered images are unknown, we cannot comment on the possible results of the advanced vessel analysis when other vendors or algorithms are being used. On the other hand, the relatively low CNR between vasculature and parenchyma,

that is essential for vessel segmentation algorithms in general, of our MIR strongly suggests that most segmentation algorithms will probably lead to the same results.

In conclusion, the use of HIR and MIR in CTA of the head and neck arteries reduces the noise and improves image quality and automated vessel analyses. While MIR has the best objective image quality, the subjective image quality is rated superior for HIR.

As the MIR reconstructions show less objective noise and more complete automatic vessel analysis, the substantially reduced noise appearance of the IMR images could be gaining more acceptance in time.

REFERENCES

1. Saake M, Goelitz P, Struffert T, Breuer L, Volbers B, Doerfler A, Kloska S. Comparison of conventional cta and volume perfusion cta in evaluation of cerebral arterial vasculature in acute stroke. *AJNR Am J Neuroradiol*. 2012;33:2068-2073
2. Josephson SA, Bryant SO, Mak HK, Johnston SC, Dillon WP, Smith WS. Evaluation of carotid stenosis using ct angiography in the initial evaluation of stroke and tia. *Neurology*. 2004;63:457-460
3. Westerlaan HE, Gravendeel J, Fiore D, Metzemaekers JD, Groen RJ, Mooij JJ, Oudkerk M. Multislice ct angiography in the selection of patients with ruptured intracranial aneurysms suitable for clipping or coiling. *Neuroradiology*. 2007;49:997-1007
4. Fleischmann D, Boas FE. Computed tomography--old ideas and new technology. *Eur Radiol*. 2011;21:510-517
5. Yanagawa M, Honda O, Kikuyama A, Gyobu T, Sumikawa H, Koyama M, Tomiyama N. Pulmonary nodules: Effect of adaptive statistical iterative reconstruction (asir) technique on performance of a computer-aided detection (cad) system-comparison of performance between different-dose ct scans. *Eur J Radiol*. 2012;81:2877-2886
6. Deak Z, Grimm JM, Treitl M, Geyer LL, Linsenmaier U, Korner M, Reiser MF, Wirth S. Filtered back projection, adaptive statistical iterative reconstruction, and a model-based iterative reconstruction in abdominal ct: An experimental clinical study. *Radiology*. 2013;266:197-206
7. Willemink MJ, de Jong PA, Leiner T, de Heer LM, Nievelstein RA, Budde RP, Schilham AM. Iterative reconstruction techniques for computed tomography part 1: Technical principles. *Eur Radiol*. 2013
8. Willemink MJ, Leiner T, de Jong PA, de Heer LM, Nievelstein RA, Schilham AM, Budde RP. Iterative reconstruction techniques for computed tomography part 2: Initial results in dose reduction and image quality. *Eur Radiol*. 2013;23:1632-1642
9. Willemink MJ, Schilham AM, Leiner T, Mali WP, de Jong PA, Budde RP. Iterative reconstruction does not substantially delay ct imaging in an emergency setting. *Insights into imaging*. 2013;4:391-397
10. Yu Z, Thibault JB, Bouman CA, Sauer KD, Hsieh J. Fast model-based x-ray ct reconstruction using spatially nonhomogeneous icd optimization. *IEEE transactions on image processing : a publication of the IEEE Signal Processing Society*. 2011;20:161-175
11. Chang W, Lee JM, Lee K, Yoon JH, Yu MH, Han JK, Choi BI. Assessment of a model-based, iterative reconstruction algorithm (mbir) regarding image quality and dose reduction in liver computed tomography. *Invest Radiol*. 2013
12. Suzuki S, Machida H, Tanaka I, Ueno E. Vascular diameter measurement in ct angiography: Comparison of model-based iterative reconstruction and standard filtered back projection algorithms in vitro. *AJR Am J Roentgenol*. 2013;200:652-657
13. Katsura M, Matsuda I, Akahane M, Sato J, Akai H, Yasaka K, Kunimatsu A, Ohtomo K. Model-based iterative reconstruction technique for radiation dose reduction in chest ct: Comparison with the adaptive statistical iterative reconstruction technique. *Eur Radiol*. 2012;22:1613-1623
14. Katsura M, Matsuda I, Akahane M, Yasaka K, Hanaoka S, Akai H, Sato J, Kunimatsu A, Ohtomo K. Model-based iterative reconstruction technique for ultralow-dose chest ct: Comparison of pulmonary nodule detectability with the adaptive statistical iterative reconstruction technique. *Invest Radiol*. 2013;48:206-212
15. Machida H, Takeuchi H, Tanaka I, Fukui R, Shen Y, Ueno E, Suzuki S, Lin XZ. Improved delineation of arteries in the posterior fossa of the brain by model-based iterative reconstruction in volume-rendered 3d ct angiography. *AJNR Am J Neuroradiol*. 2013;34:971-975
16. Machida H, Tanaka I, Fukui R, Kita K, Shen Y, Ueno E, Suzuki S. Improved delineation of the anterior spinal artery with model-based iterative reconstruction in ct angiography: A clinical pilot study. *AJR Am J Roentgenol*. 2013;200:442-446
17. Shuman WP, Green DE, Busey JM, Kolokythas O, Mitsumori LM, Koprowicz KM, Thibault JB, Hsieh J, Alessio AM, Choi E, Kinahan PE. Model-based iterative reconstruction versus adaptive statistical iterative reconstruction and filtered back projection in liver 64-mdct: Focal lesion detection, lesion conspicuity, and image noise. *AJR Am J Roentgenol*. 2013;200:1071-1076
18. Yasaka K, Katsura M, Akahane M, Sato J, Matsuda I, Ohtomo K. Model-based iterative reconstruction for reduction of radiation dose in abdominopelvic ct: Comparison to adaptive statistical iterative reconstruction. *SpringerPlus*. 2013;2:209
19. Kachelriess M. Iterative reconstruction techniques: What do they mean for cardiac ct? *Curr Cardiovasc Imaging Resp*. 2013;6:268-281
20. Mehta D TR, Morton T, Dhanantwari A, Shefer E. Iterative model reconstruction: Simultaneously lowered computed tomography radiation dose and improved image quality. *Medical Physics International*. 2013;1(2):147-155
21. Lee TY, Chhem RK. Impact of new technologies on dose reduction in ct. *Eur J Radiol*. 2010;76:28-35
22. Noel PB, Fingerle AA, Renger B, Munzel D, Rummeny EJ, Dobritz M. Initial performance characterization of a clinical noise-suppressing reconstruction algorithm for mdct. *AJR Am J Roentgenol*. 2011;197:1404-1409
23. Scibelli A. Idose^4 iterative reconstruction technique. Philips healthcare whitepaper. *Available via https://www.healthcare.philips.com/pwc_hc/main/shared/Assets/Documents/ct/idose_white_paper_452296267841.pdf*. 2011
24. Ota H, Takase K, Rikimaru H, Tsuboi M, Yamada T, Sato A, Higano S, Ishibashi T, Takahashi S. Quantitative vascular measurements in arterial occlusive disease. *Radiographics*. 2005;25:1141-1158

25. Marquering HA, Nederkoorn PJ, Smagge L, Gratama van Andel HA, van den Berg R, Majoie CB. Performance of semiautomatic assessment of carotid artery stenosis on ct angiography: Clarification of differences with manual assessment. *AJNR Am J Neuroradiol*. 2012;33:747-754

26. Korn A, Fenchel M, Bender B, Danz S, Thomas C, Ketelsen D, Claussen CD, Moonis G, Krauss B, Heuschmid M, Ernemann U, Brodoefel H. High-pitch dual-source ct angiography of supra-aortic arteries: Assessment of image quality and radiation dose. *Neuroradiology*. 2013;55:423-430

27. Waaijer A, Prokop M, Velthuis BK, Bakker CJ, de Kort GA, van Leeuwen MS. Circle of willis at ct angiography: Dose reduction and image quality--reducing tube voltage and increasing tube current settings. *Radiology*. 2007;242:832-839

28. Ertl-Wagner BB, Hoffmann RT, Bruning R, Herrmann K, Snyder B, Blume JD, Reiser MF. Multi-detector row ct angiography of the brain at various kilovoltage settings. *Radiology*. 2004;231:528-535

29. Imai K, Ikeda M, Kawaura C, Aoyama T, Enchi Y, Yamauchi M. Dose reduction and image quality in ct angiography for cerebral aneurysm with various tube potentials and current settings. *Br J Radiol*. 2012;85:e673-681

30. Gudjonsdottir J, Ween B, Olsen DR. Optimal use of aec in ct: A literature review. *Radiologic technology*. 2010;81:309-317

31. Rapalino O, Kamalian S, Payabvash S, Souza LC, Zhang D, Mukta J, Sahani DV, Lev MH, Pomerantz SR. Cranial ct with adaptive statistical iterative reconstruction: Improved image quality with concomitant radiation dose reduction. *AJNR Am J Neuroradiol*.33:609-615

32. Vorona GA, Zuccoli G, Sutcavage T, Clayton BL, Ceschin RC, Panigrahy A. The use of adaptive statistical iterative reconstruction in pediatric head ct: A feasibility study. *AJNR Am J Neuroradiol*. 2012

33. Korn A, Fenchel M, Bender B, Danz S, Hauser TK, Ketelsen D, Flohr T, Claussen CD, Heuschmid M, Ernemann U, Brodoefel H. Iterative reconstruction in head ct: Image quality of routine and low-dose protocols in comparison with standard filtered back-projection. *AJNR Am J Neuroradiol*. 2012;33:218-224

34. Kilic K, Erbas G, Guryildirim M, Arac M, Ilgit E, Coskun B. Lowering the dose in head ct using adaptive statistical iterative reconstruction. *AJNR Am J Neuroradiol*. 2011;32:1578-1582

35. Wu TH, Hung SC, Sun JY, Lin CJ, Lin CH, Chiu CF, Liu MJ, Teng MM, Guo WY, Chang CY. How far can the radiation dose be lowered in head ct with iterative reconstruction? Analysis of imaging quality and diagnostic accuracy. *Eur Radiol*. 2013;23:2612-2621

36. Katsura M, Sato J, Akahane M, Matsuda I, Ishida M, Yasaka K, Kunimatsu A, Ohtomo K. Comparison of pure and hybrid iterative reconstruction techniques with conventional filtered back projection: Image quality assessment in the cervicothoracic region. *Eur J Radiol*. 2013;82:356-360

37. Lell M, Anders K, Klotz E, Ditt H, Bautz W, Tomandl BF. Clinical evaluation of bone-subtraction ct angiography (bscta) in head and neck imaging. *Eur Radiol*. 2006;16:889-897

Summary and general discussion
Dutch summary *(Nederlandse samenvatting)*
List of publications
Acknowledgements *(Dankwoord)*
Biography *(Biografie)*

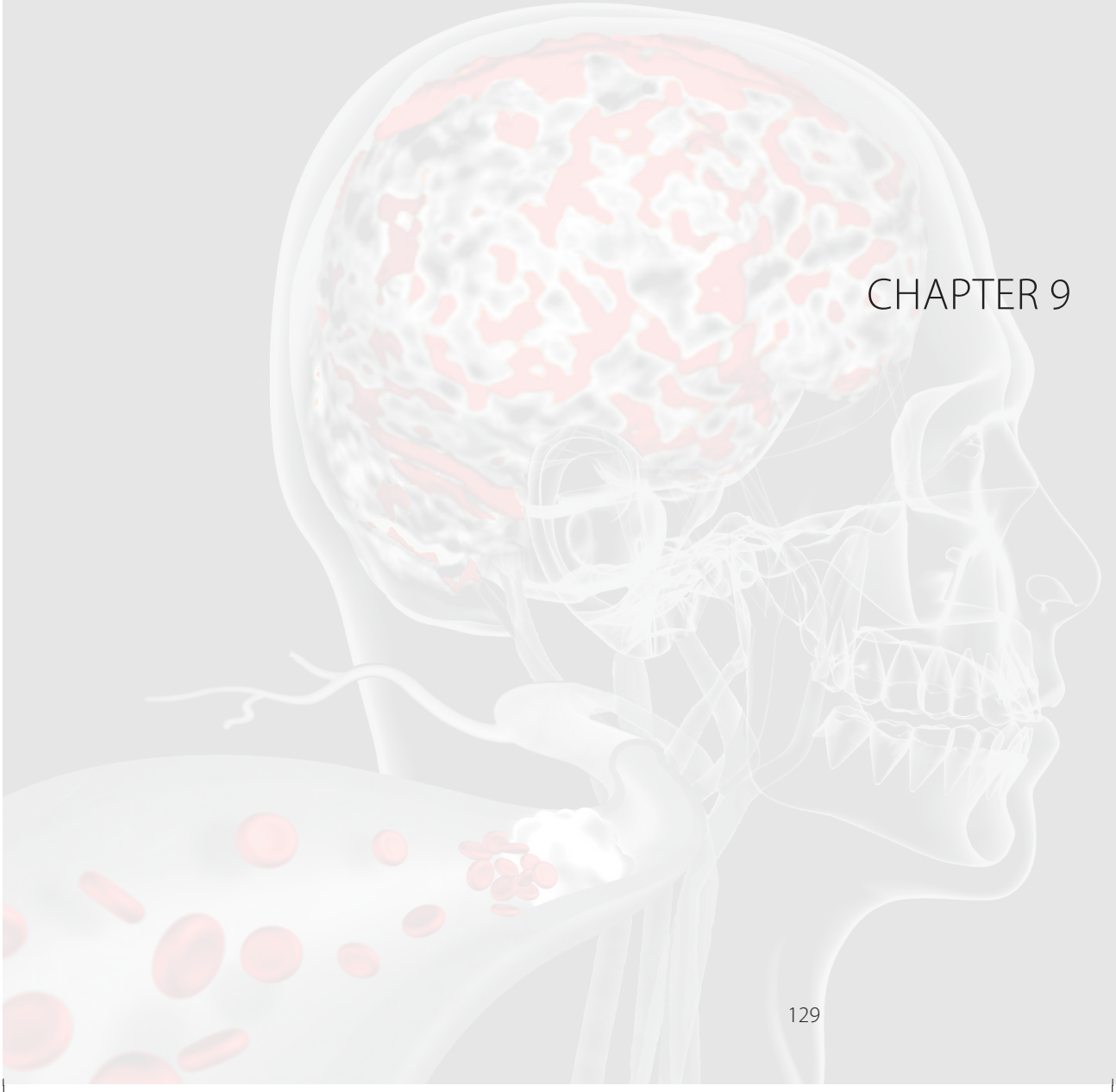

CHAPTER 9

Summary and general discussion

In this thesis two main subjects were discussed. First, histopathologic and CT characteristics of cerebral thrombi were examined. Second, techniques to increase the accuracy and to optimize CTP- and CTA-imaging were explored.
In part 1 of this thesis we investigated the relation between the cause of stroke, the success of intravenous thrombolysis and the pathologic components of thrombi with the attenuation of thrombi on NCCT. First, we looked at the relation between thrombus attenuation and the different stroke subtypes. Second, we performed a histopathologic analysis exploring the relation of thrombus components with the different stroke subtypes and thrombus attenuation. Third, we investigated whether thrombus density is related to recanalization and can predict the likelihood of a persistent occlusion after intravenous thrombolysis (IV-rtPA).
In part 2 we explored ways to optimize the diagnostic accuracy and to reduce radiation dose of CTP and to improve CTA quality. First, the diagnostic accuracy of CTP for the detection of ischemic stroke was evaluated by performing a systematic review of the literature. Second, optimization of quantitative perfusion measurements by the assessment of the vascular in- and output functions was investigated. In the third and fourth chapters the use of iterative reconstruction (IR) algorithms was explored with the goal to reduce the radiation dose with preservation of image quality in CTP and to improve image quality in CTA-imaging while keeping the radiation dose the same.

CHAPTER 9

In this chapter a summary of the major findings, limitations and future directions of these two parts are discussed.

PART 1: CT-IMAGING IN ACUTE ISCHEMIC STROKE: THROMBUS CHARACTERIZATION

The ability to predict the success of IV-rtPA with CT-imaging could improve acute stroke treatment. The combination of pathologic studies with radiologic imaging is therefore important. The attenuation of thrombi on NCCT is related to the composition of thrombi as red blood cells (RBCs) are known to increase the attenuation while platelets and cellular material decrease it [1-4]. We investigated the relation of thrombi attenuation measurements on NCCT with the subtypes of stroke and the recanalization success after IV-rtPA. In addition the pathologic components of thrombi were determined. To increase the generalizability of our findings both the absolute and relative HU (=HU thrombus / HU contralateral vessel, correcting for hematocrit and vendor specific characteristics) were used for analyses.

Major findings

In **chapter 2** we presented the relation between the thrombus attenuation and the presence of a dense vessel sign on 1-mm thin slice NCCT with different stroke subtypes (defined as large artery atherosclerosis, cardioembolism and dissection according to the TOAST criteria) [5]. We found that cardioembolic thrombi showed the least dense vessel signs and the lowest attenuation, followed by thrombi due to large artery atherosclerosis, while dissection thrombi nearly always showed a hyperdense vessel sign and had the highest attenuation. Since the presence of hyperdense vessel sign and attenuation are related to the RBC-component our findings suggest that the thrombi from dissection subtype contains the highest proportion of RBCs, followed by large artery atherosclerosis thrombi, and that cardioembolic thrombi exhibit the least RBCs.

The high numbers of RBCs in the dissection thrombi are easy to understand as dissection typically begins with a tear on the innermost intimal layer or the middle layer of the blood vessel wall. This allows blood to enter the vascular wall under arterial pressure, resulting in an acute intramural hematoma with consequent luminal stenosis or thromboembolic event [6, 7]. As this hematoma consists mostly out of RBCs, dissection thrombi will have high numbers of RBCs. Our finding however that cardioembolic thrombi have less RBCs than large artery atherosclerosis thrombi is contrary to the traditional vision. This traditional hypothesis emphasizes that so called "red thrombi", containing mainly a mixture of fibrin and RBCs, originate from low flow regions, as would be expected in cardioembolic thrombi; while "white thrombi", containing mainly platelets and high amount of fibrin, were thought to arise in regions of fast moving blood, as to be expected in large artery atherosclerosis thrombi [8, 9]. We therefore took a closer look at the validity of this traditional hypothesis and the pathogenesis of the different stroke subtypes. We found that histopathologic information about thrombi leading to cerebral stroke is limited, and interpretations have mainly been derived from thrombus studies of the coronary arteries. In these studies thrombi are all thought to originate from a localised plaque rupture of a pre-existing atherosclerotic process. Recently, it has however been shown that RBCs in particular cause instability with rupture and re-hemorrhage in the ulcerated atherosclerotic plaques, promoting the transition from a stable to an unstable lesion causing coronary occlusions [10-14]. It is therefore more likely that thrombi originating from (unstable) atherosclerotic plaques contain high amounts of RBCs, especially in cerebral thrombi where the majority of atherosclerotic thrombi are due to acute thromboembolic events immediately after intraplaque haemorrhage. The three histopathological studies performed on cerebral thrombi all disprove the traditional assumption. These investigators found similar cell components of thrombi derived from either arterial or cardiac sources and also demonstrated that atherosclerotic thrombi contain significant amounts of RBCs [15-17]. Furthermore, the only study investigating the histopathology of cardioembolisms by either extraction from atrial thrombi (11 patients) or by removal of embolized cardioembolic thrombi from ilio-femoral and subclavian-brachial arteries (11 pa-

tients), concluded that most cardiac thrombi consisted of fibrin, platelets and debris [18]. Embolized thrombi showed twice as much platelet-rich domains (40% of total) compared to non-embolized atrial thrombi (20%).

These recent insights and studies underline our findings (contrary to the traditional assumptions) that thrombi from large artery atherosclerosis could contain more RBCs than cardioembolic thrombi.

As a next step, in **chapter 3** we performed a histopathologic analysis on 22 cerebral thrombi to further explore the relation between composition of thrombi with the stroke subtype and with thrombus attenuation on NCCT. There was a moderate positive correlation (p=0.049) between the attenuation on NCCT and RBC-component of thrombi, which could be even stronger in reality as attenuation was measured before thrombolysis while most thrombi were investigated after thrombolysis (probably influencing thrombus composition). We found that the majority of cerebral thrombi was fresh and, in concordance with the findings of chapter 2, that thrombi originating from large artery atherosclerosis had a higher percentage of RBCs than cardioembolisms, and that large artery atherosclerosis was the only stroke subtype with red (RBC-rich) thrombi.

Because RBC-rich thrombi are more sensitive to IV-rtPA and have higher density on NCCT, we investigated in **chapter 4** the relationship between thrombus density and recanalization and whether persistent occlusions can be predicted by Hounsfield Units (HU)-measurements. We found that the thrombus density on thin-slice NCCT was indeed related to the likelihood of recanalization in patients treated with IV-rtPA only. Lower absolute HU and relative HU were independently (multivariate odds-ratio 3.1 and 4.1, respectively) related to persistent occlusion and HU-measurements significantly increased discriminative performance in a multivariate model with other known predictors for recanalization (subtype of stroke, time to thrombolysis, clot burden score and site of occlusion). Cut-off values of <56.5 absolute HU and relative HU of <1.38 showed the most optimal predictive values for persistent occlusion and may help to select IV-rtPA treated stroke patients who could benefit from (additional) intra-arterial treatment.

Limitations

Exploring the relation of thrombi attenuation measurements on NCCT with the subtypes of stroke, the recanalization success after IV-rtPA and the pathologic components of thrombi, should be considered with some caution. First, in the reports involving the subtype of stroke it was not always possible to determine the cause with certainty, e.g. if atherosclerosis was present in combination with a possible cardiac cause such as atrial fibrillation. Therefore some patients were placed in an "unknown" group. However, the theoretical misclassification of some patients in the wrong stroke subtypes would have probably biased our results towards less strong results, therefore the signifi-

cant differences found in our study will only increase if the possible misclassification would not have happened. Second, in chapter 3 and 4 only a relative small number of patients were investigated, which made it hard to draw solid conclusions. Third, the follow-up CTA performed to assess the rate of recanalization in chapter 4 took place after 1-4 days, which was relatively late. As the occurrence of spontaneous recanalization is known to increase within time [19], part of the recanalization on CTA could have been occurred due to spontaneous recanalization rather than due to a direct effect of IV-rtPA. On the other hand, as the clinical outcome is significantly better in patients who show recanalization on late follow-up our findings were still clinically important despite the reason for recanalization [20].

Future directions

The new insights discussed in chapter 2, 3 and 4 are important in understanding the etiopathogenesis of cerebral thrombi and relating the pathologic characteristics of thrombi with CT-imaging.
To our knowledge, our studies were the first to extensively describe the finding that large artery atherosclerosis thrombi could contain more RBCs than cardioembolic thrombi. Hence, our investigations could change the way we think about the etiopathogenesis of cerebral thrombi and could be a first step into adjustment of treatment based on thrombi characteristics and corresponding attenuation measurements on NCCT.

The findings of chapter 2 that thrombus attenuation was significantly related to the stroke subtype, help to gain insight in the etiopathogenesis of stroke and in making an accurate estimation of the cause of stroke. However, our findings should be validated by future larger multicentre studies.
The findings discussed in chapter 4 that the thrombus density on thin-slice NCCT was indeed related to the likelihood of recanalization in patients treated with IV-rtPA can lead to other treatment management based on the thrombus attenuation measurements and could therefore have clinically important meanings for future interpretation of the NCCT. If a thrombus exhibits a low HU-value for example, IV-rtPA is expected to be unsuccessful and alternative treatments as mechanical thrombectomy could be applied sooner. These thresholds should first be validated in another group of acute stroke patients. After validation further studies could focus on the possible adjustments of treatment based on the thrombi characteristics and corresponding attenuation measurements on NCCT.

PART 2: CT-IMAGING IN ACUTE ISCHEMIC STROKE: TECHNIQUE OPTIMIZATION

With CTP we can visualise information about hemodynamics of the brain complementary to the NCCT. CTP has the ability to determine the extent of infarct core and penumbra and can help in treatment decision making. A CTA of the head and neck is important in evaluating acute and chronic neurovascular diseases [21].

Major findings

Chapter 5 reviewed the literature on the accuracy of CTP in determining ischemic stroke. In a total of 1107 patients, a pooled analysis resulted in a high sensitivity of 80% and a very high specificity of 95%. Almost two-thirds of the false negatives were due to small lacunar infarcts; the remaining false negatives were mostly due to limited coverage of the CT acquisition. By optimizing CTP techniques and increasing spatial coverage sensitivity for the detection of lacunar infarcts could be improved.

Adding CTP and CTA to the NCCT increases ionising radiation dose about 3-fold, which raises concerns about radiation dose [22, 23]. Therefore, techniques that reduce radiation dose without altering image quality are important subjects to investigate.

In **chapter 6** the objective image quality (quantitative perfusion values, attenuation, image noise, penumbra and infarct area) and subjective image quality (diagnostic and overall image quality) of a standard dose CTP with the standard filtered back projection (FBP) were compared with half dose CTP reconstructed with IR algorithms. We found that with by using IR in CTP imaging it was possible to examine patients with half the radiation dose without significantly altering the objective and diagnostic image quality. However, the standard dose with FBP was still preferable considering the superior subjective image quality in about one quarter of patients.

The accuracy of the quantitative perfusion maps can be improved by selecting an artery with the least partial volume effects as the AIF. With the introduction of the 256-(or more-)MDCT systems the perfusion slab coverage increased [24], providing the opportunity to also select the internal carotid arteries and basilar artery as the arterial input function (AIF) instead of only the anterior cerebral artery (ACA) and middle cerebral artery (MCA). To improve the accuracy and reproducibility of CTP imaging, we described in **chapter 7** that selecting the internal carotid artery as the AIF and continuing the use of a venous sinus as the venous output function (VOF) improved the accuracy of CTP. We found that the selection of AIF had significant effects on the accuracy of quantitative perfusion measurements, leading to major differences (up to 13% for the MTT, 25% for the CBV and more than 50% for CBF). Selection of the internal carotid artery instead of ACA, MCA or basilar artery as the AIF improved the accuracy

of absolute quantitative values in CTP. Deleting the VOF was detrimental for the validity of perfusion results in the majority of patients and was therefore inadvisable.

In **chapter 8** we compared head and neck CTA images reconstructed with three techniques: the standard FBP; a so-called hybrid IR algorithm; and a model-based IR algorithm. Comparison was based on objective and subjective image quality (including carotid stenosis measurement and the ability to perform automatic vessel analysis). No differences were found in the measurement of the carotid stenosis between the reconstructions. However, we did find that the use of model-based IR of the head and neck reduced the noise, improved automated vessel analysis and objective image quality compared to hybrid IR, which was in turn superior to FBP. While the model-based IR had the best objective image quality, the subjective image quality was superior in hybrid IR.

Limitations

Besides the above mentioned increase in radiation dose, another important limitation of CTP is the vendor dependent parameters that are being used. There is a great heterogeneity in the image acquisition, the software package that processes the data and IR reconstruction algorithms. Our results are based on a 64- or 256-slice Philips CT scanner and the accompanying software, therefore it is hard to comment on other vendors and software. Indeed, in the review of chapter 4 the sensitivity of CTP varied considerably between the different studies, which is probably mainly due to heterogeneity in CTP scanning and post processing methods. Although in chapter 6, 7 and 8 we assumed that our results are also valid for other vendors and algorithms, we did not have the possibility of investigating other manufacturers or software. Furthermore, in chapter 8 we used a prototype of the model-based IR algorithm, which is currently only available for research purposes. Reconstructions were time consuming with this prototype, but are expected to improve before implementation in clinical practice. As the clinically introduced version could be slightly different, the final version of IMR could also lead to other results.

Future directions

Our findings discussed in part 2 of this thesis, show how the accuracy and image quality of CTP and CTA can be improved and how the radiation dose can be minimized. Selection of the internal carotid artery will increase the validity of perfusion results, providing a robust way to get the best result from CTP-imaging. Furthermore, it is an important step to deal with the problem of a lack of standardization in CTP-imaging. A wide variety of CTP techniques has become available to assess vascular lesions and brain parenchyma in acute ischemic stroke patients; different vendors have their own scanners and apply their own filters, their own thresholds and their own post-processing software [25]. Even within the same vendor, different software possibilities are often offered, all possibly leading to other estimations of the ischemic lesions.

Therefore there is a great need for standardization of the CTP methods and future large studies should compare all possible methods and advise on the best standard method to evaluate CTP scans.
We showed that IR algorithms are promising techniques in CTP- and CTA-imaging and are able to either substantially lower the radiation dose without affecting the objective CTP-image quality or to improve the CTA-image quality with the same dose. Advanced CT scanners that allow imaging of the entire brain are more often introduced in institutions and this will further increase ionising radiation dose [23]. Our findings will help to minimize the increase in radiation dose. Future studies should focus on the influence and the possibility of IR algorithms in reducing radiation dose or improving image quality in other vendors. For CTA-imaging future technical studies should work on improving the objective image quality without affecting the subjective image quality. As quick evaluation is important, investigations should also focus on how to perform these reconstructions as fast as possible, hopefully leading to standard fast and robust algorithms that will improve image quality or reduce radiation dose even further.

REFERENCES

1. Caplan LR. Antiplatelet therapy in stroke prevention: Present and future. *Cerebrovasc Dis*. 2006;21 Suppl 1:1-6
2. Kim EY, Heo JH, Lee SK, Kim DJ, Suh SH, Kim J, Kim DI. Prediction of thrombolytic efficacy in acute ischemic stroke using thin-section noncontrast ct. *Neurology*. 2006;67:1846-1848
3. Moulin T, Tatu L, Vuillier F, Cattin F. [brain ct scan for acute cerebral infarction: Early signs of ischemia]. *Revue neurologique*. 1999;155:649-655
4. Kirchhof K, Welzel T, Mecke C, Zoubaa S, Sartor K. Differentiation of white, mixed, and red thrombi: Value of ct in estimation of the prognosis of thrombolysis phantom study. *Radiology*. 2003;228:126-130
5. Adams HP, Jr., Bendixen BH, Kappelle LJ, Biller J, Love BB, Gordon DL, Marsh EE, 3rd. Classification of subtype of acute ischemic stroke. Definitions for use in a multicenter clinical trial. Toast. Trial of org 10172 in acute stroke treatment. *Stroke*. 1993;24:35-41
6. Mohan IV. Current optimal assessment and management of carotid and vertebral spontaneous and traumatic dissection. *Angiology*. 2013
7. Stevic I, Chan HH, Chan AK. Carotid artery dissections: Thrombosis of the false lumen. *Thrombosis research*. 2011;128:317-324
8. Chaves CJ, Caplan LR. Heparin and oral anticoagulants in the treatment of brain ischemia. *Journal of the neurological sciences*. 2000;173:3-9
9. Molina CA, Montaner J, Arenillas JF, Ribo M, Rubiera M, Alvarez-Sabin J. Differential pattern of tissue plasminogen activator-induced proximal middle cerebral artery recanalization among stroke subtypes. *Stroke*. 2004;35:486-490
10. Vila A, Korytowski W, Girotti AW. Spontaneous transfer of phospholipid and cholesterol hydroperoxides between cell membranes and low-density lipoprotein: Assessment of reaction kinetics and prooxidant effects. *Biochemistry*. 2002;41:13705-13716
11. Kockx MM, Cromheeke KM, Knaapen MW, Bosmans JM, De Meyer GR, Herman AG, Bult H. Phagocytosis and macrophage activation associated with hemorrhagic microvessels in human atherosclerosis. *Arteriosclerosis, thrombosis, and vascular biology*. 2003;23:440-446
12. Kolodgie FD, Gold HK, Burke AP, Fowler DR, Kruth HS, Weber DK, Farb A, Guerrero LJ, Hayase M, Kutys R, Narula J, Finn AV, Virmani R. Intraplaque hemorrhage and progression of coronary atheroma. *The New England journal of medicine*. 2003;349:2316-2325
13. Rao DS, Goldin JG, Fishbein MC. Determinants of plaque instability in atherosclerotic vascular disease. *Cardiovascular pathology : the official journal of the Society for Cardiovascular Pathology*. 2005;14:285-293
14. Virmani R, Kolodgie FD, Burke AP, Finn AV, Gold HK, Tulenko TN, Wrenn SP, Narula J. Atherosclerotic plaque progression and vulnerability to rupture: Angiogenesis as a source of intraplaque hemorrhage. *Arteriosclerosis, thrombosis, and vascular biology*. 2005;25:2054-2061
15. Liebeskind DS, Sanossian N, Yong WH, Starkman S, Tsang MP, Moya AL, Zheng DD, Abolian AM, Kim D, Ali LK, Shah SH, Towfighi A, Ovbiagele B, Kidwell CS, Tateshima S, Jahan R, Duckwiler GR, Vinuela F, Salamon N, Villablanca JP, Vinters HV, Marder VJ, Saver JL. Ct and mri early vessel signs reflect clot composition in acute stroke. *Stroke*. 2011;42:1237-1243
16. Marder VJ, Chute DJ, Starkman S, Abolian AM, Kidwell C, Liebeskind D, Ovbiagele B, Vinuela F, Duckwiler G, Jahan R, Vespa PM, Selco S, Rajajee V, Kim D, Sanossian N, Saver JL. Analysis of thrombi retrieved from cerebral arteries of patients with acute ischemic stroke. *Stroke*. 2006;37:2086-2093
17. Almekhlafi MA, Hu WY, Hill MD, Auer RN. Calcification and endothelialization of thrombi in acute stroke. *Ann Neurol*. 2008;64:344-348
18. Wysokinski WE, Owen WG, Fass DN, Patrzalek DD, Murphy L, McBane RD, 2nd. Atrial fibrillation and thrombosis: Immunohistochemical differences between in situ and embolized thrombi. *Journal of thrombosis and haemostasis : JTH*. 2004;2:1637-1644
19. Rha JH, Saver JL. The impact of recanalization on ischemic stroke outcome: A meta-analysis. *Stroke*. 2007;38:967-973
20. Yeo LL, Paliwal P, Teoh HL, Seet RC, Chan BP, Liang S, Venketasubramanian N, Rathakrishnan R, Ahmad A, Ng KW, Loh PK, Ong JJ, Wakerley BR, Chong VF, Bathla G, Sharma VK. Timing of recanalization after intravenous thrombolysis and functional outcomes after acute ischemic stroke. *JAMA neurology*. 2013;70:353-358
21. Korn A, Fenchel M, Bender B, Danz S, Thomas C, Ketelsen D, Claussen CD, Moonis G, Krauss B, Heuschmid M, Ernemann U, Brodoefel H. High-pitch dual-source ct angiography of supra-aortic arteries: Assessment of image quality and radiation dose. *Neuroradiology*. 2013;55:423-430
22. Abels B, Villablanca JP, Tomandl BF, Uder M, Lell MM. Acute stroke: A comparison of different ct perfusion algorithms and validation of ischaemic lesions by follow-up imaging. *Eur Radiol*. 2012
23. Kloska SP, Fischer T, Sauerland C, Buerke B, Dziewas R, Fischbach R, Heindel W. Increasing sampling interval in cerebral perfusion ct: Limitation for the maximum slope model. *Acad Radiol*. 2010;17:61-66

24. Dorn F, Muenzel D, Meier R, Poppert H, Rummeny EJ, Huber A. Brain perfusion ct for acute stroke using a 256-slice ct: Improvement of diagnostic information by large volume coverage. *Eur Radiol*. 2011;21:1803-1810

25. Kudo K, Sasaki M, Yamada K, Momoshima S, Utsunomiya H, Shirato H, Ogasawara K. Differences in ct perfusion maps generated by different commercial software: Quantitative analysis by using identical source data of acute stroke patients. *Radiology*. 2010;254:200-209

Dutch summary
(Nederlandse samenvatting)

In dit proefschrift worden twee hoofdonderwerpen besproken. Het eerste deel gaat over de karakterisering van cerebrale thrombi op non-contrast CT (NCCT). Het tweede gedeelte bespreekt de mogelijkheden en het optimaliseren van CT-perfusie (CTP) en CT-angiografie (CTA).
Een herseninfarct wordt veroorzaakt door een thrombus dat een slagader (i.e. arterie) afsluit waardoor het hersenparenchym niet of in mindere mate wordt voorzien van zuurstofrijk bloed. Het doel van therapie (waarvan intraveneuze trombolyse de eerstelijns behandeling vormt) is om recanalizatie van deze arterie te bewerkstelligen maar wordt slechts in ongeveer de helft van de gevallen bereikt. De componenten van een thrombus houden mogelijk verband met de effectiviteit van deze therapie. Bij patiënten die symptomen van een acuut herseninfarct vertonen, wordt vaak op de eerste hulp eerst een NCCT gemaakt. Met behulp van de NCCT kan eerst een onderscheid gemaakt worden tussen twee vormen van beroerte; hersenbloeding en -infarct. Indien na het beoordelen van de NCCT een hersenbloeding uitgesloten is, worden patiënten in vele centra met een CTP en CTA gescand. Middels de CTP kan de doorbloeding van de hersenen getoond worden. In patiënten met een herseninfarct kan deze techniek gebruikt worden om de irreversibele infarctkern te onderscheiden van het potentieel nog te redden "penumbra". De CTA wordt gebruikt om de oorzaak van de arteriële occlusie, de collaterale circulatie en de mate van extracraniale arteriële stenosen te onderzoeken.

In deel 1 beschrijven wij onderzoeken die tot meer kennis over de thrombussamenstelling en de relatie met de kenmerken ervan op NCCT leiden en laten wij zien hoe het voorspellen van succes van trombolyse op basis van NCCT-beeldvorming te verbeteren is.
In deel 2 onderzochten wij manieren om tot verbetering van de kwaliteit en accuraatheid van CTP en CTA-technieken te komen en om de radiatiedosis zo laag mogelijk te houden.

DEEL 1
CT-BEELDVORMING BIJ ACUUT HERSENINFARCT: THROMBUSKARAKTERISERING

Ongeveer een derde van de arteriële occlusies die herseninfarcten veroorzaken ontstaat door arteriosclerose, een derde door een embolie vanuit het hart en een relatief kleiner gedeelde door een dissectie. Ongeacht de oorzaak van de afsluitende thrombus, is het doel van therapie het recanalizeren van de geoccludeerde arterie. Om dit te bereiken zijn verschillende therapieën voor handen. Intraveneuze trombolyse met recombinant tissue-type plasmino-

gen activator (IV-rtPA) is de enige FDA-goedgekeurde behandeling. De toediening hiervan dient plaatst te vinden binnen 3 uur na het ontstaan van de klachten en is in ongeveer de helft van de gevallen succesvol. Hoewel recente onderzoeken laten zien dat deze tijd window misschien wel tot 4.5 uur verlengd kan worden, wordt de kans op falen of het optreden van een bloeding na deze periode vooralsnog te groot geacht.

Patiënten waarvan de IV-rtPA gefaald heeft of die überhaupt niet geschikt waren voor deze behandeling, kunnen in aanmerking komen voor intra-arteriële thrombolyse of mechanische thrombectomie. Hoewel het percentage succesvolle recanalizaties van deze behandeling groot is, gaan deze procedures gepaard met een grote kans op mortaliteit of andere ernstige complicaties.

Een NCCT is het enige onderzoek wat vereist is voor de beoordeling tot behandeling met IV-rtPA. In vele ziekenhuizen is dit ook de enige beschikbare CT-techniek en daarnaast wordt in andere klinieken direct na de NCCT (en nog voor het vervaardigen van de CTP en CTA) overgegaan tot wel of niet toedienen van IV-rtPA. De mogelijkheid om op de NCCT te kunnen voorspellen welke patiënten niet zullen recanalizeren na IV-rtPA zal de keuze tot het overgaan op de andere behandelingen vergemakkelijken. Om dit zo goed mogelijk te kunnen onderzoeken is het belangrijk meer te weten te komen over de pathofysiologie van een thrombus en de verhouding daarvan met de NCCT-karakteristieken. In de literatuur wordt beschreven dat de samenstelling van een thrombus, welke voornamelijk bestaat uit rode bloed cellen (eryhtrocyten), bloedplaatjes (thrombocyten) en fibrine, verband houdt met de gevoeligheid voor IV-rtPA en de verschillende infarcttypen. Aangezien erytrocyten een positieve lineaire en bloedplaatjes een negatieve relatie hebben met de aankleuring (densiteit) van een thrombus op NCCT, onderzochten wij in deel één van dit proefschrift de relaties tussen de thrombusdensiteit op NCCT met de subtypen, de histopathologische samenstelling van thrombus en de kans op recanalizatie.

In **hoofdstuk 2** laten we de resultaten zien van het onderzoek naar de relatie van de thrombusdensiteit (gemeten in Hounsfield Units (HU)) op NCCT met de verschillende subtypen van infarct. Wij vonden dat er een significante relatie bestaat tussen de densiteit en de origine van thrombi. Een thrombus van cardioembolische origine had de laagste densiteit en liet de minste "dense vessel signs" zien, in oplopende volgorde gevold door arteriosclerose en dissectie. Vanwege de lineaire relatie van erythrocyten met de densiteit, suggereerden deze bevindingen ook dat het gemiddelde percentage van erythrocyten in een thrombus dezelfde sequentie heeft. Deze bevindingen zijn in tegenstelling tot de traditionele opvatting dat zogenaamde "rode" thrombi, die veel erythrocyten bevatten, voornamelijk in lagere bloedstroomgebieden (i.e. cardioembolieen) ontstaan en dat witte thrombi (met thrombocyten als belangrijkste component) vanuit hoge stroomgebieden voortkomen, zoals verwacht bij arteriosclerose.

Om onze theorie en de onjuistheid van de traditionele opvatting te kunnen bevestigen presenteren wij in **hoofdstuk 3** de histopathologische samenstelling van 22 thrombi. In overeenstemming met onze bevindingen van hoofdstuk 2 vonden wij dat thrombi ontstaan vanuit arteriosclerose een hoger percentage erythrocyten bevat dan cardioembolische thrombi. Wij vonden ook dat alle als rood geclassificeerde thrombi van arteriosclerotische origine waren en dat geen enkele rode thrombus van cardioembolische origine afkomstig was.

Om een andere belangrijk doel, het voorspellen van de succeskans van IV-rtPA op basis van de NCCT, onder het licht te brengen presenteren wij in **hoofdstuk 4** de relatie tussen de densiteit van thrombi en de kans op recanalizatie. Wij vonden dat de kans op recanalizatie inderdaad verband houdt met de thrombusdensiteit gemeten op de NCCT. Een lagere densiteitmeting geeft een hogere kans op het persisteren van een occlusie. Bovendien kunnen densiteitmetingen van grote voorspellende waarden zijn bovenop andere bekende predictoren en zijn drempelwaarden van <56.5 absolute HU en <1.38 relatieve HU de nauwkeurigste waarden voor het voorspellen van IV-rtPA falen.

In de hoofdstukken van deel 1 van dit proefschrift bediscussiëren we ook de tot nu toe bestaande onderzoeken over de traditionele opvatting en de gedachten waarom deze theorie niet meer geldig is. Wij laten zien dat deze theorie over de origine van rode en witte thrombi voornamelijk gebaseerd is op studies naar cardiale thrombi en dat er tot nu toe weinig histopathologisch onderzoek verricht is op hersenthrombi. We vonden dat de enige drie cerebrale histopathologische studies die totnogtoe beschreven zijn de traditionele theorie tegenspreken en dat een andere belangrijke studie onze bevinding dat cardioembolische thrombi voornamelijk bloedplaatsjes bevat onderstreept.

DEEL 2
CT-BEELDVORMING BIJ ACUUT HERSENINFARCT: TECHNIEKOPTIMALISATIE

CT-perfusie (CTP) is een waardevolle modaliteit in de evaluatie van patiënten met een verdenking op een herseninfarct en andere neurologische ziekten. Door middel van kwantitatieve parameters, zoals Cerebral Blood Volume (CBV), Cerebral Blood Flow (CBF), en Mean Transit Time (MTT), kan de bloeddoorstroming van de hersenen gemeten en gevisualiseerd worden. CBV meet het totale volume aan bloed in een bepaald volume van de hersenen, CBF is gedefinieerd als het totale volume aan bloed in een bepaald volume van de hersenen per tijdeenheid en MTT als de gemiddelde tijd dat bloed erover doet om door een bepaald hersengebeid te stromen.
Het gebruik van CTP biedt, naast de toegevoegde diagnostische waarde,

meerdere voordelen; het is een snel en relatief goedkoop onderzoek en in veel ziekenhuizen 24 uur per dag beschikbaar. Aan de andere kant heeft het ook enkele limitaties zoals de extra stralingsdosis die patiënten ondervinden en de variatie in resultaten die voortkomen uit de meerdere bedienerafhankelijke stappen die genomen dienen te worden.

Naast het vervaardigen van een CTP, kan ook de toevoeging van de CT-angiografie (CTA) tot essentiële extra informatie leiden in de beeldvorming van patiënten met een herseninfarct. Middels CTA kan de plaats en oorzaak van occlusie, de mate van collaterale circulatie en stenosegraad van vaten in beeld gebracht worden. Een goede beeldkwaliteit van de CTA is belangrijk om tot de best mogelijke interpretatie ervan te komen. Dit hoeft niet alleen op basis van de "directe" CTA-beelden te gebeuren maar vindt ook vaak plaats middels het snellere "automatische vat analyse" waarbij de vaten op een overzichtelijke manier zonder de beïnvloeding van andere structuren worden getoond. De CTA dient daarnaast niet alleen voor een goede beoordeling van het vaatstelsel in de acute fase, het is ook deel van de work-up van infarctpatiënten. Een nauwkeurige meting van de stenosegraad van de carotiden is namelijk belangrijk omdat de uitkomst hiervan de beslissing tot het overgaan op een chirurgische behandeling beïnvloedt.

Ondanks het feit dat meerdere studies de sensitiviteit van CTP voor het aantonen van ischemie onderzochten, ontbreekt in de literatuur een duidelijk overzicht van dit belangrijk onderwerp. In **hoofdstuk 5** van dit proefschrift onderzoeken wij daarom de accuratesse van CTP door het uitvoeren van een systematische review. Wij vonden dat CTP erg accuraat is in het aantonen van ischemische gebieden met een sensitiviteit van 80% en een specificiteit van 95%. Bijna tweederde van alle vals-negatieve gevallen waren het gevolg van kleine lacunaire infarcten, terwijl de resterende een derde door een gelimiteerde breindekking van de CT-scanner kwam. Met de verbeterende CTP technieken en de steeds geavanceerder wordende CT-scanners zal de sensitiviteit naar alle waarschijnlijkheid in de komende jaren verder toenemen.

In **hoofdstuk 6** onderzoeken wij een manier om tot een reductie in stralingsdosis te kunnen komen. Wij creëerden CTP datasets met slechts de helft van het normale aantal stralingsdosis en reconstrueerden deze data met het normale Filtered Back Projection (FBP) en een zogenaamd hybride iteratieve reconstructie algoritme. Dit algoritme kan door middel van het verminderen van ruis in de zogenaamde ruwe data zorgen voor een gelijkwaardige beeldkwaliteit wanneer er met minder straling wordt gescand. Wij zagen dat met het gebruik van dit algoritme het mogelijk is om patiënten met de helft van de dosis een CTP te laten ondergaan zonder dat de diagnostische beeldkwaliteit en objectieve paramaters significant worden aangetast. Aan de andere kant zagen we wel dat in ongeveer één kwart van de patiënten de algemene beeldkwaliteit minder werd.

Hoofdstuk 7 behandelt een bedienerafhankelijke stap die tot veel variatie in resultaten kan leiden; de selectie van de arteriële input functie (AIF) en veneuze output functie (VOF). Een AIF dient als referentievat voor de software om kwantitatieve paramaters te kunnen berekenen terwijl de VOF wordt geselecteerd om de AIF te optimaliseren. De introductie van de 256(-of-meer-) slice-scanners en de daarmee gepaard gaande grotere coverage biedt de mogelijkheid om ook de carotiden als AIF te selecteren en zou daarnaast het selecteren van een VOF overbodig kunnen maken. Wij vonden dat de selectie van verschillende AIFs kan leiden tot grote significante verschillen in de kwantitatieve paramaters (tot 13% in MTT, 25 % in CBV en meer dan 50% in CBF). De selectie van de carotiden als AIF zorgde voor de meest accurate resultaten terwijl de selectie van de VOF nog steeds nodig bleek.

In **hoofdstuk 8** vergelijken wij de kwaliteit van de FBP-gereconstrueerde CTA van het hoofd en de nek met de kwaliteit voortkomend uit twee recent ontwikkelde algoritmen; naast het in hoofdstuk 6 al geïntroduceerde hybride iteratieve reconstructie algoritme, is dat het nog recenter ontwikkelde modelgebaseerde iteratieve reconstructie algoritme.
In metingen van de graad van de carotis stenosen werd geen verschil gevonden tussen de verschillende reconstructies. Wel zagen wij dat in zowel CTA van het hoofd als van de nek het modelgebaseerde iteratieve reconstructie algoritme de ruismetingen, de objectieve beeldkwaliteit en de automatische vat analyse verbeterde in vergelijking met het hybride iteratieve reconstructie algoritme en met FBP. Toch was er ook een nadeel; de observers vonden de subjectieve beeldkwaliteit van het modelgebaseerde iteratieve reconstructie algoritme namelijk slechter en hun voorkeur ging hierin uit naar de middels hybride iteratieve algoritme gereconstrueerde CTA-beelden. Ondanks dat de resultaten van dit onderzoek uiteenlopend waren, werd wel duidelijk dat er veel kwaliteitswinst te winnen is door het gebruik van iteratieve reconstructie algoritmen in CTA-beeldvorming.

List of publications

J.M. Niesten, I.C. van der Schaaf, A.J. Riordan, H.W.A.M. de Jong, W.P.T.M. Mali, B.K. Velthuis Optimisation of vascular input and output functions in CT-perfusion imaging using 256 (or more)-slice multidetector CT. *European Radiology. 2013;23(5):1242-9.*

J.M. Niesten joint first authorship J.M. Biesbroek, J.W. Dankbaar, G.J. Biessels, B.K. Velthuis, J.B. Reitsma, I.C. van der Schaaf. Diagnostic accuracy of CT-perfusion imaging for detecting acute Ischemic stroke: a systematic review and meta-Analysis. *Cerebrovascular diseases. 2013;35(6):493-501*

J.M. Niesten, I.C. van der Schaaf, G.J. Biessels, A.E. van Otterloo, T. van Seeters, A.D. Horsch, M.J.A. Luitse, Y. van der Graaf, L.J. Kappelle, W.P.T.M. Mali, B.K. Velthuis, on behalf of the Dutch acute Stroke Trial (DUST) Relationship between thrombus attenuation and different stroke subtypes. *Neuroradiology. 2013;55(9):1071-9*

J.M. Niesten, I.C. van der Schaaf, L. Van Dam, A. Vink, J.A. Vos, W.J. Schonewille, P.C. de Bruin, W.P.T.M. Mali, B.K. Velthuis. Histopathologic composition of cerebral thrombi of acute stroke patients is correlated with stroke subtype and thrombus attenuation. *Plos One. 2014; Ahead of publication.*

J.M. Niesten, I.C. van der Schaaf, Y. van der Graaf, LJ. Kappelle, GJ. Biessels, A.D.Horsch, J.W.Dankbaar, E.J. Smit, W.P.Th.M. Mali, B.K. Velthuis, on behalf of the DUtch acute Stroke Trial (DUST). Predictive value of thrombus attenuation on thin-slice non-contrast CT for persistent occlusion after intravenous thrombolysis. *Cerebrovascular diseases. 2014;37(2):116-122.*

J.M. Niesten, I.C. van der Schaaf, A.J. Riordan, H.W.A.M. de Jong, A.D. Horsch, D. Eijspaart, E.J. Smit, W.P.T.M. Mali, B.K. Velthuis. Radiation dose reduction in cerebral CT perfusion imaging using iterative reconstruction. *European Radiology. 2013; 24(2):484-493*

J.M. Niesten, I.C. van der Schaaf, M.J. Willemink, P.C. Vos, B.K. Velthuis. Improving head and neck CTA with hybrid and model-based iterative reconstruction techniques. *Submitted.*

Acknowledgements *(Dankwoord)*

Mijn promotietijd heb ik met veel plezier doorlopen door alle mensen die daarbij betrokken waren. Het was een prachtige tijd waarvan dit proefschrift slechts een kleine weerspiegeling is. Dit proefschrift is met de hulp van veel personen tot stand gekomen. Een aantal van hen wil ik nog nadrukkelijk bedanken.

Mijn copromotoren, Dr. I.C. van der Schaaf en Dr. B.K. Velthuis, Irene en Birgitta, ik kan niets anders dan mijn dankwoord met jullie te beginnen. Dankzij jullie heb ik mijn onderzoek kunnen opstarten en afronden. Jullie inzet, kennis en enthousiasme heeft me in die jaren veel geboden. Altijd stonden jullie klaar om te overleggen en eventuele problemen op te lossen. Het was fijn om altijd laagdrempelig langs te kunnen lopen of even op te kunnen bellen om te overleggen. Daarnaast was het nuttig en leuk om vrijwel elke donderdag met een bakje koffie uit de juiste machine bij elkaar te komen om te overleggen over de voortgang van de DUST, artikelen, het begeleiden van studenten en soms ook om even te roddelen. Birgitta, bedankt voor de prettige samenwerking. Ondanks het feit dat je zoveel projecten hebt lopen, vond je altijd de tijd om mij te begeleiden, mijn stukken van commentaar te voorzien en met nieuwe ideeën te komen. Dankzij jouw fijne karakter wist jij als hoofdonderzoeker van de DUST altijd een fijne sfeer te creëren en heb ik de afgelopen drie jaar met veel plezier kunnen werken. Irene, bedankt voor je directe begeleiding, je inzet, gezelligheid en doortastendheid. Zonder jou was dit proefschrift er nooit gekomen en ik heb in die jaren veel van jou kunnen leren. Dankzij onze vele brainstormsessies en jouw uitgebreide feedback heeft het proefschrift inhoud gekregen. Ik zal jullie in het vervolg van mijn loopbaan missen!

Prof. dr. Mali, Willem, mijn promotor, ik wil ook u van harte bedanken. Dankzij u heb ik de mogelijkheid gehad om op deze afdeling onderzoek te doen. Daarnaast heb ik, met name op het begin en aan het eind, uw pragmatische hulp mogen ontvangen bij het totstandkoming van artikelen en het proefschrift.

De leden van de beoordelingscommissie, prof dr. Rinkel, prof. dr. Van Diest, prof. dr. Algra en prof. dr. Majoie, dank voor uw interesse en voor de moeite die u heeft gestoken in het beoordelen van mijn proefschrift en voor de bereidheid zitting te nemen in de oppositie.

Mijn dank gaat ook uit naar de professoren die bij de DUST betrokken zijn geweest en mijn proefschrift mede mogelijk hebben gemaakt: prof. dr. Biessels, Geert Jan, prof. dr. Kappelle, Jaap, prof. dr. van der Graaf, Yolanda, bedankt voor jullie inzet en hulp.

Daarnaast heb ik met de andere promovendi en collega's van de DUST ook altijd prettig kunnen samenwerken.

Voor hun neurologische bijdrage wil ik Merel, Matthijs en Marjolein bedanken. Voor alle technische inslag gaat mijn dank uit naar Alan, Edwin en Hugo. Jullie hebben mij als buurmannen vaak van goed advies voorzien.

Saskia, Anneke en Cees van het Trialbureau radiologie en Mireille wil ik bedanken voor al hun inzet. Door onder andere het overzichtelijk krijgen van alle data, het maken en invoeren van de radiologische database en het voorbereiden van alle scans hebben wij als onderzoekers onze aandacht op de DUST-hoofdzaken kunnen houden. Daarnaast was het ook altijd gezellig om even bij te praten of te overleggen.

Fotografie, Roy, Karin, Chris en Jan, bedankt voor het produceren van posters, kerstkaarten, stickers, proefschriften, afbeeldingen en natuurlijk ook voor de gezelligheid.

Stafsecretariaat radiologie, en met name Marja, bedankt voor jullie inzet bij het coördineren van vergaderingen, het plaatsen van bestellingen, het regelen van vele andere dingen en de gezelligheid.

Trialbureau neurologie, Ans, Marrit, Paut en Dorien, bedankt voor jullie hulp.

Technisch cluster, Rudy, Sven, Kees, Richard en Martijn, bedankt voor het faciliteren van de DUST en mijn onderzoek. Rudy, met name jouw inzet heeft mij vaak snel op gang geholpen, hoewel jouw praatjes mij daar vervolgens weer net zo snel vanaf hielden.

Mijn (oud)collega's; Alexander, Alexandra, Andor, Anita, Anja, Anouk, Anouk, Arthur, Beatrijs, Bertine, Björn, Cecile, Charlotte, Dominika, Ewoud, Floortje, Gisela, Hamza, Hanke, Herwi, Hugo, Jesse, Jill, Jip, Joost, Laura, Maarten, Marlijne, Martin, Maurice, Merel, Niek, Nikki, Nolan, Onno, Pushpa, Richard, Stan, Suzanne, Tim, Tom, Wouter bedankt voor de gezellige lunches, congressen en andere uitstapjes.

Mijn kamergenoten op E2: Tom, Alexander, Thijs en Jan Willem. Bedankt voor de leuke sfeer die er altijd was met de vele kopjes koffie, de leuke en trieste verhalen, de grapjes en het luisterend oor dat jullie boden. Tom, dankzij jouw voorbereidend werk kon ik gelijk van start gaan met het schrijven van DUST-manuscripten. Veel dank hiervoor en ik hoop dat ook jij snel je proefschrift zal afronden. Alexander, jouw levenservaring en de daaruit voortkomende verhalen waren altijd leuk om naar te luisteren. Thijs, jij kwam pas het laatste jaar op mijn kamer maar hebt een onvergetelijk indruk op mij en mijn trommelvliezen achter gelaten in die zin. Jan Willem, jouw vaak bespotte gebrek aan lengte wist jij goed te compenseren door mij op sarcastische wijze

van dictatoriaal advies te voorzien, vaak begeleid door tranen van het lachen. Dank jullie voor je interesse, humor en vriendschap, ook buiten het werk om.

Mijn vrienden buiten de radiologie, dank voor jullie steun en de andere vele waardevolle momenten die er zijn geweest en nog zullen komen. Het is een genot om elkaar zo vaak te zien.

Mijn paranimfen,
Maarten, al sinds de 1e klas van de middelbare school volgen wij hetzelfde pad en zijn wij vrienden. Bedankt voor de gezelligheid en jouw humor, welke mij veel plezier hebben gebracht. Ik hoop dat het "potje-potje" nog lang door zal gaan.
Gawein, vanaf het moment dat we in elkaars werkgroep kwamen zijn we samen met Ronnie een hecht trio geworden. Ik weet zeker dat we elkaar in de toekomst nog vaak zullen zien en mooie momenten zullen beleven.

Lieve familie van Vilsteren,
Bedankt voor jullie interesse, vertrouwen en steun de afgelopen jaren. Het is altijd erg fijn om me in jullie gezelschap te bevinden.

Lieve zus en broer,
Jullie hebben al vanaf mijn geboorte een grote en gelukkig ook goede invloed gehad op de persoon die ik geworden ben. Het was kostbaar om met jullie op te groeien en het is nog steeds erg fijn om jullie als broer en zus, samen met Gijs en Lieke, om me heen te hebben.

Lieve mama, papa,
Veel dank voor de onvoorwaardelijke liefde, belangstelling en steun die ik altijd van jullie gekregen heb en nog steeds krijg. Dankzij jullie heb ik de mogelijkheid gehad om mezelf steeds verder te ontwikkelen. Bedankt voor alles wat jullie voor mij gedaan hebben en voor alles wat jullie samen met respectievelijk Bert,en Petri nog voor mij zullen betekenen.

Lieve Sita,
Vanaf het eerste moment dat wij elkaar zagen, ben jij mijn vreugde, mijn geluk, mijn alles. Het is een heerlijkheid om met jou naast mijn zijde door het leven te gaan. Samen zijn wij één en ik wil je bedanken voor al je liefde.

Biography

Joris Martijn Niesten was born on 30th of December 1984 in Nijmegen, the Netherlands. There he spent his first eighteen years and graduated from high school (Stedelijk Gymnasium) in 2003. In that same year he moved to Utrecht and started studying Medicine at the University of Utrecht. In 2010 he graduated from medical school and immediately after that followed clinical internship at the department of Surgery in Diakonessenhuis Utrecht. In 2011 he started as a PhD-student at the University Medical Center Utrecht on a project written by dr. IC. van der Schaaf, dr. BK. Velthuis and prof. dr. WPThM. Mali. As of December 2013 he started his residency in Radiology under supervision of dr. Montauban van Swijndrecht at the Onze Lieve Vrouwe Gasthuis in Amsterdam.

Biografie

Joris Martijn Niesten werd geboren op 30 december 1984 in Nijmegen. De eerste 18 jaar van zijn leven woonde hij aldaar en behaalde hij zijn VWO-diploma aan het Stedelijk Gymnasium. In datzelfde jaar startte hij zijn studie Geneeskunde aan de Universiteit van Utrecht, welke hij in 2010 afrondde. Gelijk hierna werkte hij een tijd als AGNIO chirurgie in het Diakonessenhuis te Utrecht. Begin 2011 begon hij met een promotietraject onder leiding van IC. van der Schaaf, dr. BK. Velthuis en prof. dr. WPthM. Mali, wat geleid heeft tot dit proefschrift. In december 2013 is hij vervolgens met zijn opleiding tot radioloog onder supervisie van dr. Montauban van Swijndrecht in het Onze Lieve Vrouwe Gasthuis in Amsterdam begonnen.